Asymmetric Rotor Examples – Part 1 Ver 21.10

Important Note:

This simplified feature presented in Ver 21.10 is replaced by a more generalized FEA in Ver 21.20 that allows for analyzing more practical and complex models. For more information, see V21_Asymmetric_Rotor_Examples_Part_2.pdf. The examples presented using this simplified approach are also modeled using the general models in Ver 21.20. In Part 2 of the ducument, only the inputs and outputs are presented, no detailed discussion is presented. The dynamic characteristics are well described in the examples using this simplified model. Please read through this document and then read through the Part 2 document. This simplified model tool will be removed in the new release in the future.

Introduction

Seven rotor configurations are considered to demonstrate the dynamic characteristics of the asymmetric (anisotropic) rotor systems. The anisotropic properties occur in the rotating components (rotor and disk) only and the bearings are either rigid for the flexible rotors or isotropic for the rigid rotors. The basic configurations included in DyRoBeS are shown in Fig. 1:

0 – Pure translation motion
1 – Pure rotational motion
2 – Flexible cantilever rotor
3 – Flexible straddle rotor (disk located within the bearing span)
4 – Flexible overhung rotor (disk located outside the bearing span)
5 – Rigid straddle rotor (Center of Mass located within the bearing span)
6 – Rigid overhung rotor (Center of Mass located outside the bearing span)

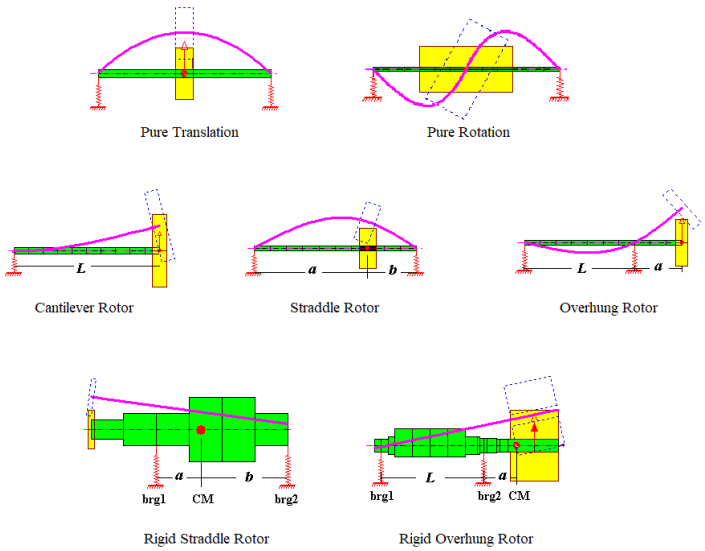

Fig. 1 – Rotor Configurations

For the anisotropic rotor systems, the solutions are solved from the equations of motion expressed in the rotating coordinate system, several axis-symmetric rotor systems are used to validate the solution algorithms. They are:

Asymmetric_Rotor_Verification_Type0_01.rotA
Asymmetric_Rotor_Verification_Type0_32.rotA
Asymmetric_Rotor_Verification_Type0_33.rotA
Asymmetric_Rotor_Verification_Type1_34.rotA
Asymmetric_Rotor_Verification_Type2_01.rotA
Asymmetric_Rotor_Verification_Type3_32.rotA
Asymmetric_Rotor_Verification_Type3_42a.rotA
Asymmetric_Rotor_Verification_Type3_42b.rotA
Asymmetric_Rotor_Verification_Type4_01.rotA
Asymmetric_Rotor_Verification_Type4_02.rotA
Asymmetric_Rotor_Verification_Type5_41.rotA
Asymmetric_Rotor_Verification_Type6_01.rotA

Most of them are taken from the book "Introduction to the Dynamics of Rotor-Bearing Systems". They are used to validate and interpret the results calculated from the rotating coordinate system. These results can be compared to those calculated from the conventional fixed (stationary) coordinate system to ensure the validity of the solution algorithms.

Several examples for the asymmetric (anisotropic) rotors are also included to illustrate the unique features of the anisotropic rotor systems. They are:

Asymmetric_Rotor_Example_1A.rotA
Asymmetric_Rotor_Example_1B.rotA
Asymmetric_Rotor_Example_2A.rotA
Asymmetric_Rotor_Example_2B.rotA
Asymmetric_Rotor_Example_2C.rotA
Asymmetric_Rotor_Example_2D.rotA
Asymmetric_Rotor_Example_2E.rotA
Asymmetric_Rotor_Example_3A1.rotA
Asymmetric_Rotor_Example_3A2.rotA
Asymmetric_Rotor_Example_3B1.rotA
Asymmetric_Rotor_Example_3C1.rotA
Asymmetric_Rotor_Example_4A.rotA
Asymmetric_Rotor_Example_4B.rotA
Asymmetric_Rotor_Example_4C.rotA
Asymmetric_Rotor_Example_5A.rotA
Asymmetric_Rotor_Example_5B.rotA
Asymmetric_Rotor_Example_5C.rotA

Program Description

Since the rotor model and analysis results for the asymmetric rotors are quite different from the axis-symmetric rotor systems, a menu “Asymmetric-Rotor”, as shown in Fig. 2, is created in the Rotor main menu. Users can enter and edit the data, perform the file manipulation, run the analysis from the sub-menu “Asymmetric Rotor Simulation”, and view the results from the sub-menu “Asymmetric Rotor PostProcessor”. As stated before, currently seven basic configurations can be analyzed. Once the Rotor Type is selected, the associated and required data will be shown in the dialog box and a graphic representation will appear in the right-lower corner of the screen as shown in Fig. 2. Enter the data, select the desired analysis and click Analyze. The computational time for the analysis is very short. Once the analysis is complete, leave this input dialog box open, and simply go to the PostProcessor menu, as shown in Fig. 3, and select the desirable output presentation. Note that in every graphics, user can switch the results between the rotating coordinate system (rotating frame) and the fixed coordinate system (stationary frame).

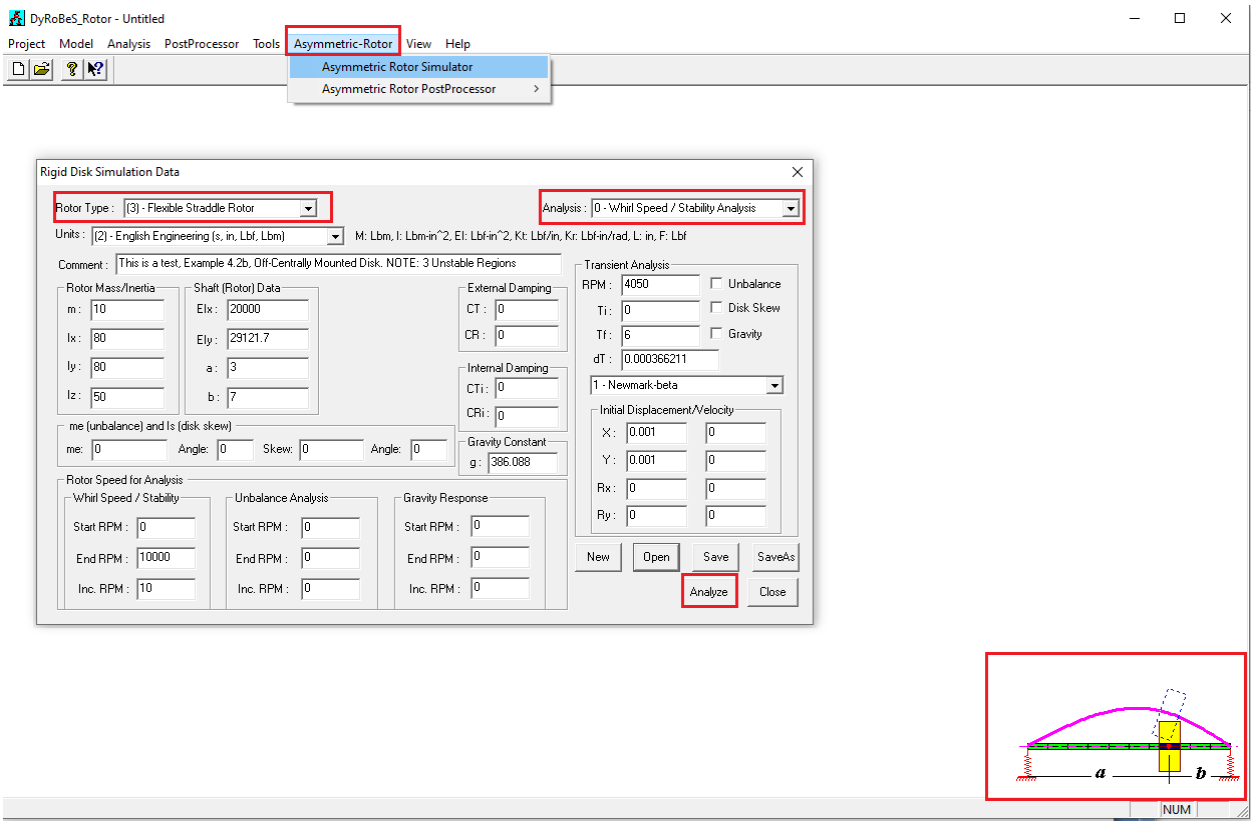

Fig. 2 – Program Menu

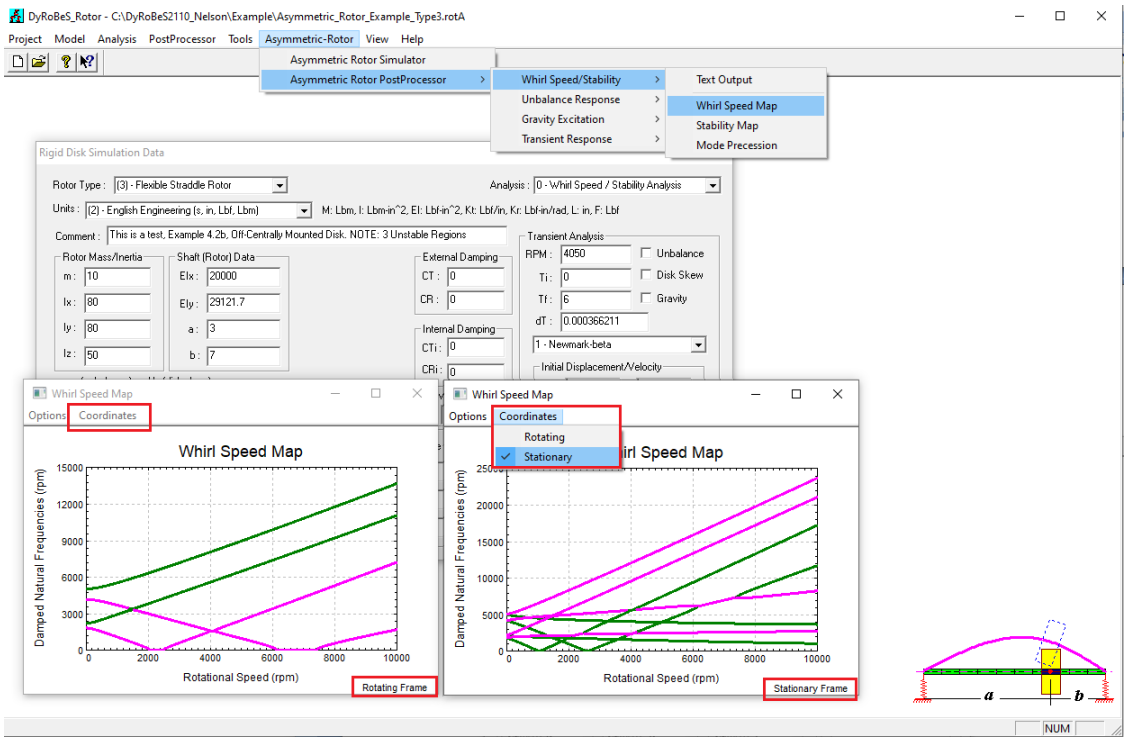

Fig. 3 – PostProcessor Menu

Asymmetric Rotor Examples

Several examples are used to validate the algorithms and hopefully to illustrate some unique dynamic characteristics present in the asymmetric rotor systems.

1. Example 1 – 2DOF Translational Motion

A Jeffcott rotor system, as shown in Fig. 1-1, supported by rigid bearings is utilized in this example. A rigid disk is located at the midspan of a flexible massless shaft. Since the fundamental translational and rotational motions are decoupled in this system, we will focus on the translational motion in this example. This rotor was analyzed with isotropic shaft properties in details in books "Introduction to the Dynamics of Rotor-Bearing Systems", Example 3.2, and "Practical Rotordynamics and Fluid Film Bearing Design", page 89-97.

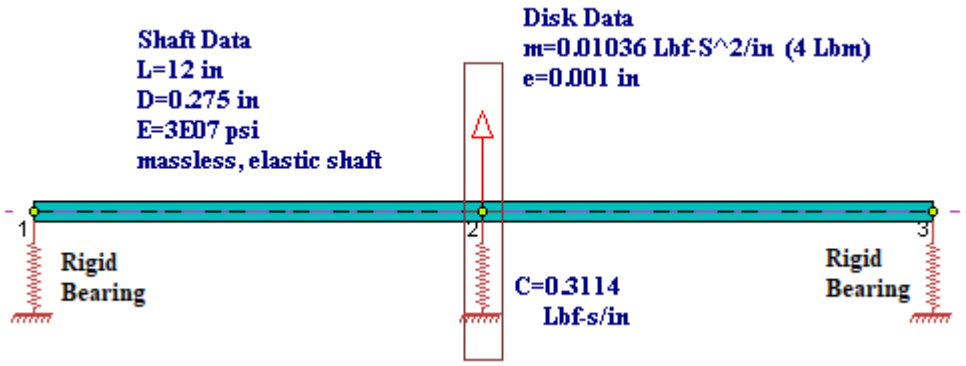

Fig. 1-1 Jeffcott Rotor

m = 4.0 Lbm (0.01036 Lbf-s^2/in) (disk mass)
L = 12.0 in (total length)
D = 0.275 in (shaft diameter for the axis-symmetric case)
E = 3.0E07 psi (Young's modulus)
C = 0.3114 Lbf-s/in (viscous damping at disk)
e = 0.001 in (mass eccentricity)
me=0.004 Lb-in = 0.064 oz-in (mass unbalance)

The translational stiffnesses at the midspan of the asymmetric shaft due to bending are:

$$k_x = \frac{48EI_y}{L^3}, \qquad k_y = \frac{48EI_x}{L^3} \tag{1-1}$$

For the axis-symmetric shaft (I_x=I_y), the shaft translational stiffness is:

$$k_x = k_y = \frac{48EI}{L^3} = 233.95 \text{ Lbf/in}, \quad \text{where } I = \frac{\pi D^4}{64} \tag{1-2}$$

Consider an anisotropic rotor with the bending stiffness of k_x and k_y in the rotating coordinate x and y axes, respectively. The equations of motion for this purely translational motion in the fixed coordinate system (Stationary Frame) are:

$$\begin{bmatrix} m & 0 \\ 0 & m \end{bmatrix}\begin{Bmatrix} \ddot{X} \\ \ddot{Y} \end{Bmatrix}+\begin{bmatrix} c & 0 \\ 0 & c \end{bmatrix}\begin{Bmatrix} \dot{X} \\ \dot{Y} \end{Bmatrix}+\begin{bmatrix} k_x\cos^2\Omega t+k_y\sin^2\Omega t & \dfrac{(k_x-k_y)}{2}\sin 2\Omega t \\ \dfrac{(k_x-k_y)}{2}\sin 2\Omega t & k_x\sin^2\Omega t+k_y\cos^2\Omega t \end{bmatrix}\begin{Bmatrix} X \\ Y \end{Bmatrix}=\begin{Bmatrix} F_X \\ F_Y \end{Bmatrix} \tag{1-3}$$

The stiffness matrix $\boldsymbol{K}$ in the fixed coordinate system is obtained from the stiffness matrix $\boldsymbol{k}$ in the rotating coordinate system through the coordinate transformation:

$$\boldsymbol{K}=\boldsymbol{T}\boldsymbol{k}\boldsymbol{T}^T=\begin{bmatrix} \cos\Omega t & -\sin\Omega t \\ \sin\Omega t & \cos\Omega t \end{bmatrix}\begin{bmatrix} k_x & 0 \\ 0 & k_y \end{bmatrix}\begin{bmatrix} \cos\Omega t & \sin\Omega t \\ -\sin\Omega t & \cos\Omega t \end{bmatrix} \tag{1-4}$$

The equations of motion in the rotating coordinate system (Rotating Frame) are:

$$\begin{bmatrix} m & 0 \\ 0 & m \end{bmatrix}\begin{Bmatrix} \ddot{x} \\ \ddot{y} \end{Bmatrix}+\begin{bmatrix} c & -2\Omega m \\ 2\Omega m & c \end{bmatrix}\begin{Bmatrix} \dot{x} \\ \dot{y} \end{Bmatrix}+\begin{bmatrix} k_x-\Omega^2 m & -\Omega c \\ \Omega c & k_y-\Omega^2 m \end{bmatrix}\begin{Bmatrix} x \\ y \end{Bmatrix}=\begin{Bmatrix} F_x \\ F_y \end{Bmatrix} \tag{1-5}$$

The stiffness coefficients in the stationary frame are periodic and the closed-form solution is not feasible. However, the coefficients in the rotating frame are constant at a specific rotor speed and the linear solutions can be easily calculated from the algebraic equations. The stability characteristics of the anisotropic rotor systems is closed related to the synchronous forward critical speeds excited by the mass unbalance. The unbalance force in the stationary coordinate system is a synchronous excitation, but is a constant expressed in the rotating coordinate system. The steady-state unbalance response in the rotating frame is obtained from the following algebraic equations:

$$\begin{bmatrix} k_x-\Omega^2 m & -\Omega c \\ \Omega c & k_y-\Omega^2 m \end{bmatrix}\begin{Bmatrix} x_o \\ y_o \end{Bmatrix}=\begin{Bmatrix} me_x\Omega^2 \\ me_y\Omega^2 \end{Bmatrix} \tag{1-6}$$

For the undamped system c=0, we have:

$$\begin{Bmatrix} x_o \\ y_o \end{Bmatrix}=\begin{Bmatrix} \dfrac{e_x\Omega^2}{\left(\dfrac{k_x}{m}\right)-\Omega^2} \\ \dfrac{e_y\Omega^2}{\left(\dfrac{k_y}{m}\right)-\Omega^2} \end{Bmatrix}=\begin{Bmatrix} \dfrac{e_x\Omega^2}{\omega_x^2-\Omega^2} \\ \dfrac{e_y\Omega^2}{\omega_y^2-\Omega^2} \end{Bmatrix} \qquad \text{where } \omega_x=\sqrt{\frac{k_x}{m}},\quad \omega_y=\sqrt{\frac{k_y}{m}} \tag{1-7}$$

The steady-state synchronous unbalance response in the fixed coordinate system has the form:

$$X_c=Y_s=x_o, \qquad Y_c=-X_s=y_o$$

There are two potential distinct critical speeds due to mass unbalance, $\Omega_{cr} = \omega_x$ and $\Omega_{cr} = \omega_y$, where the steady state response due to mass unbalance is unbounded for the undamped system. For this purely translational motion without gyroscopic effect, the forward synchronous critical speeds are the system natural frequencies. For systems with adequate damping, these two critical speeds can merge into one response peak.

For the stability analysis, consider the eigenvalue problem for a homogeneous equation. The eigensolution has the form:

$$\begin{Bmatrix} x(t) \\ y(t) \end{Bmatrix} = \begin{Bmatrix} \bar{x} \\ \bar{y} \end{Bmatrix} e^{\lambda t} \tag{1-8}$$

The eigenvalue problem is defined as the following:

$$\left(\lambda^2 \begin{bmatrix} m & 0 \\ 0 & m \end{bmatrix} + \lambda \begin{bmatrix} c & -2\Omega m \\ 2\Omega m & c \end{bmatrix} + \begin{bmatrix} k_x - \Omega^2 m & -\Omega c \\ \Omega c & k_y - \Omega^2 m \end{bmatrix} \right) \begin{Bmatrix} \bar{x} \\ \bar{y} \end{Bmatrix} = \begin{Bmatrix} 0 \\ 0 \end{Bmatrix} \tag{1-9}$$

or

$$\begin{bmatrix} \lambda^2 m + \lambda c + \left(k_x - \Omega^2 m\right) & -\lambda 2\Omega m - \Omega c \\ \lambda 2\Omega m + \Omega c & \lambda^2 m + \lambda c + \left(k_y - \Omega^2 m\right) \end{bmatrix} \begin{Bmatrix} \bar{x} \\ \bar{y} \end{Bmatrix} = \begin{Bmatrix} 0 \\ 0 \end{Bmatrix} \tag{1-10}$$

For an undamped system *c*=0, the characteristic equation has the following simple form:

$$m^2\lambda^4 + \left[\left(k_x - \Omega^2 m\right) m + \left(k_y - \Omega^2 m\right) m + 4\Omega^2 m^2 \right] \lambda^2 + \left(k_x - \Omega^2 m\right)\left(k_y - \Omega^2 m\right) = 0 \tag{1-11}$$

or

$$\lambda^4 + \left[\left(\omega_x^2 - \Omega^2\right) + \left(\omega_y^2 - \Omega^2\right) + 4\Omega^2 \right] \lambda^2 + \left(\omega_x^2 - \Omega^2\right)\left(\omega_y^2 - \Omega^2\right) = 0 \tag{1-12}$$

The eigenvalues are:

$$\lambda_i^2 = -\frac{1}{2}\left(\omega_x^2 + \omega_y^2 + 2\Omega^2\right) \pm \sqrt{\frac{1}{4}\left(\omega_x^2 + \omega_y^2 + 2\Omega^2\right)^2 - \left(\omega_x^2 - \Omega^2\right)\left(\omega_y^2 - \Omega^2\right)} \qquad i = 1, 2 \tag{1-13}$$

The eigensolution depends on the rotor speed Ω and the product of $\left(\omega_x^2 - \Omega^2\right)\left(\omega_y^2 - \Omega^2\right)$. When the rotor speed is below the first critical speed and above the second critical speed, i.e.,

$$\left(\omega_x^2 - \Omega^2\right)\left(\omega_y^2 - \Omega^2\right) > 0 \tag{1-14}$$

the eigrnvalues are complex conjugate with pure imaginary parts and the system is stable:

$$\lambda_1 = \pm j\omega_1 \qquad , \qquad \lambda_2 = \pm j\omega_2 \tag{1-15}$$

When the rotor speed is between two critical speeds:

$$\left(\omega_x^2 - \Omega^2\right)\left(\omega_y^2 - \Omega^2\right) < 0 \qquad \text{or} \qquad \Omega_{cr1} < \Omega < \Omega_{cr2} \tag{1-16}$$

The eigenvalue are:

$$\lambda_1 = \pm\sigma_1 \ \text{(real parts)} \qquad , \qquad \lambda_2 = \pm j\omega_2 \ \text{(imaginary parts)} \tag{1-17}$$

In this region, one natural motion is exponentially increase with time and the system is unstable due to the positive damping exponent $+\sigma$. At critical speeds, $\left(\omega_x^2 - \Omega^2\right)\left(\omega_y^2 - \Omega^2\right) = 0$, the system is at the stability boundary. At the first critical speed, the rotor is in the transition from the stable to unstable state. And at the second critical speed, the rotor is in the transition from the unstable to stable state. For the isotropic system, there is only one critical speed and the system is always stable.

$$\Omega_{cr} = \omega_x = \omega_y \tag{1-18}$$

and

$$\left(\omega_x^2 - \Omega^2\right)\left(\omega_y^2 - \Omega^2\right) = \left(\Omega_{cr}^2 - \Omega^2\right)^2 \ \geq \ 0 \tag{1-19}$$

For the anisotropic rotor, another unique feature is the steady-state response caused by the gravity excitation. The gravity excitation is constant in the fixed coordinate system, but synchronous (1X) in the rotating coordinate system. The steady state response due to gravity is a simple 1X harmonic motion in the rotating coordinate system for an anisotropic rotor, but is a summation of an eccentricity and a 2X harmonic circular and forward motion in the fixed coordinate system. Again, the steady state solution can be solved in the rotating coordinate system for the gravity harmonic excitation:

$$\begin{bmatrix} k_x - 2\Omega^2 m & -\Omega c & \Omega c & -2\Omega^2 m \\ \Omega c & k_y - 2\Omega^2 m & 2\Omega^2 m & \Omega c \\ -\Omega c & 2\Omega^2 m & k_x - 2\Omega^2 m & -\Omega c \\ -2\Omega^2 m & -\Omega c & \Omega c & k_y - 2\Omega^2 m \end{bmatrix} \begin{Bmatrix} x_c \\ y_c \\ x_s \\ y_s \end{Bmatrix} = -mg \begin{Bmatrix} 0 \\ 1 \\ 1 \\ 0 \end{Bmatrix} \tag{1-20}$$

For the undamped system, c=0, the response in the rotating coordinate system becomes:

$$\begin{Bmatrix} x_c \\ y_c \\ x_s \\ y_s \end{Bmatrix} = -mg \begin{Bmatrix} 0 \\ \dfrac{A - C}{\left(AB - C^2\right)} \\ \dfrac{B - C}{\left(AB - C^2\right)} \\ 0 \end{Bmatrix} = -mg \begin{Bmatrix} 0 \\ \dfrac{k_x - 4\Omega^2 m}{k_x k_y - 2\Omega^2 m\left(k_x + k_y\right)} \\ \dfrac{k_y - 4\Omega^2 m}{k_x k_y - 2\Omega^2 m\left(k_x + k_y\right)} \\ 0 \end{Bmatrix} \tag{1-21}$$

Where

$$A = k_x - 2\Omega^2 m \tag{1-22}$$

$$B = k_y - 2\Omega^2 m \tag{1-23}$$

$$C = 2\Omega^2 m \tag{1-24}$$

and

$$\begin{aligned} AB-C^2 &= \left(k_x-2\Omega^2 m\right)\left(k_y-2\Omega^2 m\right)-\left(2\Omega^2 m\right)^2 \\ &= k_x k_y-2\Omega^2 m\left(k_x+k_y\right)=m^2\omega_x^2\omega_y^2-2\Omega^2 m^2\left(\omega_x^2+\omega_y^2\right) \\ &= m^2\left[\omega_x^2\omega_y^2-2\Omega^2\left(\omega_x^2+\omega_y^2\right)\right] \end{aligned} \tag{1-25}$$

The steady state response due to gravity excitation is unbounded at the rotor speed where the denominator in Eq. (1-21) is zero.

$$AB-C^2=0 \quad \Rightarrow \quad \omega_x^2\omega_y^2-2\Omega^2\left(\omega_x^2+\omega_y^2\right)=0 \;\Rightarrow\; \Omega_{cr,g}=\frac{\omega_x\omega_y}{\sqrt{2\left(\omega_x^2+\omega_y^2\right)}} \tag{1-26}$$

For small rotor anisotropy, the gravity critical speed is about half of the unbalance critical speed.

$$\omega_x \approx \omega_y \;\Rightarrow\; \Omega_{cr,g}=\frac{\omega}{2} \tag{1-27}$$

The steady state response due to gravity excitation in the fixed coordinate system is the sum of a static eccentricity and a 2X harmonic response. The static eccentricity is:

$$\begin{Bmatrix} X_o \\ Y_o \end{Bmatrix}=\begin{Bmatrix} \dfrac{\left(x_c-y_s\right)}{2} \\ \dfrac{\left(x_s+y_c\right)}{2} \end{Bmatrix}=-mg\begin{Bmatrix} 0 \\ \dfrac{A+B-2C}{2\left(AB-C^2\right)} \end{Bmatrix} \tag{1-28}$$

and the components of the 2X harmonic response are:

$$X_c=Y_s=\frac{\left(x_c+y_s\right)}{2}=0 \tag{1-29}$$

$$Y_c=-X_s=\frac{\left(y_c-x_s\right)}{2}=-mg\left(\frac{A-B}{2\left(AB-C^2\right)}\right) \tag{1-30}$$

For the axis-symmetric rotor, k_x=k_y and A=B, the harmonic response due to gravity in the fixed coordinates vanishes ($X_c = X_s = Y_c = Y_s = 0$) and only the constant static eccentricity in the gravity direction remains (X_o= 0, and Y_o=–mg/k). For the asymmetric rotor, both the harmonic response and static eccentricity are not zero and dependent on the rotor speed. Unlike the response caused by the mass unbalance, which may have two apparent critical speeds (response peaks), the response caused by the gravity only has one critical speed. The maximum harmonic response occurs at the rotor speed where AB–C^2=0.

Before we go into the anisotropic rotor, let us analyze the isotropic system first to validate the solution algorithm and get familiar with the results presented in the rotating coordinate system.

A) Isotropic System

The undamped natural frequency, damping factor, logarithmic decrement and damped natural frequency for this isotropic system are:

$$\omega_n = \sqrt{\frac{K}{M}} = \sqrt{\frac{233.95}{0.01036}} = 150.3\, rad/\sec = 1435\,\text{rpm}$$

$$\xi = \frac{C}{C_c} = \frac{C}{2M\omega_n} = 0.1 \qquad \text{i.e. 10 percent critical damping}$$

$$\delta = \frac{2\pi\xi}{\sqrt{1-\xi^2}} = 0.631$$

$$\omega_d = \omega_n\sqrt{1-\xi^2} = 149.5\, rad/\sec = 1428\,\text{rpm}$$

$$\Omega = \omega_n = 1435\,\text{rpm} \qquad |x| = |y| = \frac{e}{2\xi} = 0.005$$

$$\Omega = \frac{\omega_n}{\sqrt{1-2\xi^2}} = 1450\,\text{rpm} \qquad |x| = |y| = \frac{e}{2\xi\sqrt{1-\xi^2}} = 0.005025 \text{ Peak Amplitude}$$

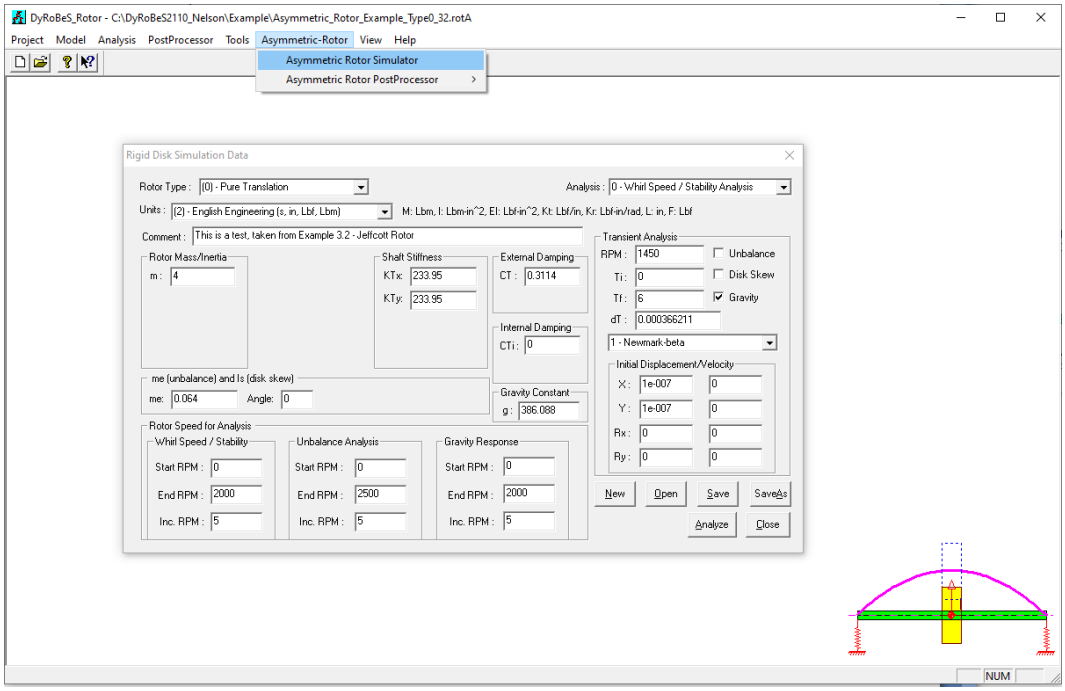

Fig. 1-2 Example 1a: Isotropic Rotor

Whirl Speed and Stability Analysis

The Whirl Speed Maps (damped natural frequencies ω vs. rotor speed Ω) in the rotating and stationary frames are shown in Fig. 1-3 below:

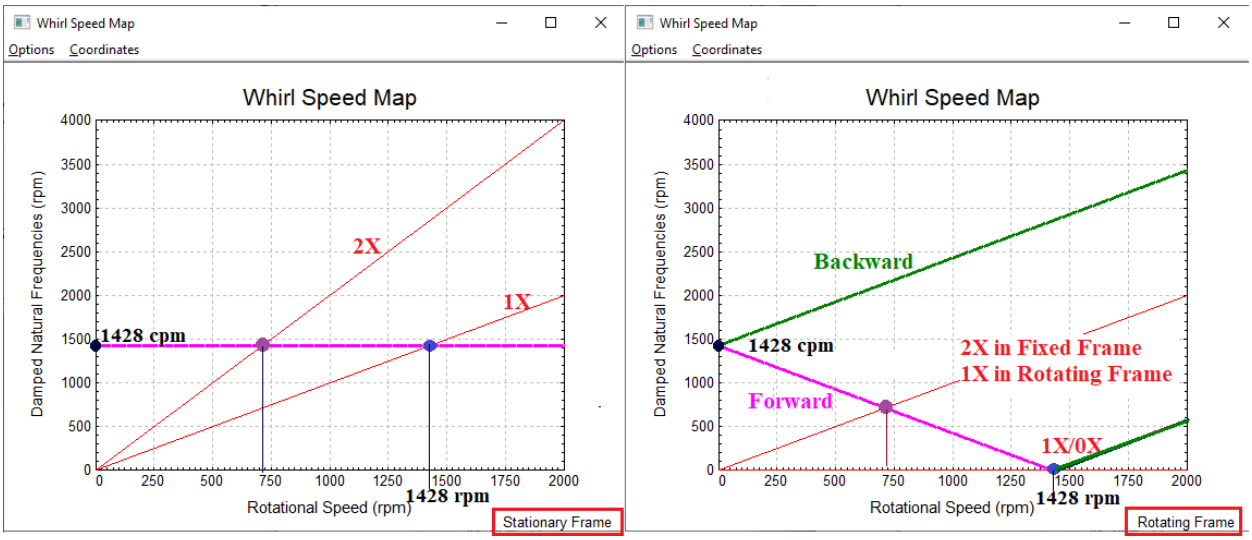

Fig. 1-3 Whirl Speed Map

Traditionally, a synchronous whirl line (1X) is drawn in the Whirl Speed Map in the stationary frame to obtain the synchronous critical speeds (ω=Ω) due to mass unbalance, and a 2X line for the critical speeds (ω=2Ω) due to gravity excitation for the anisotropic rotor systems. However, there will be 0X and 1X whirl lines in the rotating frame, since the rotating frame rotates with 1X velocity. Note that the critical speed determined from the Whirl Speed Map is not exactly the speed where the peak response occurs for the damped system, but in the vicinity of the peak response speed. Fig. 1-3 shows the damped natural frequency is a constant of 1428 cpm in the stationary frame. This is an isotropic system without gyroscopic effect, two natural frequencies are identical, one is forward circular and the other is backward circular. Therefore, it shows one line in the stationary frame, but two split straight lines in the rotating frame. Since the eigenvalues are solved in the rotating coordinate system, the frequencies in the stationary frame are obtained from the frequencies calculated from the rotating frame. (ω+Ω) is the frequency for the forward mode and (ω–Ω) is the frequency for the backward mode in the stationary frame, where ω is the frequency calculated from the rotating frame.

Let us examine the modal motions at 1,000 rpm. The first mode, as shown in Fig. 1-4, is a forward mode with a frequency of 428 cpm in the rotating frame. Since this is an isotropic system, the orbit is circular. Therefore, there is NO backward component. The precessional motion (mode shape) in the rotating frame and stationary frame are identical in shape with different whirl frequency, 428 cpm in the rotating frame and 1,428 = 428+1,000 cpm in the stationary frame. The second mode, as shown in Fig. 1-5, is a backward mode with a frequency

of 2,428 cpm in the rotating frame. Again, this is a circular orbit, there is NO forward component. The whirl frequency in the stationary frame is 1,428 = 2,428–1,000 cpm. So, in the stationary frame, both forward and backward modes have the same frequency of 1428 cpm, only the whirling direction is different.

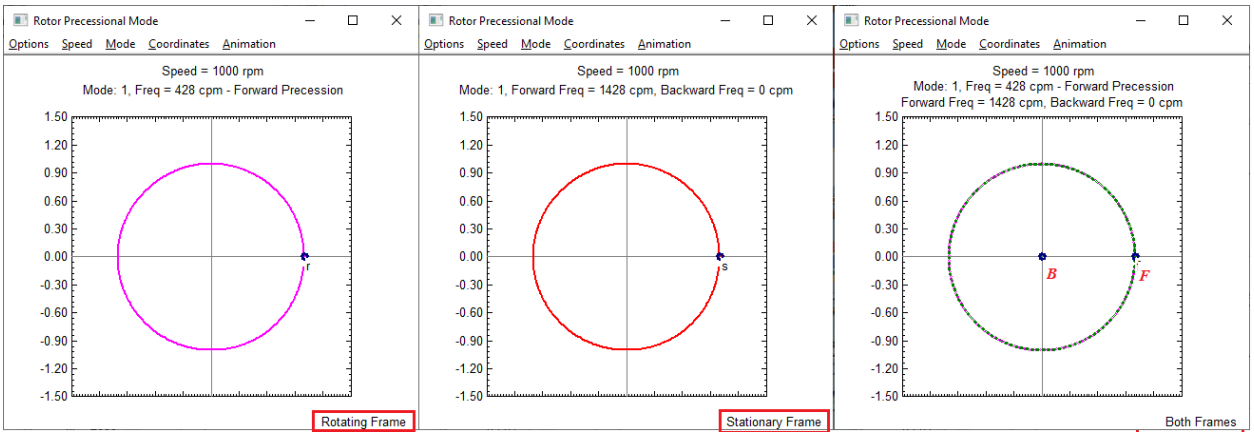

Fig. 1-4 First Mode Motion

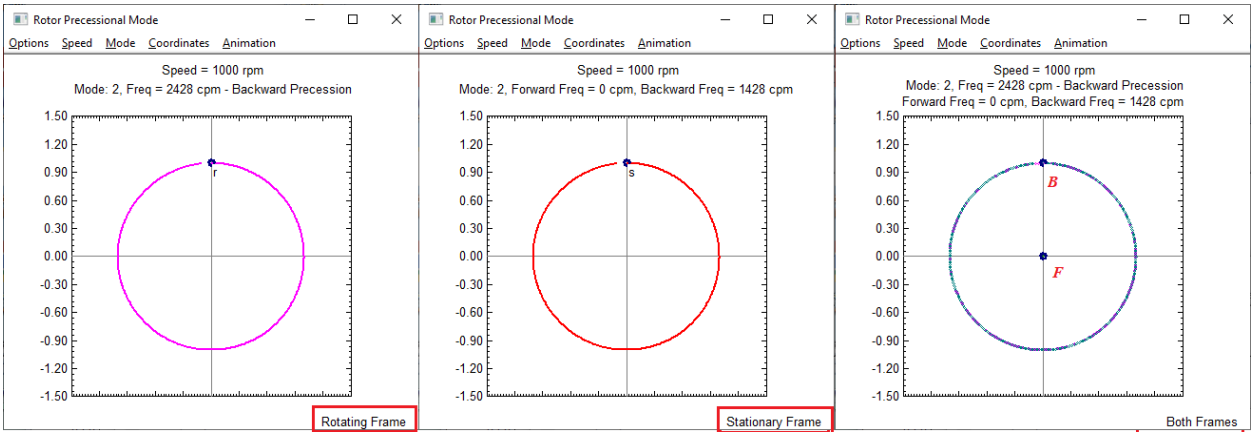

Fig. 1-5 Second Mode Motion

For the Stability Map, as shown in Fig. 1-6, damping exponents (real parts of the eigenvalues), logarithmic decrements, or damping factors can be plotted in the stationary frame, however, only damping exponents can be plotted in the rotating frame. The reason is that the frequency can be zero in the rotating frame, and the logarithmic decrement and damping factor cannot be defined. As expected, the damping factor is 0.1 in the stationary frame and the system is stable for this isotropic case.

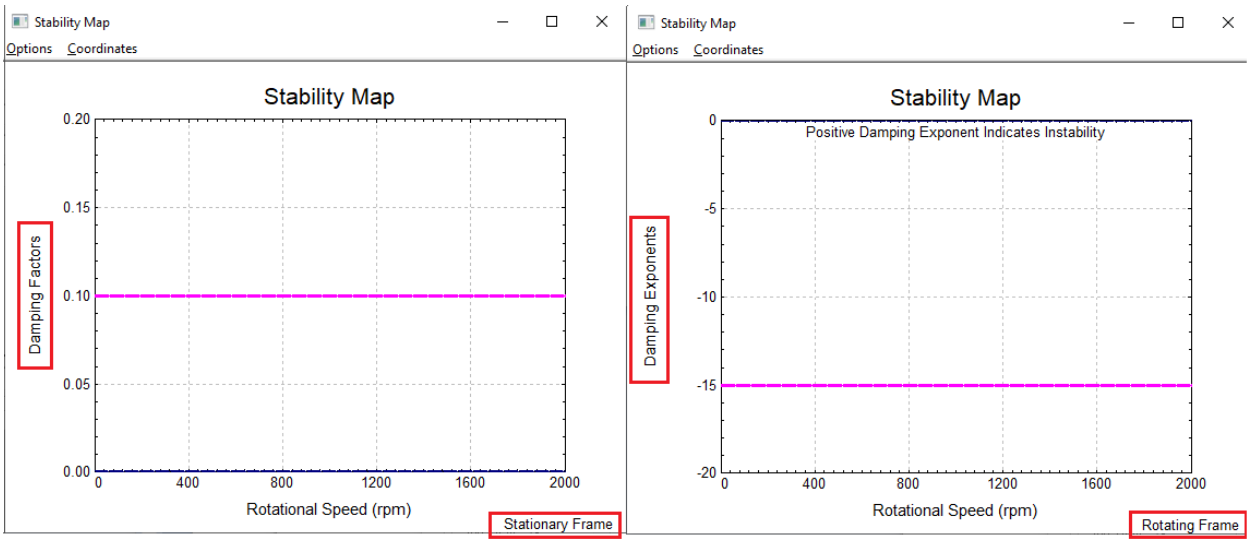

Fig. 1-6 Stability Map

Unbalance Response

The unbalance response for the isotropic system is always a forward circular orbit (1X harmonic motion) in the stationary frame, but a constant in the rotating frame. Therefore, the amplitude plots, as shown in Fig. 1-7, can be quite different for both coordinate systems. In the stationary frame, the response is circular orbit and the amplitudes in X and Y directions are identical regardless the unbalance phase angle. However, in the rotating frame, the response amplitudes in the x and y directions depend on not just the unbalance magnitude but also the unbalance phase angle. This can be easily comprehended by viewing the X-Y orbit plot as shown in Fig. 1-8. It shows the response at 1450 rpm is a forward circular orbit viewed in the stationary frame and a constant in the rotating frame.

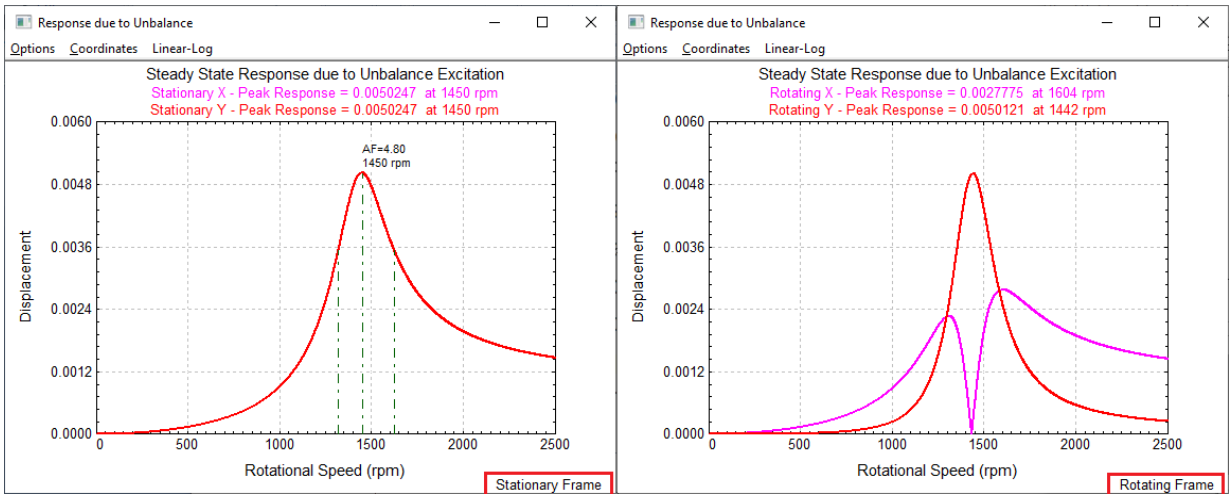

Fig. 1-7 Unbalance Response

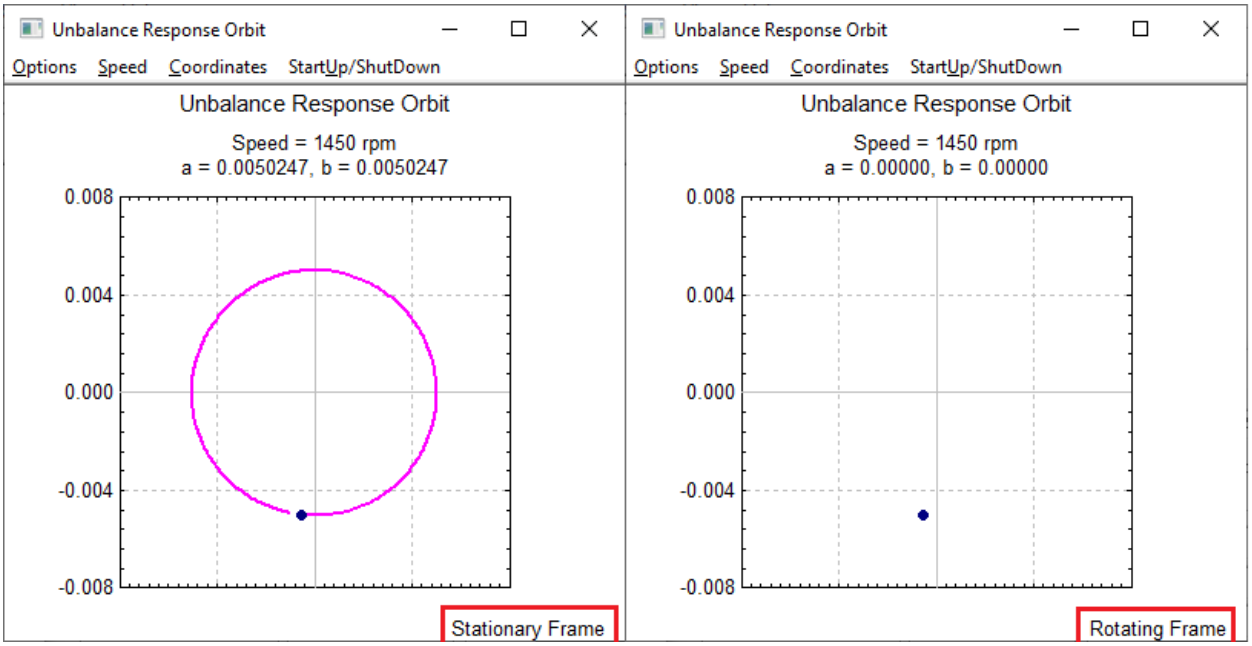

Fig. 1-8 Unbalance Response at 1450 rpm

Gravity Response

As stated before, the gravity excitation is a constant in the stationary frame, but 1X harmonic excitation in the rotating frame. For this isotropic system, the response in the stationary frame is a constant without any harmonics, and it is 1X harmonic motion with the same amplitude in the rotating frame, as shown in Fig. 1-9. The gravity critical speed can only be observed for the anisotropic system, not for the isotropic system. The static equilibrium position can be easily calculated from mg/K = 4/233.95 = 0.0171 inches for the verification purposes.

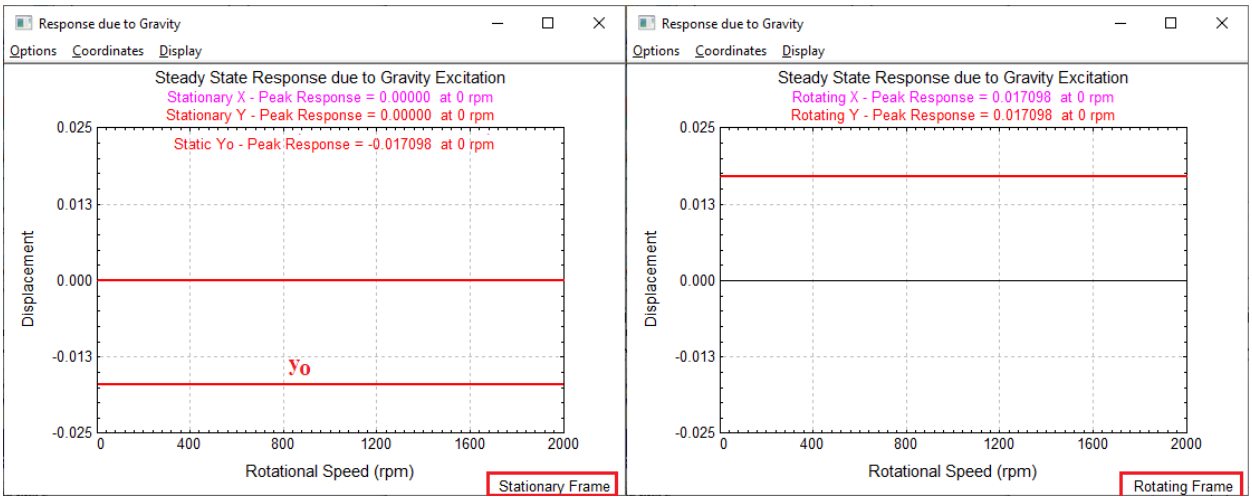

Fig. 1-9 Gravity Response

Fig. 1-10 shows the response due to gravity at 1450 rpm. Again, it is a constant in the stationary frame, but a backward circular orbit in the rotating frame, in this case.

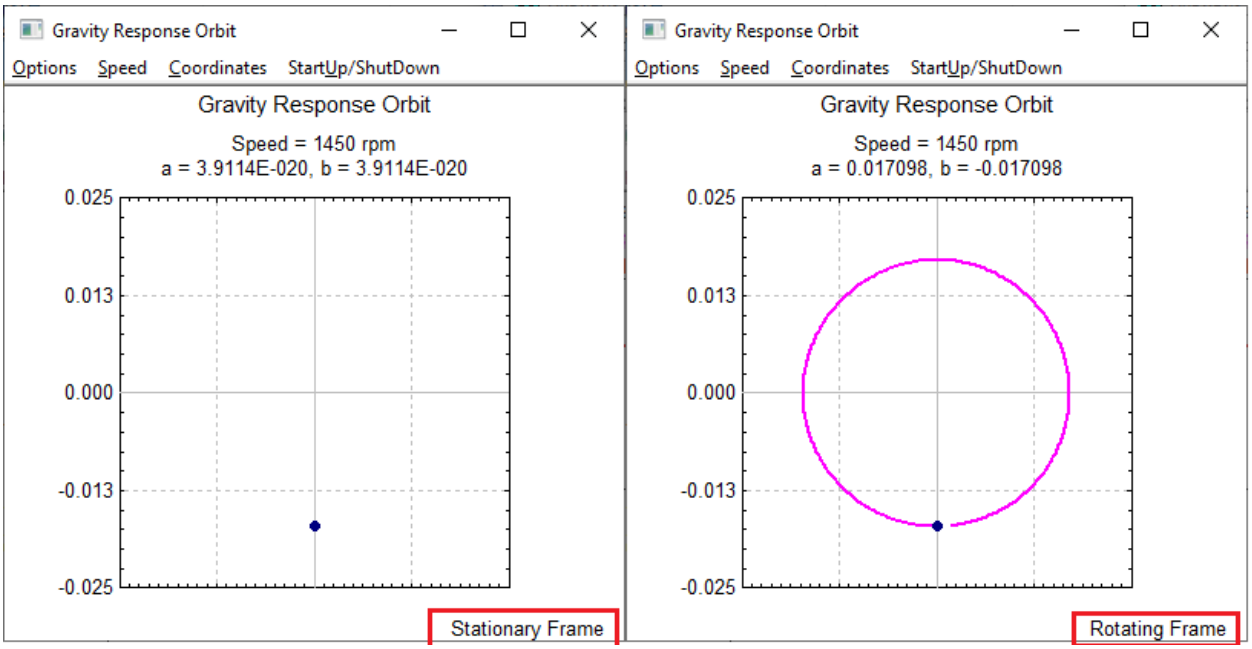

Fig. 1-10 Gravity Response at 1450 rpm

B) Anisotropic System

Let us consider the shaft is anisotropic in this case, for instance, the cross-session of the shaft is not circular which produces different bending stiffnesses in the different body axes. One unique feature for the asymmetric rotor system is the system instability present even when the system is lightly damped and no known traditionally instability mechanism except the anisotropy in the rotor. Let us change the bending stiffness in the x direction (body axis) from 233.95 to 113.615 Lbf/in. This will produce two distinct natural frequencies for each direction. At zero rpm, the undamped natural frequencies, damping factors, and damped natural frequencies are:

$$\omega_{nx} = \sqrt{\frac{113.615}{4/386.088}} = 104.72 \text{ rad/sec} = 1000 \text{ cpm}$$

$$\omega_{ny} = \sqrt{\frac{233.95}{4/386.088}} = 150.27 \text{ rad/sec} = 1435 \text{ cpm}$$

$$\xi_x = \frac{c}{2m\omega_{nx}} = \frac{0.3114}{2\times(4/386.088)\times 104.72} = 0.1435$$

$$\xi_y = \frac{c}{2m\omega_{ny}} = \frac{0.3114}{2\times(4/386.088)\times 150.27} = 0.1$$

$$\omega_{dx} = \omega_{nx}\sqrt{1-\xi_x^2} = 990 \text{ cpm}$$

$$\omega_{dy} = \omega_{ny}\sqrt{1-\xi_y^2} = 1428 \text{ cpm}$$

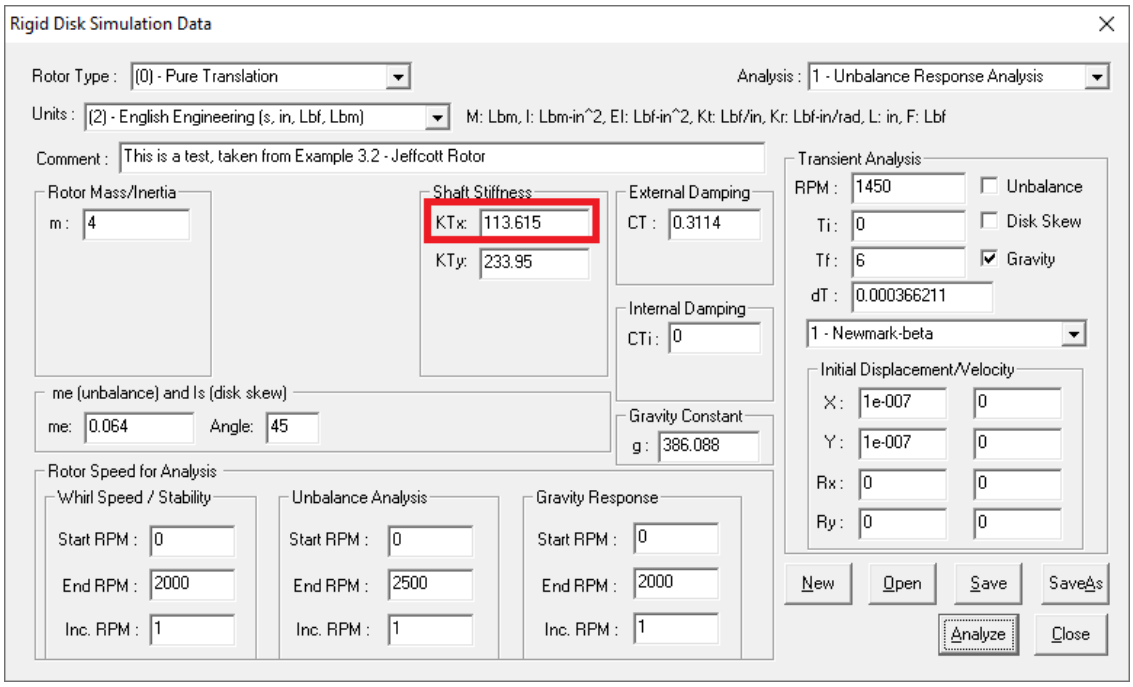

Fig. 1-11 Example 1b: Anisotropic Rotor

Whirl Speed and Stability Analysis

The whirl speed maps for the rotating and stationary frames are shown in Fig. 1-12. As described before, there are two natural modes with frequencies of ω_1 and ω_2 in the rotating frame. The first natural frequency ω_1 is a forward precession and the second natural frequency ω_2 is a backward precession in the rotating frame. Each frequency in the rotating coordinate system (ω_1 and ω_2) produces two natural frequencies in the fixed coordinate system ($\omega_{1f} = \omega_1+\Omega$, $\omega_{1b} = \omega_1-\Omega$) and ($\omega_{2f} = \omega_2+\Omega$, $\omega_{2b} = \omega_2-\Omega$), one forward precession and the other backward precession.

In the rotating frame, ω_1 starts from min(ω_{dx}, ω_{dy})=990 cpm at zero rpm and then decreases with speed, becomes zero at 990 rpm (also min(ω_{dx}, ω_{dy})) and stays at zero until the speed reaches 1,428 rpm which is the max(ω_{dx}, ω_{dy}), and then it increases with speed. ω_1=0 when rotor speed is between two damped critical speeds ω_{dx} and ω_{dy}. ω_2 starts from max(ω_{dx}, ω_{dy}) =1,428 cpm at zero rpm and then increases with speed. Since ω_2 is a backward precession mode that is not as critical as the forward mode ω_1 in practice. Unlike the isotropic rotor present before, these frequency lines are not straight lines (linear) anymore.

In the stationary frame, $\omega_{1f} = \omega_{1b} = \omega_1$ at zero speed, then ω_{1f} and ω_{1b} split as speed increases. However, ω_{1f} and ω_{1b} merges together at 990 rpm, where $\omega_{1f} = \omega_{1b} = \Omega = 990$ cpm, and stays together with the same frequency equal to the rotor speed, until the rotor speed reaches the $\max(\omega_{dx}, \omega_{dy})$ =1,428 rpm, then they split again.

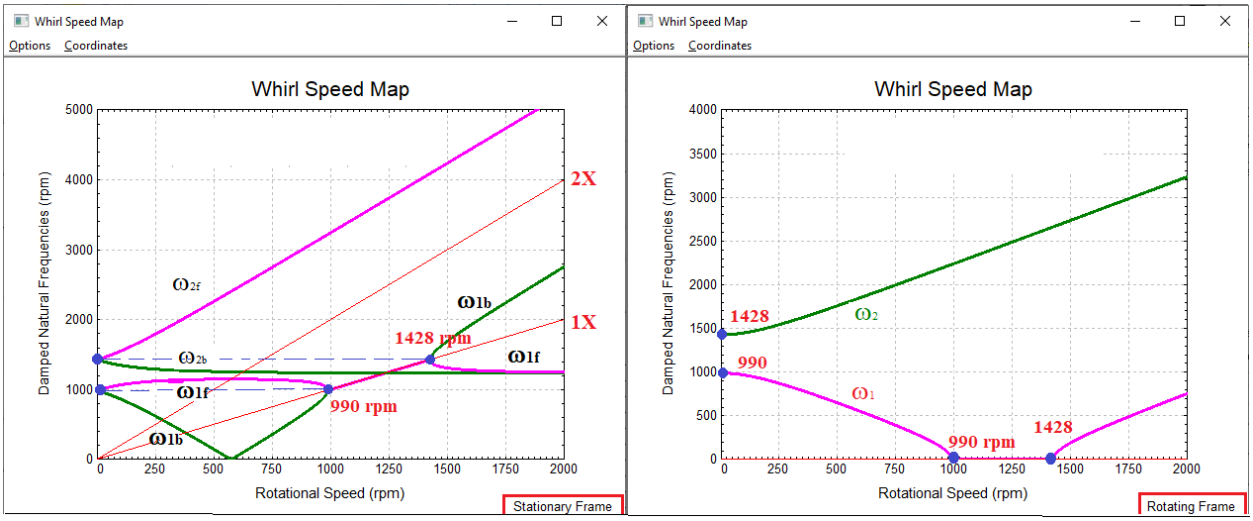

Fig. 1-12 Whirl Speed Map

Since the real parts of the eigenvalues (damping exponents) are the same for both stationary and rotating frames, they are plotted in the stationary frame as shown in Fig. 1-13. It shows that the damping exponent splits at $\min(\omega_{dx}, \omega_{dy})$=990 rpm and the forward mode goes toward the unstable region and reaches the instability threshold at 1,046 rpm, it stays unstable until the speed exceeds 1,372 rpm, then it stabilizes. The backward mode goes toward more stable region. This is a unique feature for the asymmetric rotor.

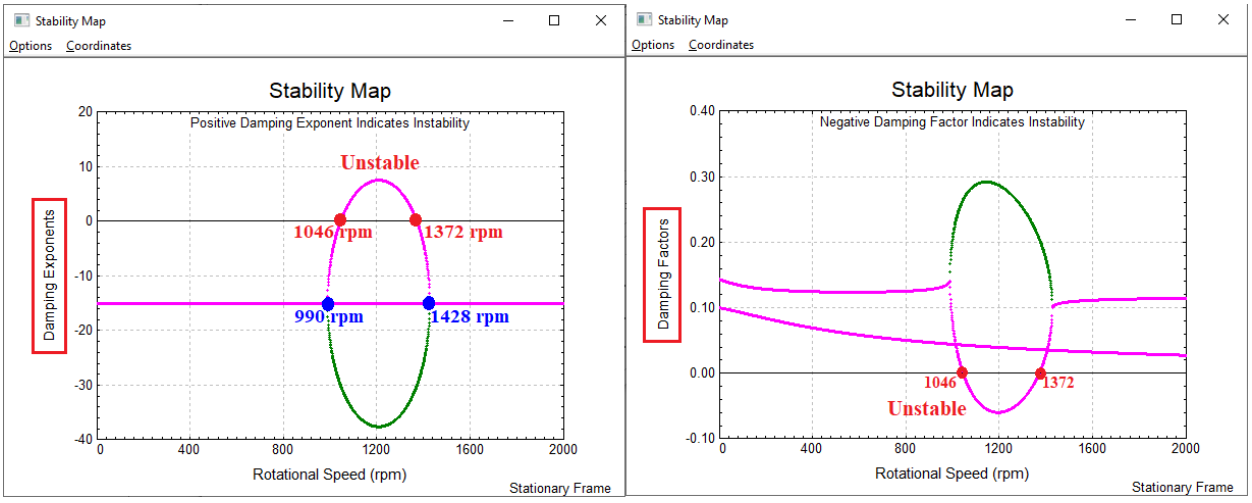

Fig. 1-13 Stability Map

Fig. 1-14 shows the unstable region versus the system damping. The unstable region is between two undamped natural frequencies (ω_{nx}, ω_{ny}) when damping is not present and then decreases as the damping increases. To decrease the rotor asymmetry and increase the damping can reduce or eliminate the unstable region,

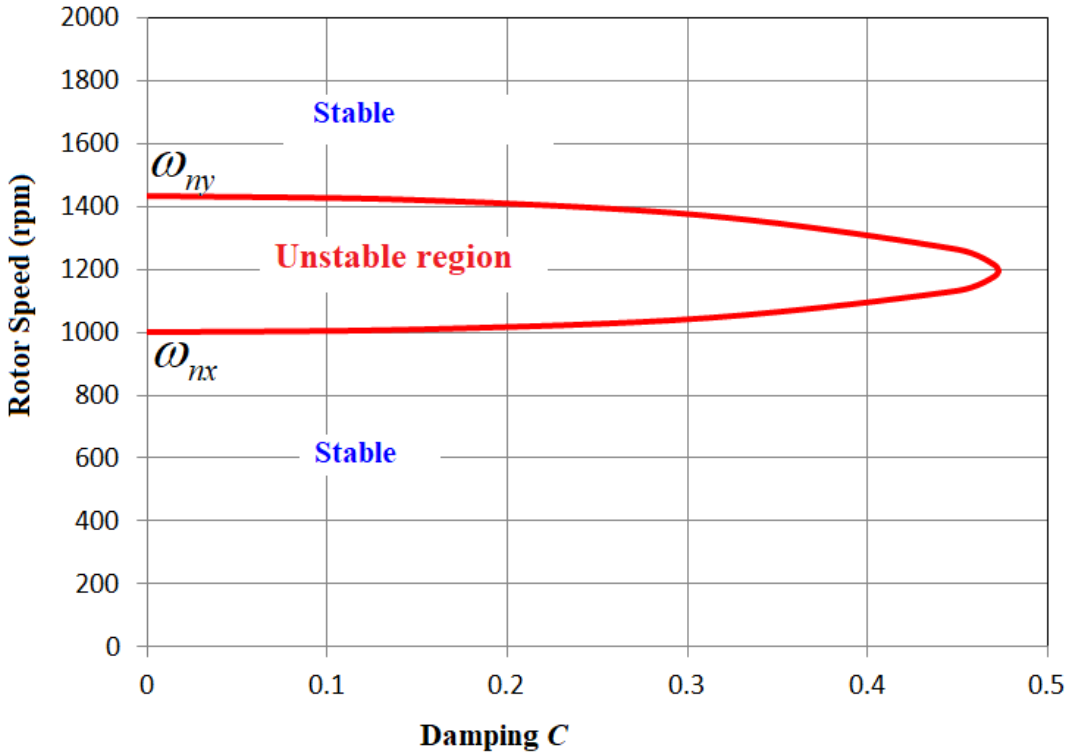

Fig. 1-14 Unstable Region for various Dampings

Unbalance Response

The steady state unbalance response is shown in Fig. 1-15. In order to excite both unbalance critical speeds (1,046 and 1,372 rpm) in the rotating frame, a non-zero unbalance phase angle (45^o) is applied such that both e_x and e_y are non-zero. It shows that the response peaks at critical speeds are extremely sharp with very high Amplification Factor (AF) for this asymmetric rotor compared to the response for the isotropic rotor presented before. Two apparent peaks can be observed in any direction in the stationary frame. Again, the response due to unbalance is synchronous in the stationary frame, but constant in the rotating frame. Also, the orbit is purely forward circular in the stationary frame, therefore, the amplitudes in the X and Y directions are identical, but they are different in the rotating frame. Interestingly, the peak speeds (1,046 rpm and 1,372 rpm) for the unbalance responses coincide with the boundaries of the instability region as shown in the Stability Map Fig. 1-13. Although we can analyze the steady state unbalance response for all the speed range, the linear theory is not applicable within this unstable region. The response orbit at 1000 rpm is shown in Fig. 1-16. It shows the response is a forward circular orbit in the fixed frame, but constant in the rotating frame.

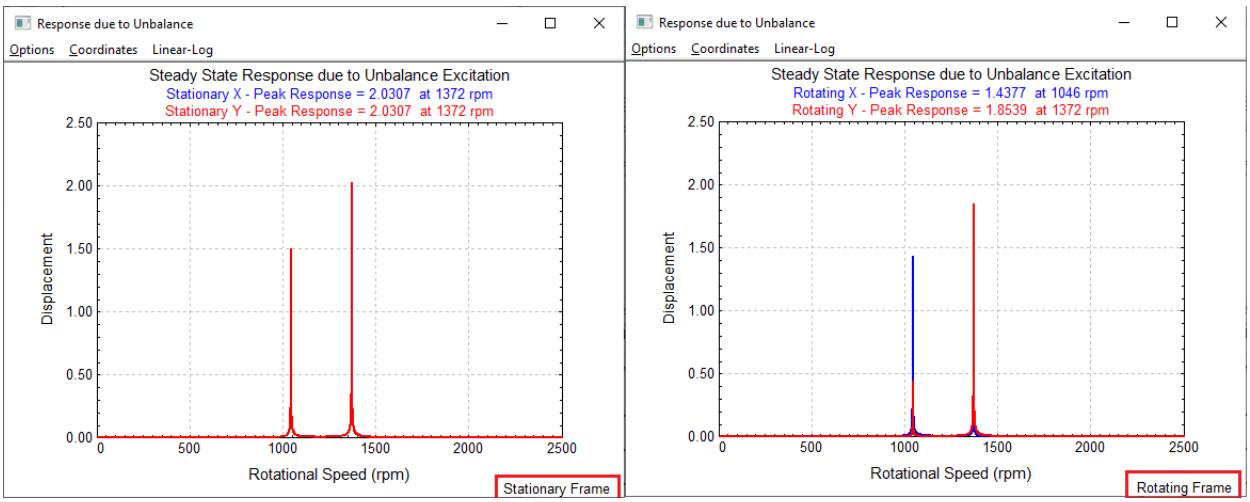

Fig. 1-15 Unbalance Response

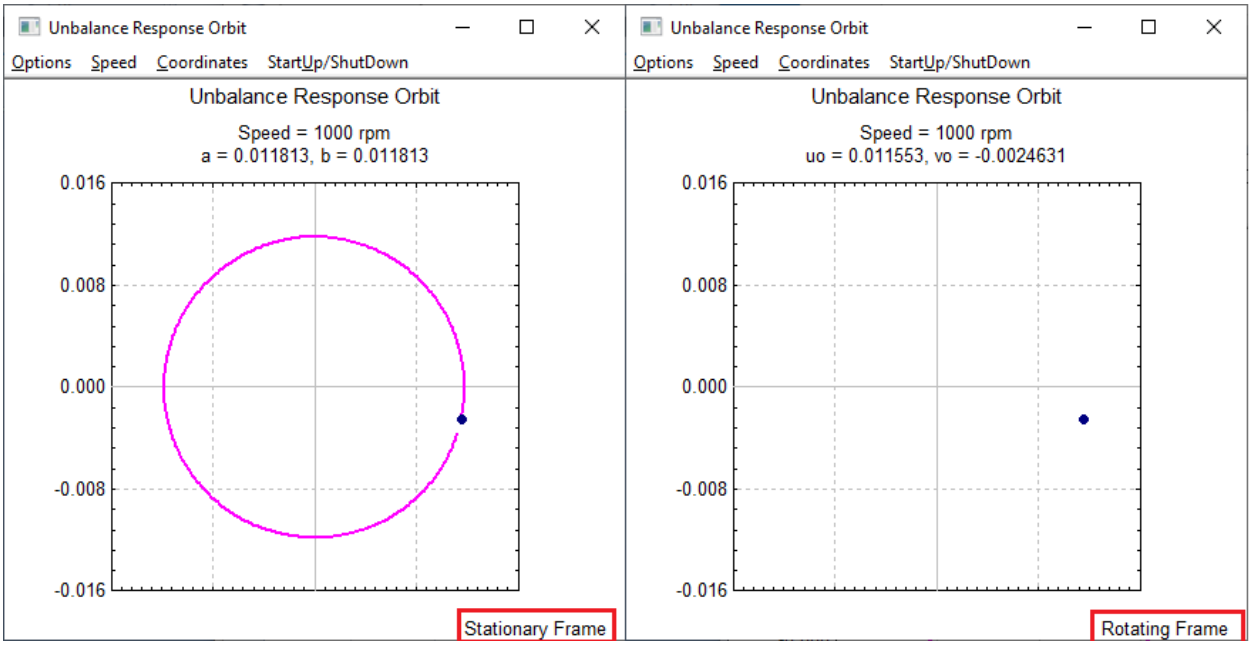

Fig. 1-16 Unbalance Response at 1000 rpm

Gravity Response

Fig. 1-17 shows the harmonic responses due to gravity excitation. The response in the rotating frame is 1X harmonic and elliptical, but the response in the stationary frame is 2X harmonic and circular, as discussed before. The peak speed, 571 rpm, can be estimated using the equation

below and is in the vicinity of the half of the first synchronous critical speed determined from the steady state unbalance response.

$$\Omega_{cr,g} \approx \frac{\omega_{dx}\omega_{dy}}{\sqrt{2\left(\omega_{dx}^2 + \omega_{dy}^2\right)}}$$

The static equilibrium position (x_o, y_o) observed in the fixed coordinate system is shown in Fig. 1-18. The non-zero x_o displacement, perpendicular to the gravity direction ($-y_o$), is caused by the damping. The response obit at 571 rpm is shown in Fig. 1-19. As described before, the harmonic response due to gravity exists only when the rotor is asymmetric. For the symmetric rotor, only a constant static equilibrium exists.

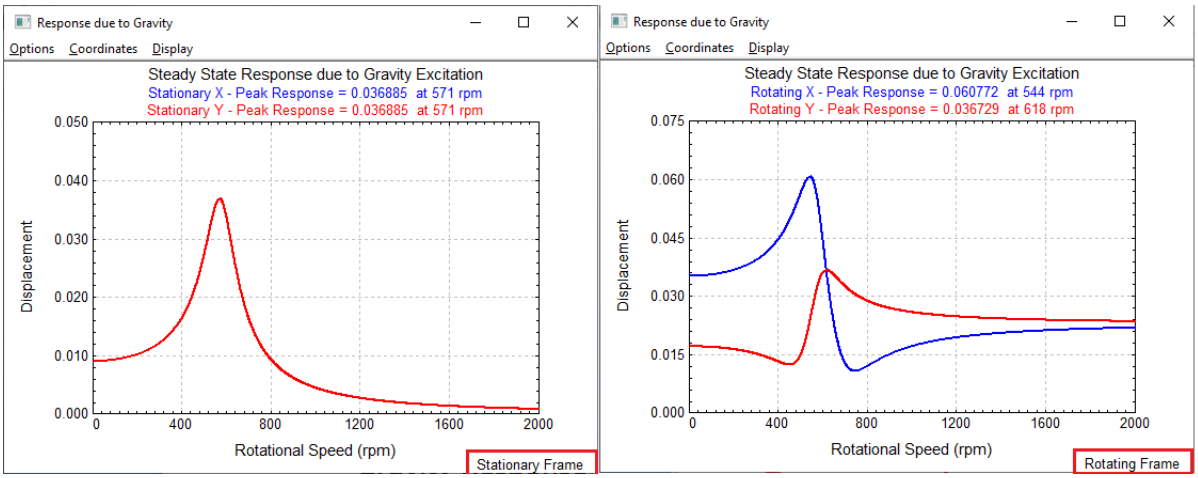

Fig. 1-17 Harmonic Response due to Gravity

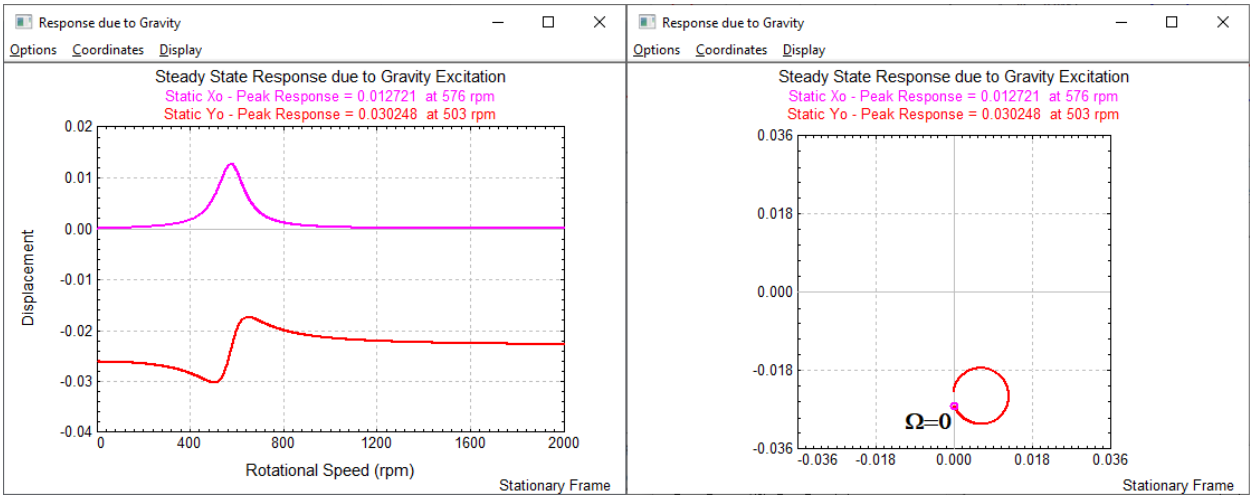

Fig. 1-18 Static Eccentricity due to Gravity

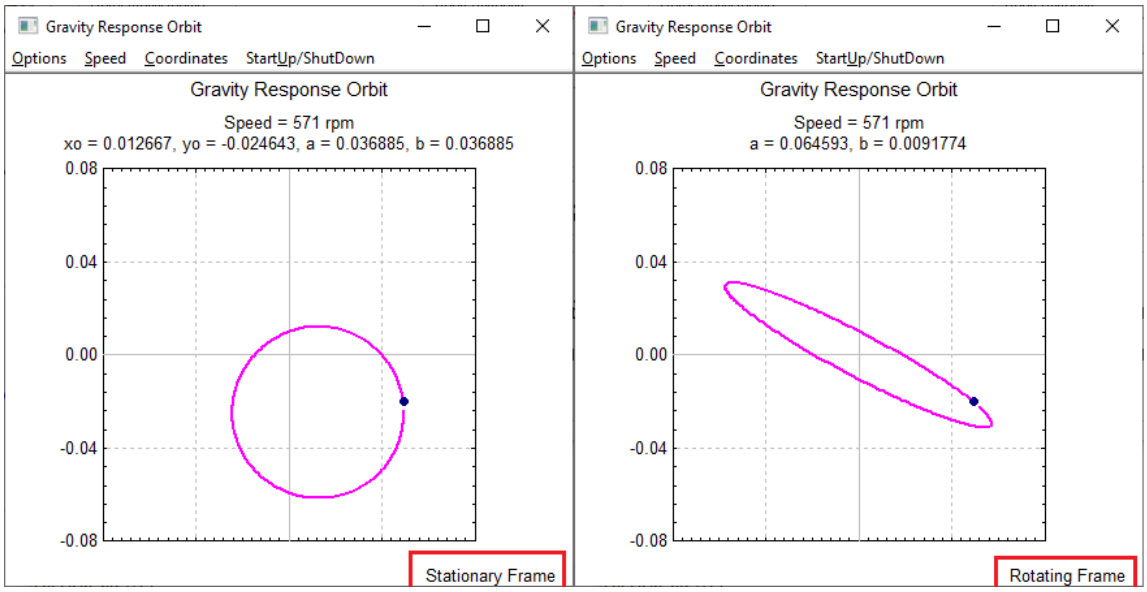

Fig. 1-19 Response due to Gravity at 571 rpm

Transient Analysis

Transient Analysis is used to validate the linear analysis discussed before. The instability threshold is 1046 rpm calculated from the Whirl Speed and Stability Analysis. Let us analyze the system with unbalance force only at 1000 and 1050 rpm. At 1000 rpm, as shown in Fig. 1-20, the motion is constrained and the response orbit due to unbalance is the same as calculated from the Unbalance Response Analysis.

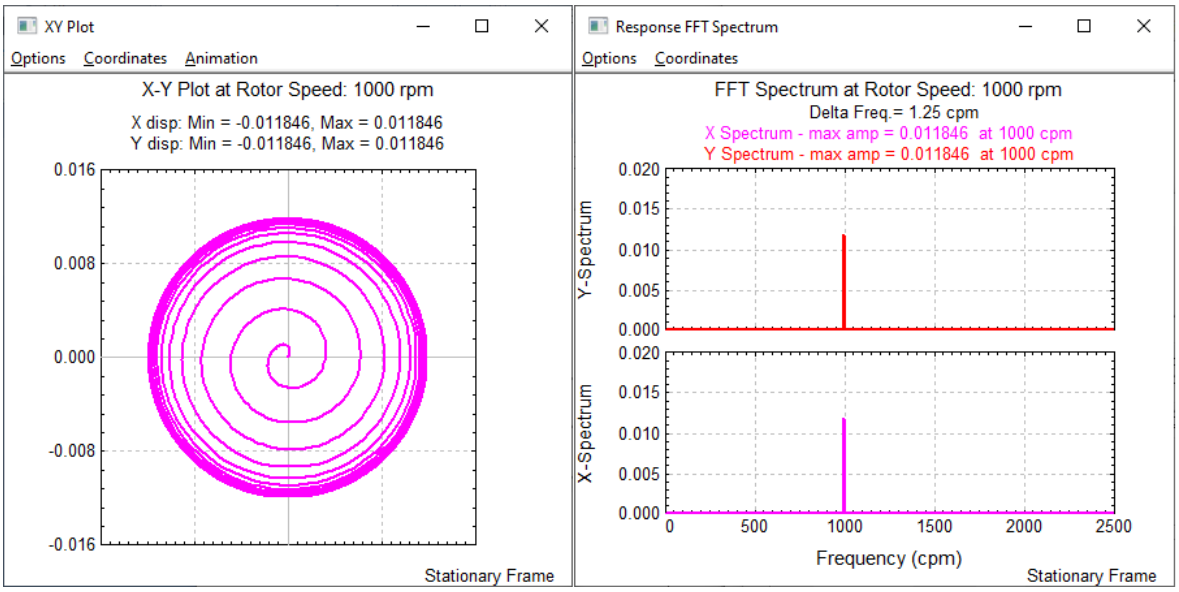

Fig. 1-20 Transient Response with Unbalance at 1000 rpm

However, at 1050 rpm, as shown in Fig. 1-21, the orbit is unconstrained and it increases exponentially since it is in the unstable region in the linear theory.

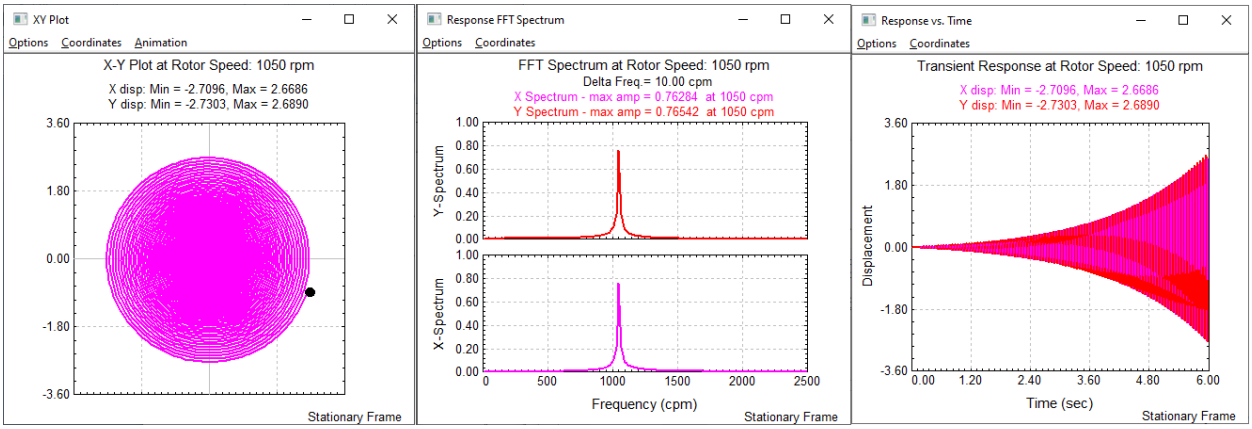

Fig. 1-21 Transient Response with Unbalance at 1050 rpm

Next, let us run the time transient analysis with the gravity only at 571 rpm. The results agree with the previous analysis.

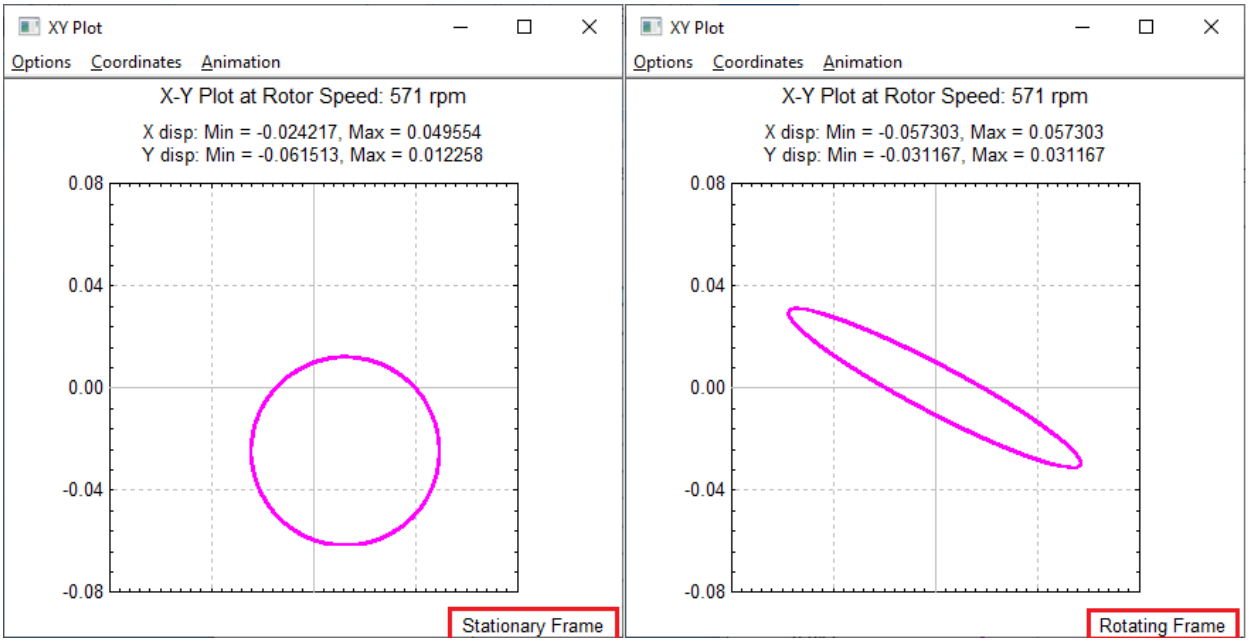

Fig. 1-22 Transient Response with Gravity at 571 rpm

2. Example 2 – 2DOF Rotational Motion

In the previous example, the asymmetry occurs in the shaft stiffness. In this example, the asymmetry occurs in the rotor inertia. Let us consider a purely rotational motion, as illustrated in Fig. 2-1. The shaft rotational stiffnesses in two principal axes for the simple Jeffcott rotor are:

$$k_x = \frac{12EI_x}{L}, \qquad k_y = \frac{12EI_y}{L}$$

Where the symbol I in EI_x and EI_y are the Second Moment of Area and should not be confused with the moment of inertia used in the kinetic energy expression and presented below. The pertinent parameters for this rotational motion are summarized below:

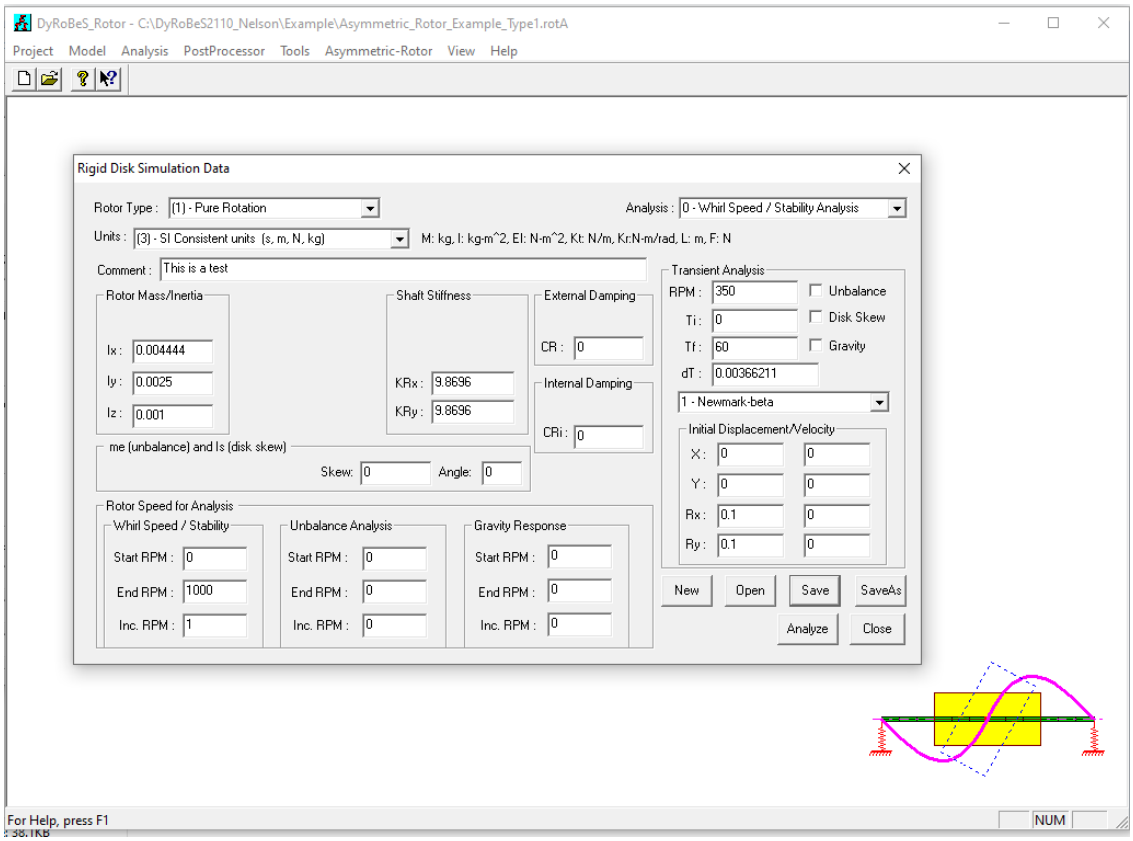

Fig. 2-1 Example 2: Purely Rotational Motion

For a purely rotational motion of an anisotropic undamped rotor, the equation of motion in the stationary frame:

$$\begin{bmatrix} I_{XX} & I_{XY} \\ I_{YX} & I_{YY} \end{bmatrix} \begin{Bmatrix} \ddot{\theta}_X \\ \ddot{\theta}_Y \end{Bmatrix} + \begin{bmatrix} c_{XX} & c_{XY} \\ c_{YX} & c_{YY} \end{bmatrix} \begin{Bmatrix} \dot{\theta}_X \\ \dot{\theta}_Y \end{Bmatrix} + \begin{bmatrix} k_{XX} & k_{XY} \\ k_{YX} & k_{YY} \end{bmatrix} \begin{Bmatrix} \theta_X \\ \theta_Y \end{Bmatrix} = \begin{Bmatrix} M_X \\ M_Y \end{Bmatrix} \tag{2-1}$$

The coefficients in the inertia and damping matrices are time dependent. Consider I_x and I_y are two diametral moments of inertia and k_x and k_y are two rotational stiffnesses in the principal body axes (x and y), respectively, and I_z is the polar moment of inertia about the spinning axis z. The matrices are:

$$\begin{aligned}\begin{bmatrix} I_{XX} & I_{XY} \\ I_{YX} & I_{YY} \end{bmatrix} &= \begin{bmatrix} \cos\Omega t & -\sin\Omega t \\ \sin\Omega t & \cos\Omega t \end{bmatrix}\begin{bmatrix} I_x & 0 \\ 0 & I_y \end{bmatrix}\begin{bmatrix} \cos\Omega t & \sin\Omega t \\ -\sin\Omega t & \cos\Omega t \end{bmatrix} \\ &= \begin{bmatrix} I_x\cos^2\Omega t + I_y\sin^2\Omega t & \dfrac{(I_x - I_y)}{2}\sin 2\Omega t \\ \dfrac{(I_x - I_y)}{2}\sin 2\Omega t & I_x\sin^2\phi + I_y\cos^2\Omega t \end{bmatrix} \\ &= \begin{bmatrix} \dfrac{(I_x + I_y)}{2} + \dfrac{(I_x - I_y)}{2}\cos 2\Omega t & \dfrac{(I_x - I_y)}{2}\sin 2\Omega t \\ \dfrac{(I_x - I_y)}{2}\sin 2\Omega t & \dfrac{(I_x + I_y)}{2} - \dfrac{(I_x - I_y)}{2}\cos 2\Omega t \end{bmatrix}\end{aligned} \tag{2-2}$$

and

$$\begin{bmatrix} c_{XX} & c_{XY} \\ c_{YX} & c_{YY} \end{bmatrix} = \Omega\begin{bmatrix} -(I_x - I_y)\sin 2\Omega t & (I_x - I_y)\cos 2\Omega t + I_z \\ (I_x - I_y)\cos 2\Omega t - I_z & (I_x - I_y)\sin 2\Omega t \end{bmatrix} \tag{2-3}$$

The stiffness matrix has the same form as the inertia matrix:

$$\begin{aligned}\begin{bmatrix} k_{XX} & k_{XY} \\ k_{YX} & k_{YY} \end{bmatrix} &= \begin{bmatrix} \cos\Omega t & -\sin\Omega t \\ \sin\Omega t & \cos\Omega t \end{bmatrix}\begin{bmatrix} k_x & 0 \\ 0 & k_y \end{bmatrix}\begin{bmatrix} \cos\Omega t & \sin\Omega t \\ -\sin\Omega t & \cos\Omega t \end{bmatrix} \\ &= \begin{bmatrix} k_x\cos^2\Omega t + k_y\sin^2\Omega t & \dfrac{(k_x - k_y)}{2}\sin 2\Omega t \\ \dfrac{(k_x - k_y)}{2}\sin 2\Omega t & k_x\sin^2\phi + k_y\cos^2\Omega t \end{bmatrix} \\ &= \begin{bmatrix} \dfrac{(k_x + k_y)}{2} + \dfrac{(k_x - k_y)}{2}\cos 2\Omega t & \dfrac{(k_x - k_y)}{2}\sin 2\Omega t \\ \dfrac{(k_x - k_y)}{2}\sin 2\Omega t & \dfrac{(k_x + k_y)}{2} - \dfrac{(k_x - k_y)}{2}\cos 2\Omega t \end{bmatrix}\end{aligned} \tag{2-4}$$

For an isotropic rotor, $I_x = I_y$ and $k_x = k_y$, the coefficients becomes constant and time independent. For an anisotropic rotor, three possible configurations can be considered: 1) anisotropic inertia with isotropic stiffness, such as asymmetric disk mounted on a symmetric flexible shaft or asymmetric rigid rotor mounted on isotropic bearings, 2) isotropic inertia with anisotropic stiffness, such as a symmetric disk mounted on an anisotropic flexible shaft, 3) anisotropic inertia with anisotropic stiffness. The equations of motion in the rotating frame are:

$$\begin{bmatrix} I_x & 0 \\ 0 & I_y \end{bmatrix}\begin{Bmatrix} \ddot{\theta}_x \\ \ddot{\theta}_y \end{Bmatrix}+\Omega\begin{bmatrix} 0 & -\left(I_x+I_y\right)+I_z \\ \left(I_x+I_y\right)-I_z & 0 \end{bmatrix}\begin{Bmatrix} \dot{\theta}_x \\ \dot{\theta}_y \end{Bmatrix}+ \\ \begin{bmatrix} k_x+\Omega^2\left(I_z-I_y\right) & 0 \\ 0 & k_y+\Omega^2\left(I_z-I_x\right) \end{bmatrix}\begin{Bmatrix} \theta_x \\ \theta_y \end{Bmatrix}=\begin{Bmatrix} M_x \\ M_y \end{Bmatrix} \tag{2-5}$$

Consider a synchronous harmonic excitation force, such as caused by the unbalance or disk skew, in the stationary coordinates:

$$\begin{Bmatrix} M_X \\ M_Y \end{Bmatrix}=\Omega^2\begin{Bmatrix} \tau\cos\left(\Omega t+\varphi\right) \\ \tau\sin\left(\Omega t+\varphi\right) \end{Bmatrix}=\Omega^2\begin{Bmatrix} \tau_x\cos\Omega t-\tau_y\sin\Omega t \\ \tau_y\cos\Omega t+\tau_x\sin\Omega t \end{Bmatrix} \tag{2-6}$$

The excitation force in the rotating coordinates is:

$$\begin{Bmatrix} M_x \\ M_y \end{Bmatrix}=\begin{bmatrix} \cos\Omega t & \sin\Omega t \\ -\sin\Omega t & \cos\Omega t \end{bmatrix}\begin{Bmatrix} \tau\ \Omega^2\cos\Omega t \\ \tau\ \Omega^2\sin\Omega t \end{Bmatrix}=\Omega^2\begin{Bmatrix} \tau_x \\ \tau_y \end{Bmatrix} \tag{2-7}$$

The response in the rotating coordinates can be solved from the following algebraic equation:

$$\begin{bmatrix} k_x+\Omega^2\left(I_z-I_y\right) & 0 \\ 0 & k_y+\Omega^2\left(I_z-I_x\right) \end{bmatrix}\begin{Bmatrix} \theta_x \\ \theta_y \end{Bmatrix}_{\mathrm{o}}=\Omega^2\begin{Bmatrix} \tau_x \\ \tau_y \end{Bmatrix} \tag{2-8}$$

and

$$\begin{Bmatrix} \theta_x \\ \theta_y \end{Bmatrix}_{\mathrm{o}}=\Omega^2\begin{Bmatrix} \dfrac{\tau_x}{k_x-\Omega^2\left(I_y-I_z\right)} \\ \dfrac{\tau_y}{k_y-\Omega^2\left(I_x-I_z\right)} \end{Bmatrix} \tag{2-9}$$

There are two possible distinct synchronous forward critical speeds where the denominators in Eq. (2-9) vanish:

$$\Omega_{cr1}=\sqrt{\frac{k_x}{I_y-I_z}} \qquad \text{and} \qquad \Omega_{cr2}=\sqrt{\frac{k_y}{I_x-I_z}} \tag{2-10}$$

Again, following the previous discussion on the eigenvalue problem in the translational motion, it can be shown that the rotor system is unstable when the rotor speed is between two synchronous forward critical speeds. That is:

$$\left(\Omega_{cr1}^2-\Omega^2\right)\left(\Omega_{cr2}^2-\Omega^2\right)\ <\ 0 \tag{2-11}$$

The eigenvalues in this region are:

$$\lambda_1=\pm\sigma_1\ \ (\text{real parts}) \qquad , \qquad \lambda_2=\pm j\omega_2\ \ (\text{imaginary parts}) \tag{2-12}$$

In this region, one natural motion is exponentially increase with time and the system is unstable due to the positive damping exponent $+\sigma$. In other speed ranges, when speed is below the first critical speed or above the second critical speed, the rotor system is stable. For the isotropic system, there is only one synchronous forward critical speed:

$$\Omega_{cr} = \Omega_{cr1} = \Omega_{cr2} \qquad \Rightarrow \qquad \left(\Omega_{cr1}^2 - \Omega^2\right)\left(\Omega_{cr2}^2 - \Omega^2\right) \geq 0 \tag{2-13}$$

The system is always stable for the isotropic system. For systems with polar moment of inertia (I_z) greater than the diametral inertia (I_x, I_y), the synchronous forward critical speeds do not exist (or infinity), the system is also always stable. In the case, if the polar moment of inertia is greater than one diametral moment of inertia and less than the other one, there is only one critical speed and the other is infinity. Then the rotor becomes unstable once it passes the first critical speed.

A) Anisotropic Rotor with isotropic stiffness

If the anisotropy occurs in the disk with asymmetric inertia and the shaft is isotropic, the shaft stiffness is:

$$k_R = k_x = k_y$$

At zero rotor speed, the natural frequencies are:

$$\omega_{nx} = \sqrt{\frac{k_x}{I_x}} = \sqrt{\frac{9.8696}{0.004444}} = 47.13 \text{ rad/sec} = 450 \text{ cpm}$$

$$\omega_{ny} = \sqrt{\frac{k_y}{I_y}} = \sqrt{\frac{9.8696}{0.0025}} = 62.83 \text{ rad/sec} = 600 \text{ cpm}$$

The synchronous forward critical speeds are:

$$\Omega_{cr1} = \sqrt{\frac{k_y}{I_x - I_z}} = \sqrt{\frac{9.8696}{0.004444 - 0.001}} = 53.53 \text{ rad/sec} = 511 \text{ rpm}$$

$$\Omega_{cr2} = \sqrt{\frac{k_x}{I_y - I_z}} = \sqrt{\frac{9.8696}{0.0025 - 0.001}} = 81.12 \text{ rad/sec} = 775 \text{ rpm}$$

The whirl speed maps in both frames are shown in Fig. 2-2. In this example, due to the gyroscopic effect, the synchronous forward critical speeds are higher than the undamped natural frequencies. Again, in the rotating frame, the first natural frequency ω_1 starts from min(ω_{nx}, ω_{ny}) = 450 cpm at zero rpm and then decreases with speed, becomes zero at 511 rpm (Ω_{cr1}) and stays at zero until the speed reaches 775 rpm (Ω_{cr2}), and then it increases with speed. That is, ω_1=0 when rotor speed is between two critical speeds, Ω_{cr1} and Ω_{cr2}. The second

natural frequency ω_2 starts from max(ω_{nx}, ω_{ny}) = 600 cpm at zero rpm and then increases with speed. Since ω_2 is a backward precessional mode that is not as critical as the forward mode ω_1 in practice. In the stationary frame, $\omega_{1f} = \omega_{1b} = \omega_1$ at zero speed, then ω_{1f} and ω_{1b} split as speed increases. However, ω_{1f} and ω_{1b} merges together at Ω_{cr1} and stays together with the same frequency equal to the rotor speed, until the rotor speed reaches the Ω_{cr2}, then they split again.

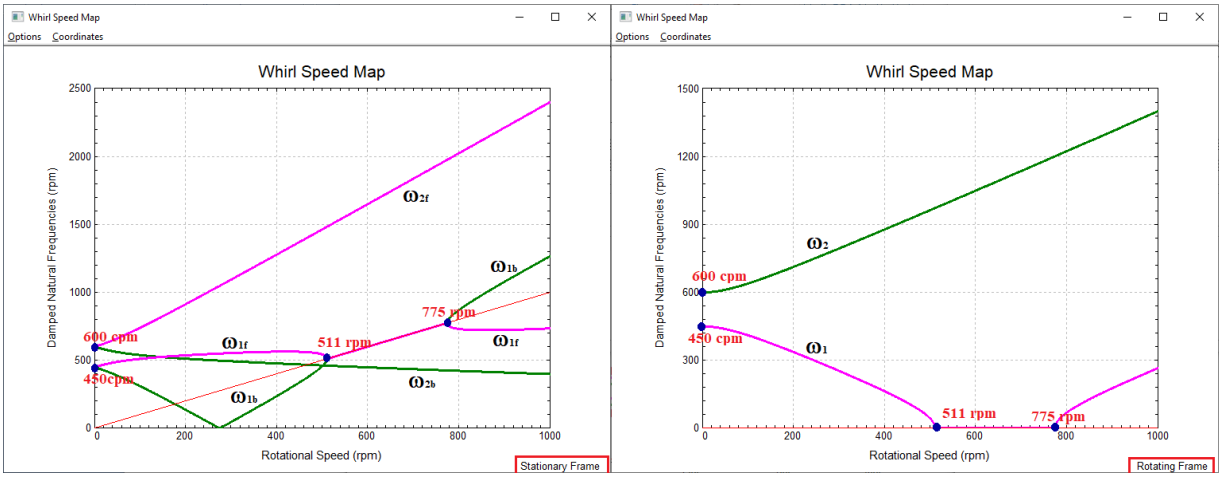

Fig. 2-2 Whirl Speed Map

The stability map, Fig. 2-3, shows the instability occurs between two critical speeds, even the system has no damping and no traditional instability mechanism, except the inertia asymmetry.

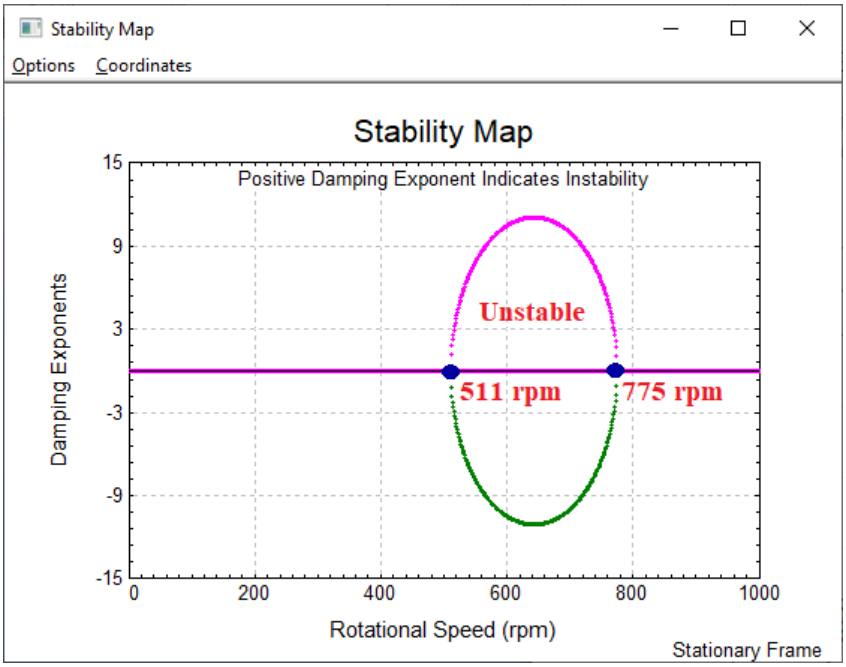

Fig. 2-3 Stability Map

B) Anisotropic Rotor with Anisotropic stiffness

Since the instability occurs between two critical speeds, let us change the rotational stiffness in x direction from 9.8696 to 4.29861, as shown below, such that the two critical speeds have the same value $\Omega_{cr1} = \Omega_{cr2} = 511$ rpm. Then the rotor system becomes stable as shown in the stability map with all the damping exponents are zero.

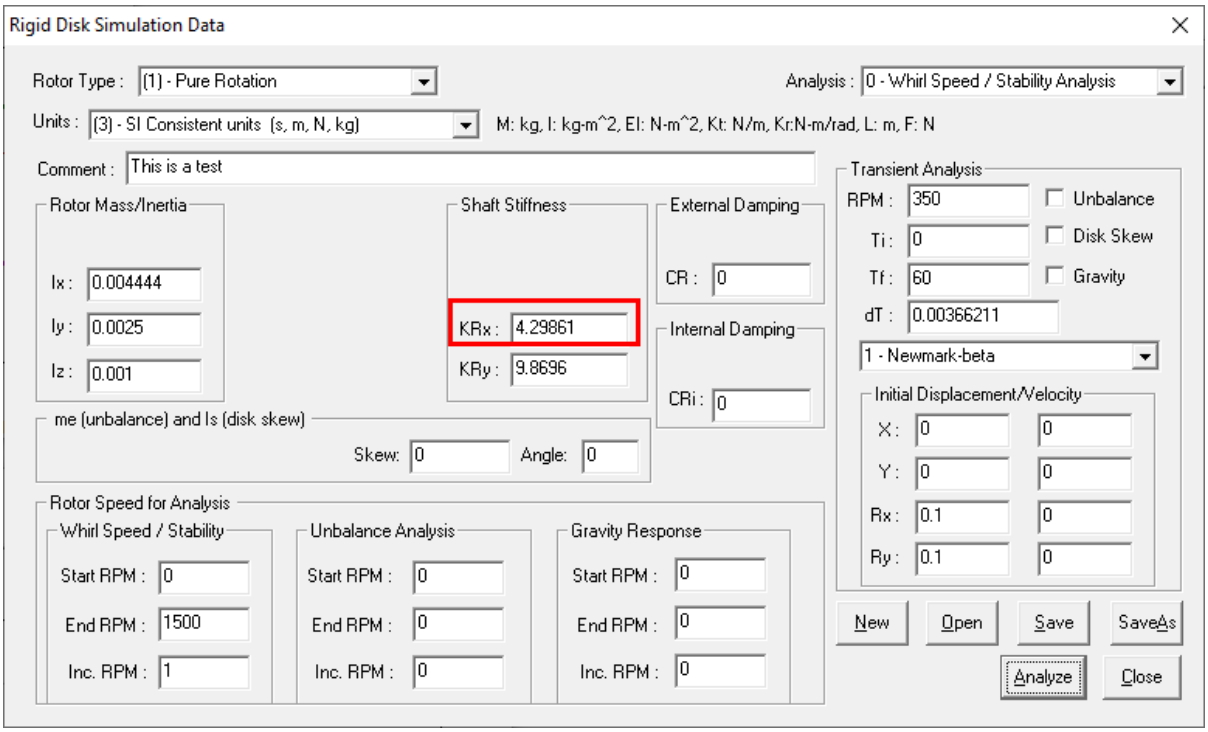

Fig. 2-4 I_x=0.004444, I_y =0.0025, I_z =0.001, k_x =4.29861, k_y =9.8696

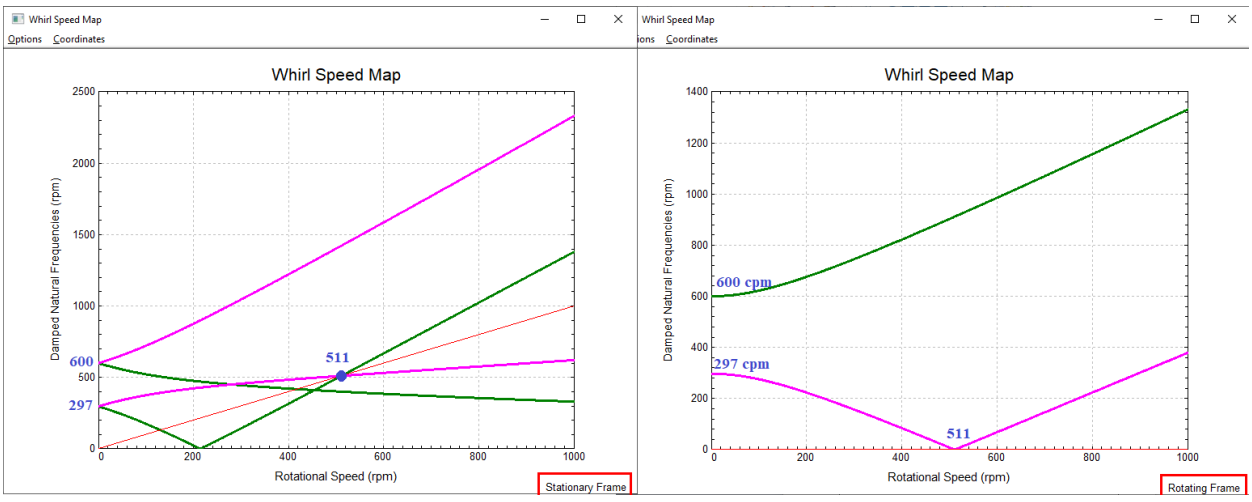

Fig. 2-5 Whirl Speed Map

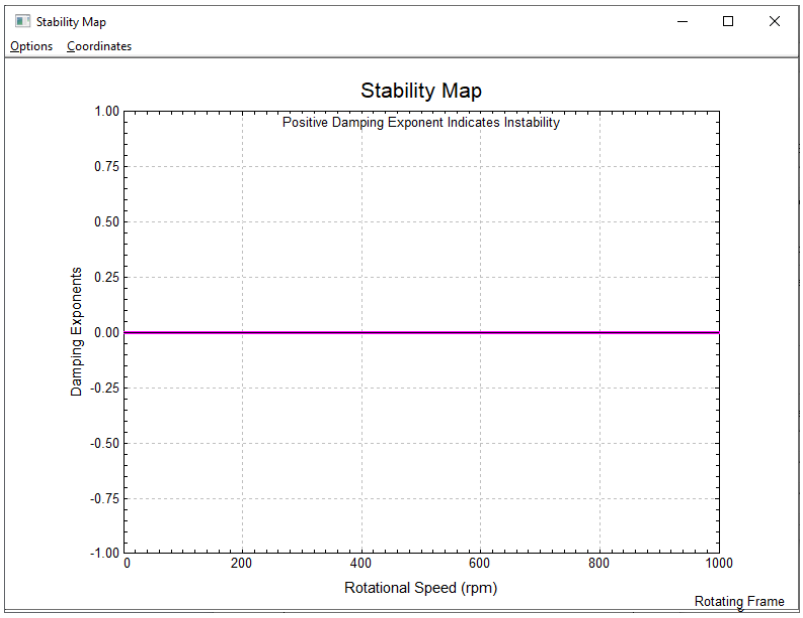

Fig. 2-6 Stability Map

If the stiffness in y direction is decreased from 9.8696 to 4.29861, as shown in Fig. 2-7, the two critical speeds become 337 rpm and 775 rpm. The system instability region actually becomes wider than before. The whirl speed map and stability map are show in Fig. 2-8 and Fig. 2-9.

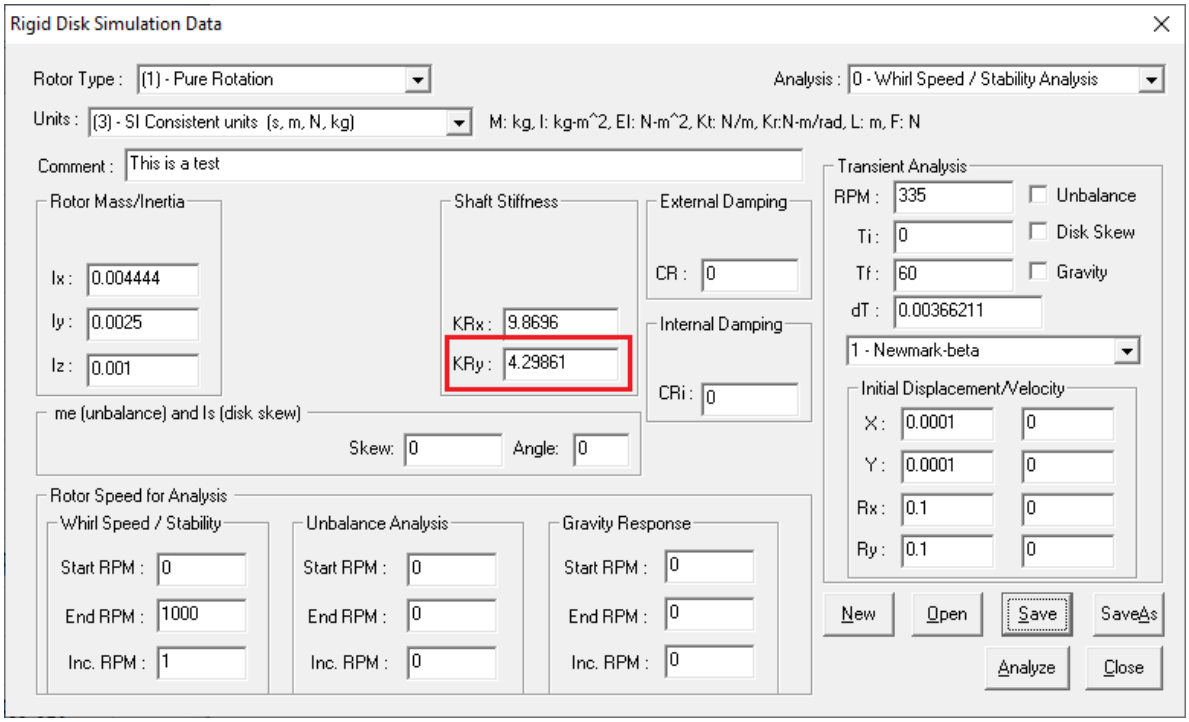

Fig. 2-7 I_x=0.004444, I_y =0.0025, I_z =0.001, k_x =9.8696, k_y =4.29861

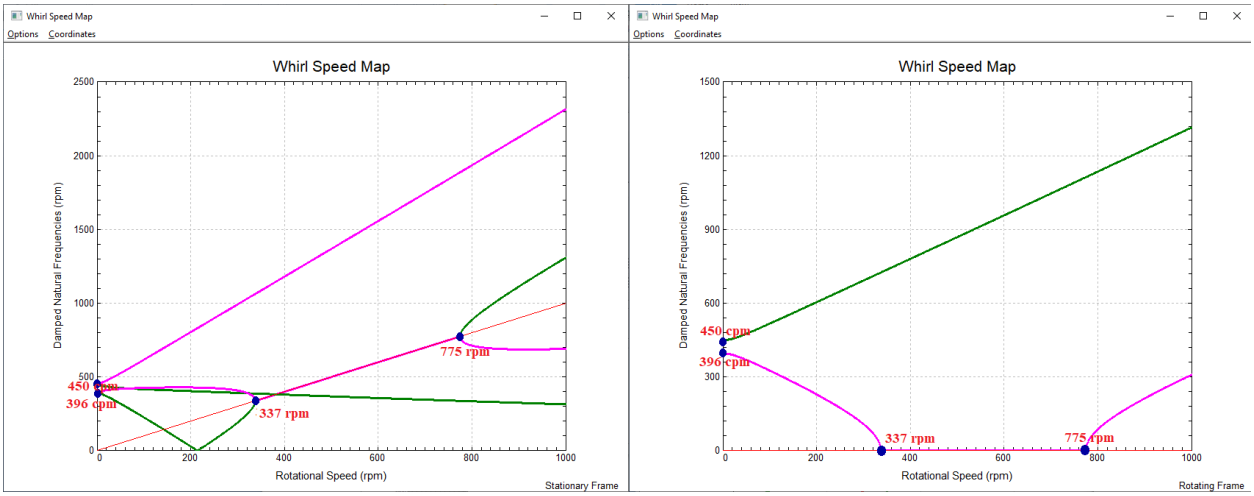

Fig. 2-8 Whirl Speed Map

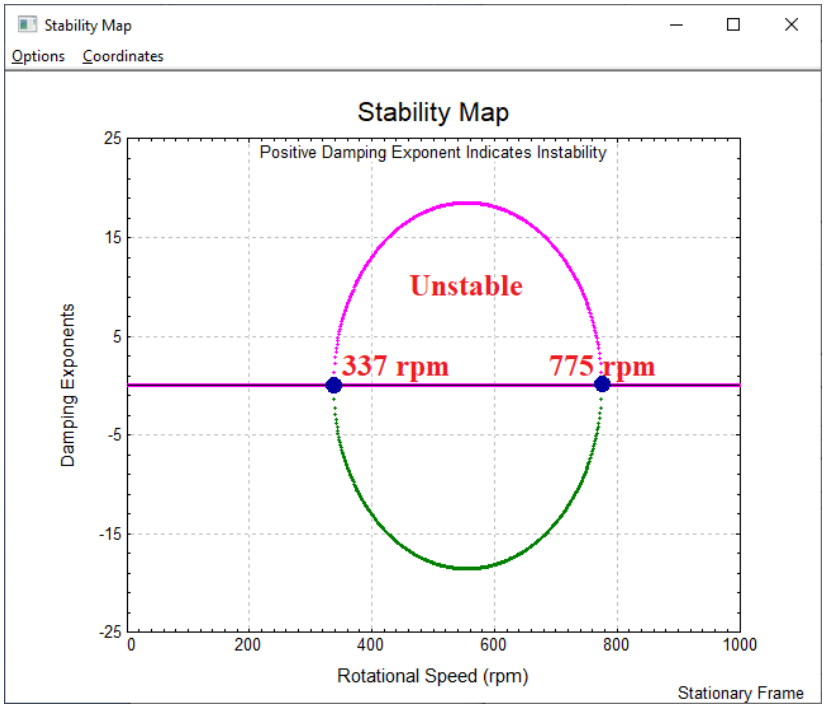

Fig. 2-9 Stability Map

Next, let us change the polar moment inertia I_z from 0.001 to 0.003 such that we have:

$$\Omega_{cr1} = \sqrt{\frac{k_y}{I_x - I_z}} = \sqrt{\frac{9.8696}{0.004444 - 0.003}} = 82.67 \text{ rad/sec} = 789 \text{ rpm}$$

and

$$\Omega_{cr2} = \infty$$

The whirl speed maps show that the first natural frequency starts from 297 cpm and reaches zero at the critical speed of 789 rpm and stays at zero afterwards in the rotating frame. That is, the ω_{1f} and ω_{1b} merge at the critical speed and stays together afterwards.

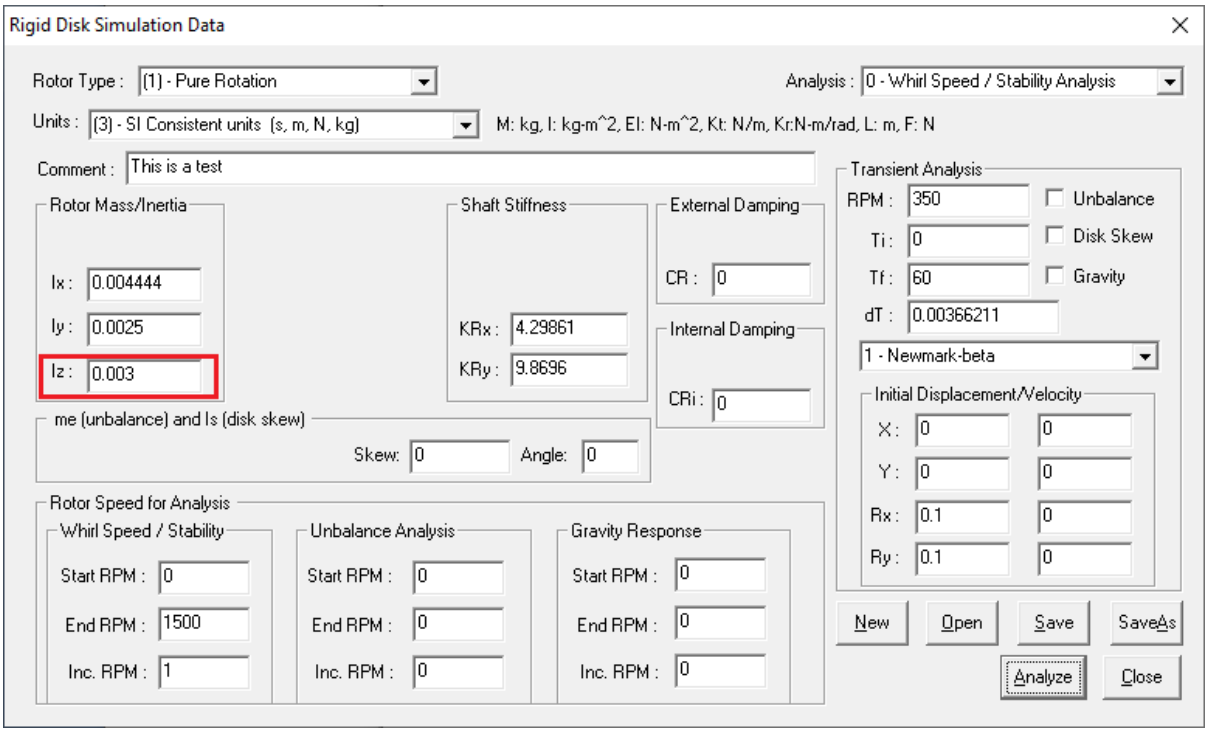

Fig. 2-10 I_x=0.004444, I_y =0.0025, I_z =0.003, k_x =4.29861, k_y =9.8696

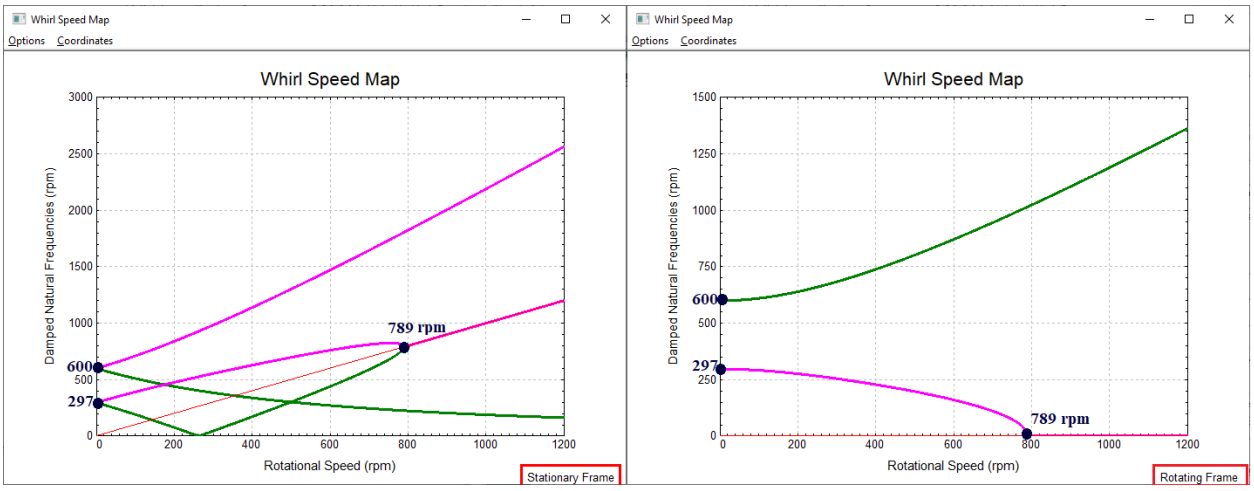

Fig. 2-11 Whirl Speed Map

Stability map shows the instability occurs after the critical speed and stays unstable as the speed increase.

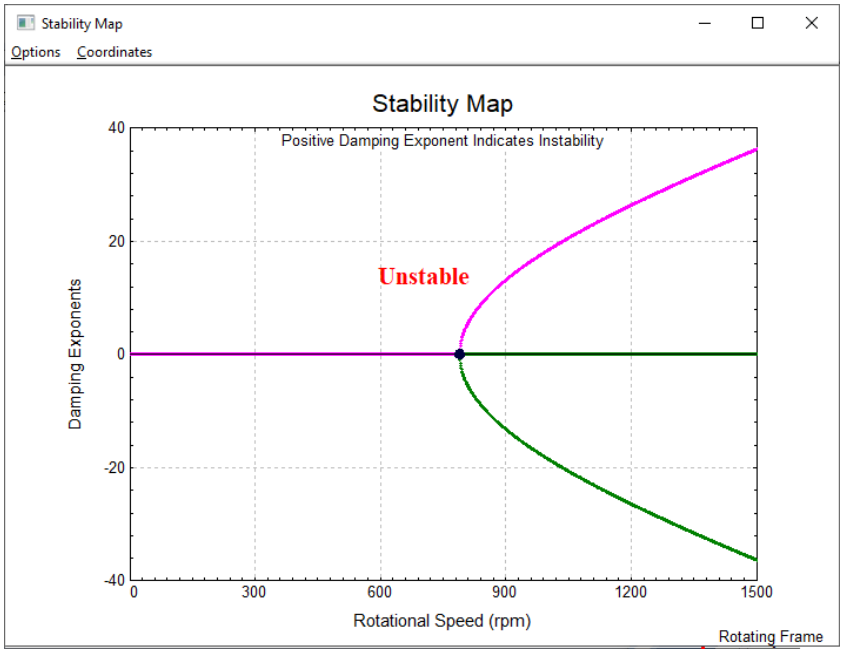

Fig. 2-12 Stability Map

Next, let us increase the polar moment of inertia to be 0.005 which is greater than both diametral moments of inertia. There is no synchronous forward critical speed present. Therefore, the system is stable in all the speed range.

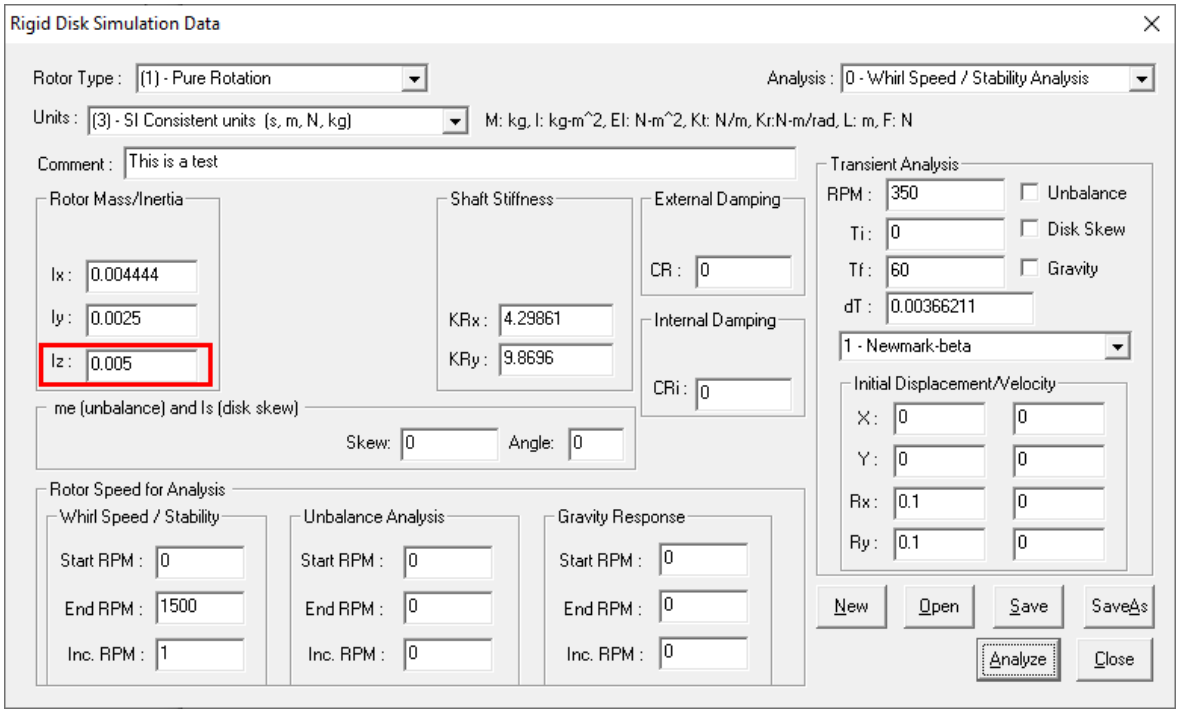

Fig. 2-13 I_x=0.004444, I_y =0.0025, I_z =0.005, k_x =4.29861, k_y =9.8696

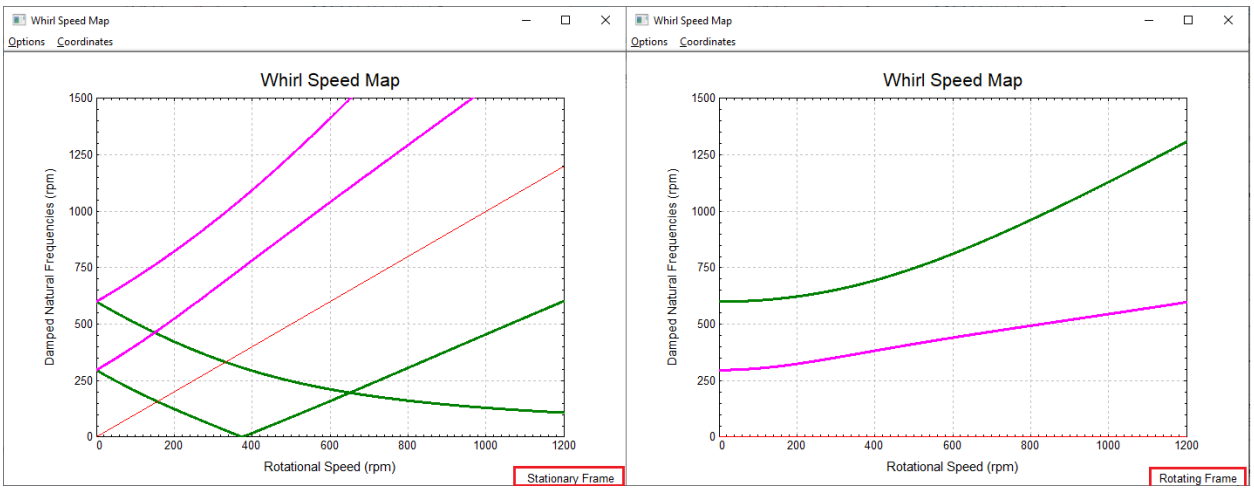

Fig. 2-14 Whirl Speed Map

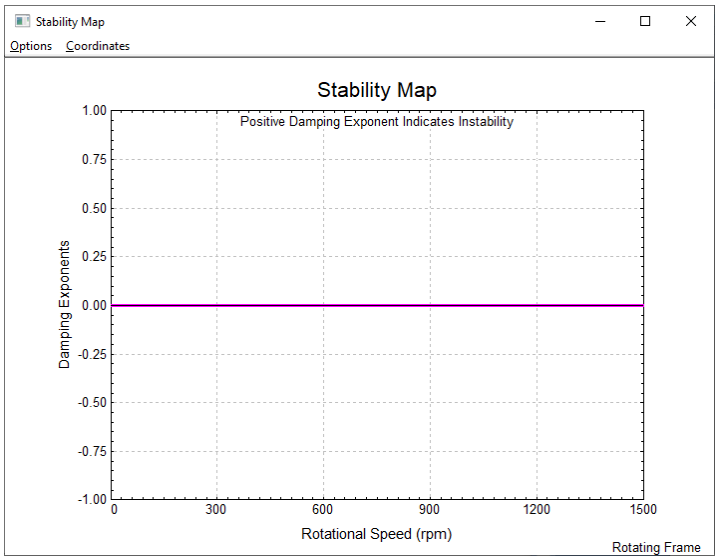

Fig. 2-15 Stability Map

The results for the example 2 are summarized below:

Parameter	Case A	Case B	Case C	Case D	Case E
I_x	0.00444	0.00444	0.00444	0.00444	0.00444
I_y	0.0025	0.0025	0.0025	0.0025	0.0025
I_z	0.001	0.001	0.001	***0.003***	***0.005***
k_x	9.8696	***4.29861***	9.8696	***4.29861***	***4.29861***
k_y	9.8696	9.8696	***4.29861***	9.8696	9.8696
Freq. at zero rpm					
$\omega_{nx} = \sqrt{\frac{k_x}{I_x}}$	450	297	450	297	297
$\omega_{ny} = \sqrt{\frac{k_y}{I_y}}$	600	600	396	600	600
Critical Speeds					
$\Omega_{cr1} = \sqrt{\frac{k_y}{I_x - I_z}}$	511	511	337	789	N/A
$\Omega_{cr2} = \sqrt{\frac{k_x}{I_y - I_z}}$	775	511	775	N/A	N/A
Unstable Region	511 – 775	Stable	337 – 775	789 –	Stable

3. Example 3 – A rigid disk mounted on a flexible rotor

A classical Jeffcott rotor system with a rigid disk located at the center of a flexible shaft, as shown in Fig. 3-1, is considered in this example. The fundamental translational and rotational are decoupled and can be analyzed separately as discussed in Examples 1 and 2. However, we will analyze this system with both translational and rotational motions together as a 4 DOF system here.

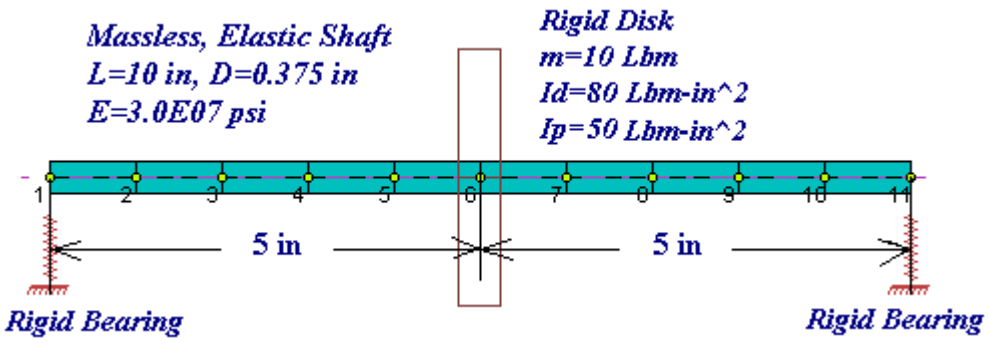

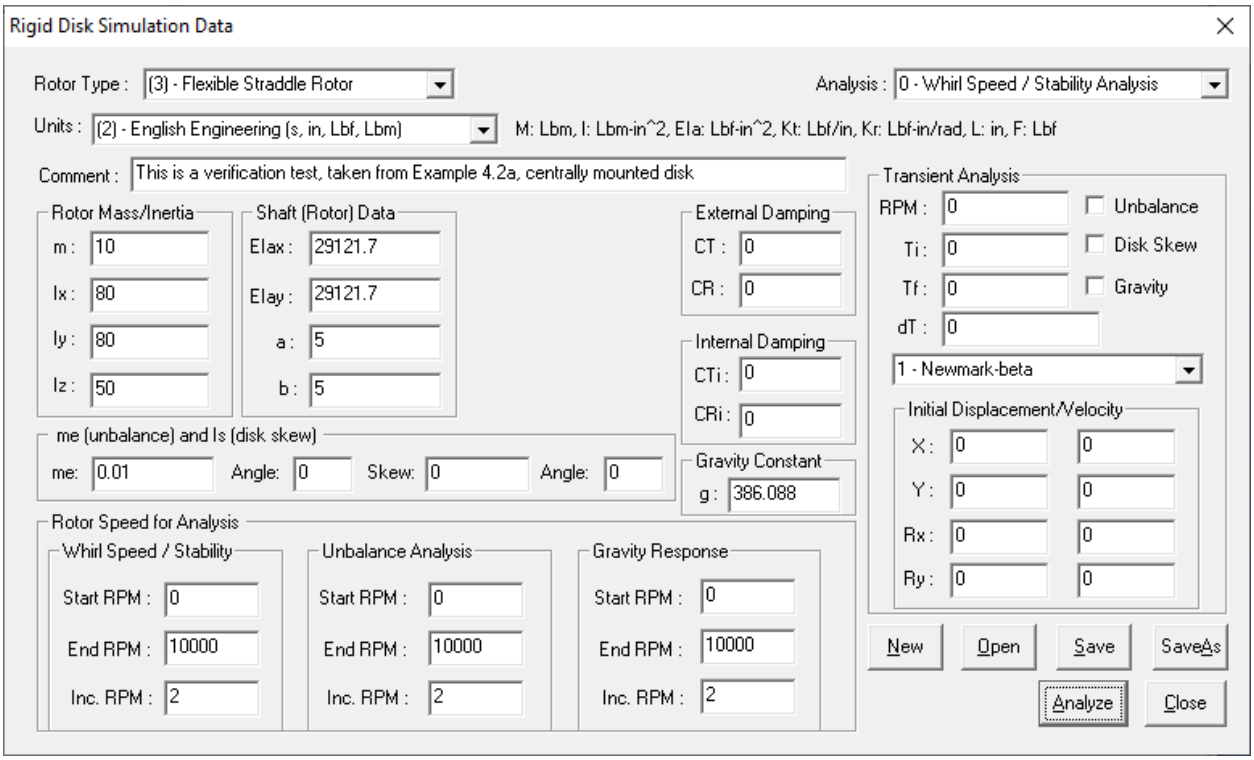

Fig. 3-1 Example 3 – a Jeffcott Rotor

A) Isotropic Rotor

We start this example with the isotropic rotor, which has been analyzed in the fixed coordinate system and presented in book "Introduction of Dynamics of Rotor-Bearing Systems", page 135-142. Here we will analyze the same system using the rotating coordinate system to verify the results. For this symmetric Jeffcott rotor system, the critical speeds can be analytically determined. The whirl speeds at zero speed, and the synchronous forward critical speeds are determined as follows, for comparison purposes:

$$k_T = k_{11} = k_{22} = \frac{48EI}{L^3} = 1397.84\,\text{Lbf/in}$$

$$k_R = k_{33} = k_{44} = \frac{12EI}{L} = 34946\,\text{Lbf - in/rad}$$

$$k_{14} = k_{41} = k_{23} = k_{32} = 0$$

For translational motion, the natural frequencies are the critical speeds since the natural frequencies are independent on the speed in this case:

$$\Omega_{cr,1b,1f} = \omega_x = \omega_y = \sqrt{\frac{k_T}{m}} = \sqrt{\frac{1397.84}{10/386.088}} = 232.3\,\text{rad/sec} = 2218\,\text{rpm}$$

For rotational motion, the natural frequencies at zero speed are:

$$\omega_{\theta x} = \omega_{\theta y} = \sqrt{\frac{k_R}{I_d}} = \sqrt{\frac{34946}{80/386.088}} = 410.7\,\text{rad/sec} = 3922\,\text{rpm}$$

The forward synchronous critical speed due to purely rotational motion is:

$$\Omega_{cr,2f} = \sqrt{\frac{k_R}{I_d - I_p}} = \sqrt{\frac{34946}{(80-50)/386.088}} = 670.6\,\text{rad/sec} = 6404\,\text{rpm}$$

The backward synchronous critical speed due to purely rotational motion is:

$$\Omega_{cr,2b} = \sqrt{\frac{k_R}{I_d + I_p}} = \sqrt{\frac{34946}{(80+50)/386.088}} = 322.2\,\text{rad/sec} = 3076\,\text{rpm}$$

Fig. 3-2 shows the Whirl Speed Map in both fixed coordinate system and rotating coordinate system. One advantage of using the rotating frame is the determination of the synchronous forward critical speeds. When the natural frequencies are zero in the rotating frame, the corresponding rotor speeds are the synchronous forward critical speeds.

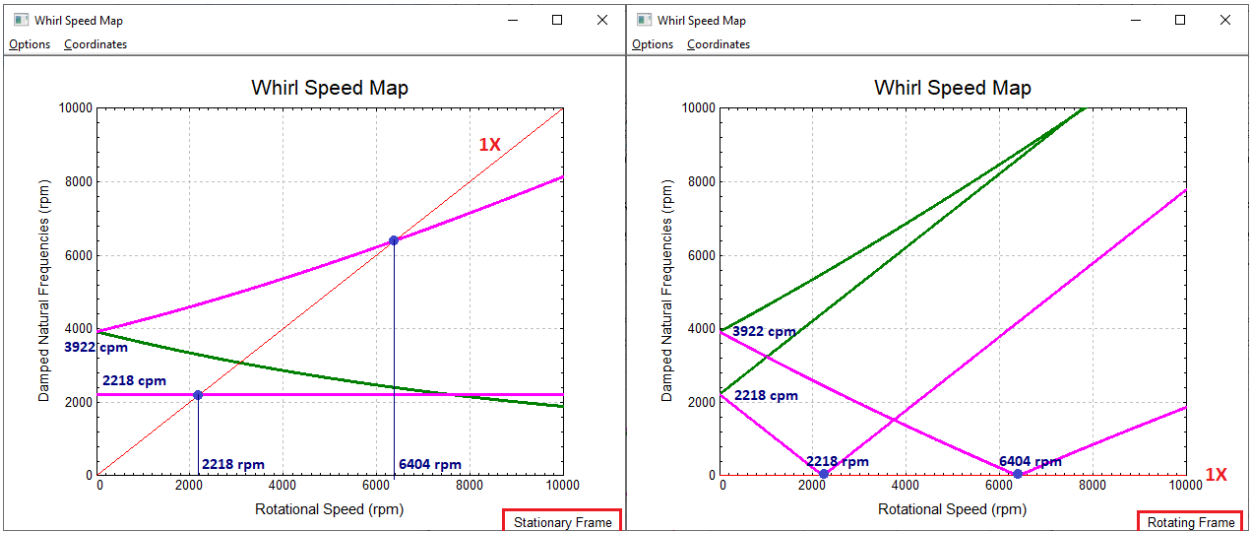

Fig. 3-2 Example 3A1 – isotropic case with EI = 29121.7

The mode shapes for the two critical speeds are shown in Fig. 3-3. It shows that the translational and rotational motions are decoupled for this centrally mounted disk system. The damping exponents are zero and the system is stable for all rotor speeds in this isotropic case and not shown here.

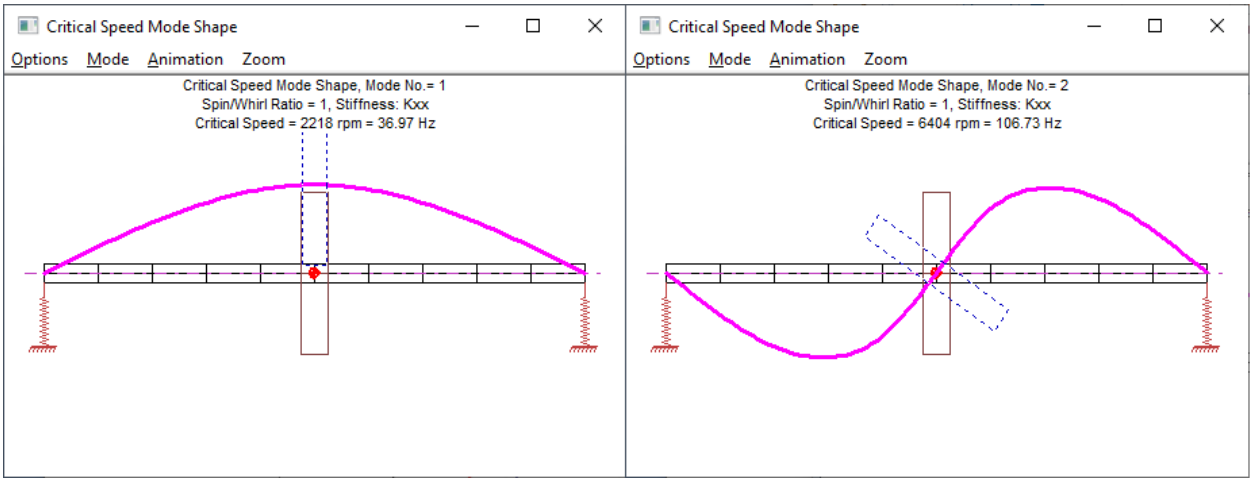

Fig. 3-3 Example 3A1 – Mode Shapes for the critical speeds with EI = 29121.7

Next, change the shaft diameter from 0.375 to 0.31769 and the corresponding EI from 29121.7 to 15000. Following the discussion before, the natural frequencies at zero speed are1592 and 2815 cpm, and the two synchronous forward critical speeds are 1592 and 4596 rpm. The associated whirl speed map is shown in Fig. 3.4.

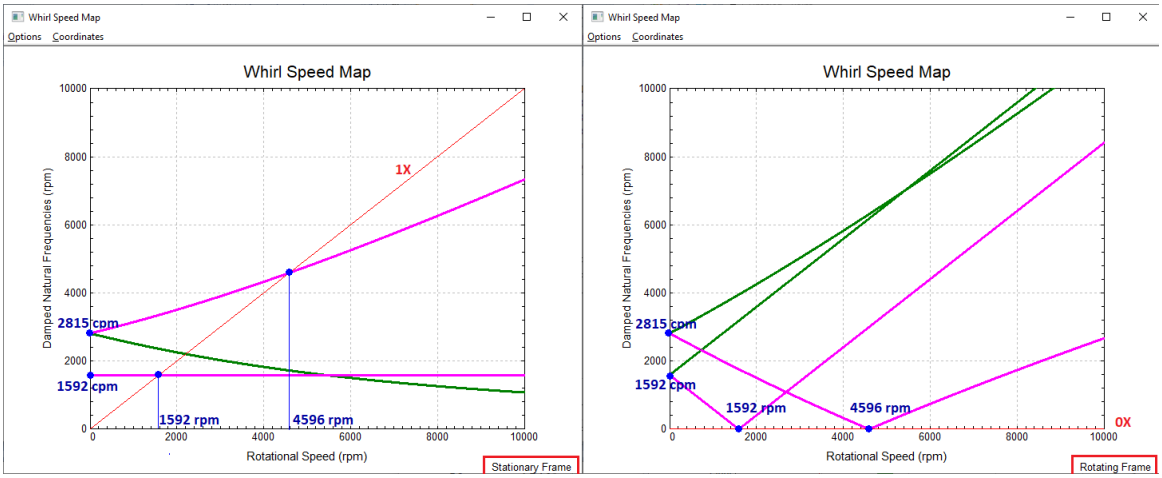

Fig. 3-4 Example 3A2 – isotropic case with EI = 15000

Again, this isotropic system is stable and the stability map is not shown here. The related inputs and results are summarized for the above two isotropic cases:

Case	$EI_x = EI_y$ = 29121.7	$EI_x = EI_y$ = 15000
Frequency (cpm) at zero rpm		
ω_1 (Translational)	2218	1592
ω_2 (Rotational)	3922	2815
Unbalance Critical Speeds, rpm		
Ω_{cr1}	2218	1592
Ω_{cr2}	6404	4596
Stability	Stable	Stable

B) Anisotropic Rotor

Now, let us consider the shaft is anisotropic with EI_x = 15000 and EI_y = 29121.7. The whirl speed map is shown in Fig. 3-5. The critical speeds due to unbalance are the intersection points between the synchronous whirl line (1X) and the system forward natural frequencies in the fixed coordinate system, but 0X in the rotating coordinate system. The critical speeds due to gravity are the intersection points between 2X whirl line and the system forward natural frequencies in the fixed coordinate system, but 1X in the rotating coordinate system. The natural frequencies at zero rpm for this anisotropic system are: 1592, 2218, 2815, 3922 cpm. The first two modes are translational motion and 3rd and 4th are the rotational motion. The unbalance critical speeds are 1592, 2218 and 4596, 6404 rpm. Again, the first two critical speeds are translational motion and 3rd and 4th are rotational motion. The whirl frequencies between two translational critical speeds (1592 – 2218) and two rotational critical speeds (4596 – 6404) are zero in the rotating frame and synchronous with the rotor speed in the fixed frame.

The gravity critical speeds can also be determined from the whirl speed map and they are 914 (Translation) and 1950 (Rotation) rpm.

The stability map, Fig 3-6, shows that there are two unstable regions where the damping exponents are greater than zero. The first region is between two translational synchronous critical speeds and the second region is between two rotational synchronous critical speeds. The severity of the instability depends on the separation margin of the associated two critical speeds. In this case, the separation between two rotational critical speeds is larger than the separation between two translational critical speeds, the damping exponents in this region is higher.

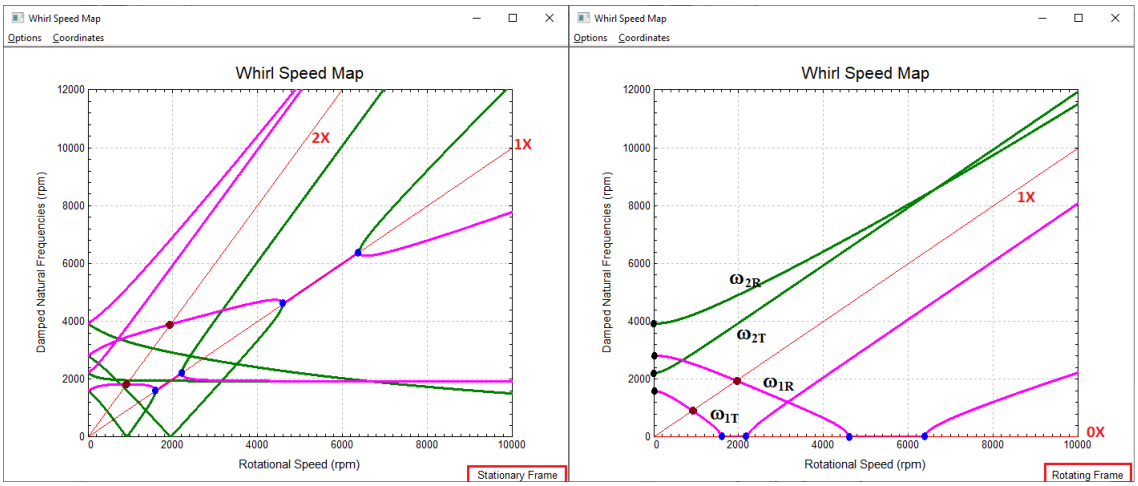

Fig. 3-5 Example 3B – Whirl Speed Map with EI_x = 15000 and EI_y = 29121.7

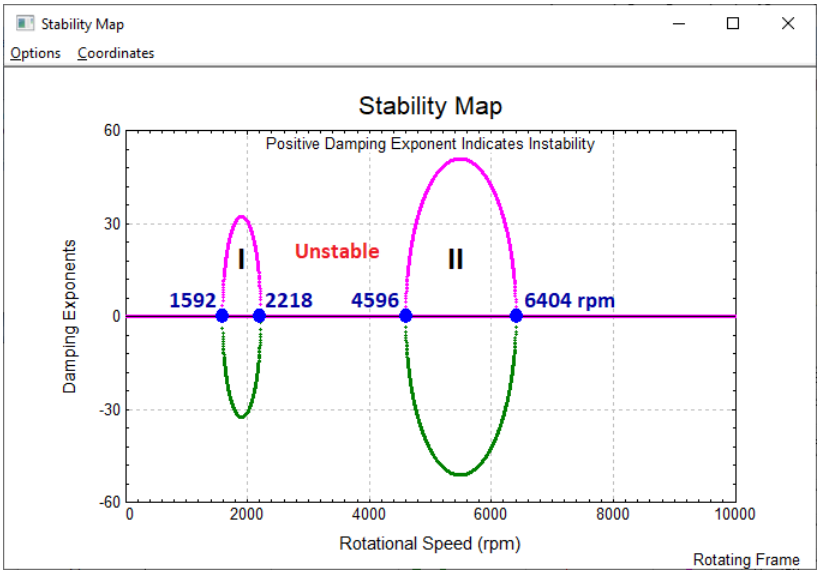

Fig. 3-6 Example 3B – Stability Map with EI_x = 15000 and EI_y = 29121.7

Fig. 3-7 shows the steady state unbalance response. Again, in order to excite both translational critical speeds, a non-zero unbalance phase angle (45°) is applied. Since the translational and rotational motions are decoupled in this system, the response due to the rotational critical speeds would not be observed in the translational displacement. The response in the rotating frame also shows that the critical speeds 1592 and 2218 rpm are associated with the y and x directions, respectively. But both critical speeds are shown in the fixed coordinate system.

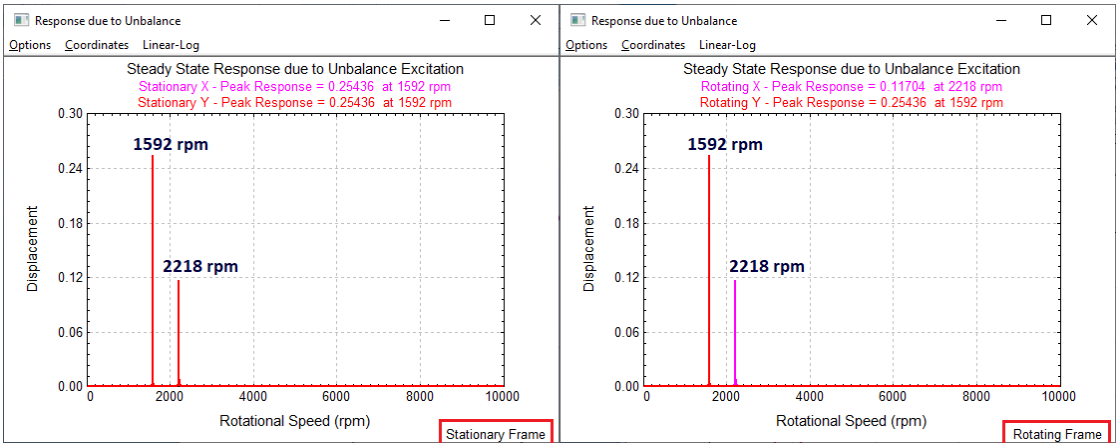

Fig. 3-7 Example 3B – Steady State Unbalance Response with EI_x = 15000 and EI_y = 29121.7

Fig. 3-8 shows the harmonic response due to gravity excitation. The gravity critical speed occurs at 914 rpm which can be obtained from the whirl speed map or estimated using Eq. (1-26). Similar to the unbalance response, the response due to rotational critical speed would not be observed in the translational displacement due to the decoupling of the two motions.

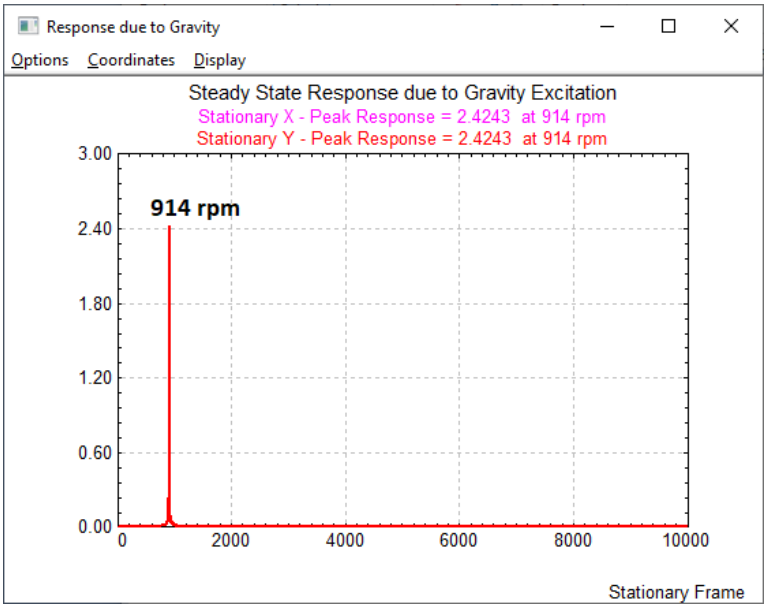

Fig. 3-8 Example 3B – Steady State Gravity Response with EI_x = 15000 and EI_y = 29121.7

C) Anisotropic Rotor and an off-centrally mounted disk

In this example, in addition to the shaft stiffness anisotropy, the disk is mounted off-center with a=3 inches and b=7 inches. The translational and rotational motions are coupled now and cannot be analyzed separately as previous cases. For an isotropic shaft, the forward synchronous critical speeds are calculated for reference. The isotropic system with EI =29,121.7 was analyzed and presented in book "Introduction of Dynamics of Rotor-Bearing Systems", page 142-147.

Critical Speed (rpm)	EI = 15,000	EI =29121.7
1st Critical Speed	1787	2490
2nd Critical Speed	5318	7410

The first critical speed is predominately a translational mode and the second critical speed is predominately a rotational mode. The translational and rotational motions are coupled by the gyroscopic effect. The related parameters are shown below.

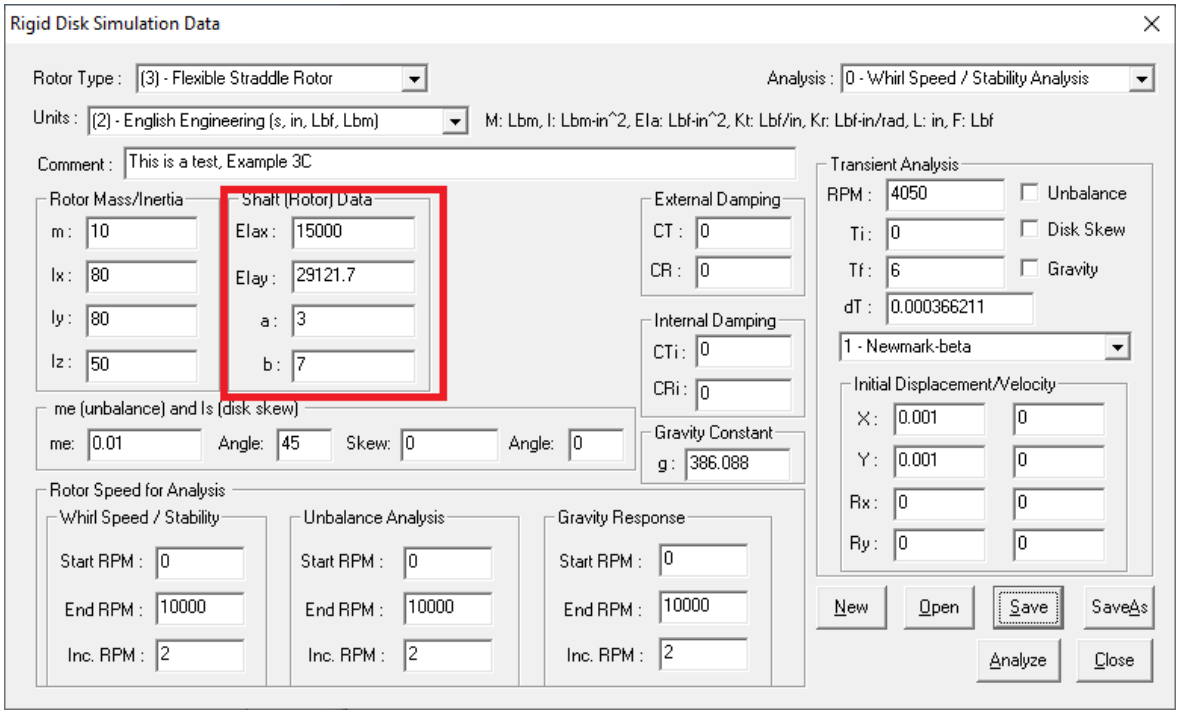

Fig. 3-9 Example 3C

The whirl speed maps in both stationary and rotating frames are shown in Fig. 3-10. As expected, there are two unstable regions (I and II) between critical speeds, 1787–2490 and 5318–7410 rpm. However, there is an additional unstable region (III) due to the coupling of the translational and rotational motions between 3656–3876 rpm where the two forward frequencies merge together and remain together in this region. The whirl frequency for the

unstable regions (I and II) between critical speeds is a single frequency equal to the rotor speed. The whirl frequency in the region (III) is not the rotor speed, but a combination of two frequencies. The stability map in Fig. 3-11 shows these three unstable regions. The range for the region III depends on the severity of the asymmetry.

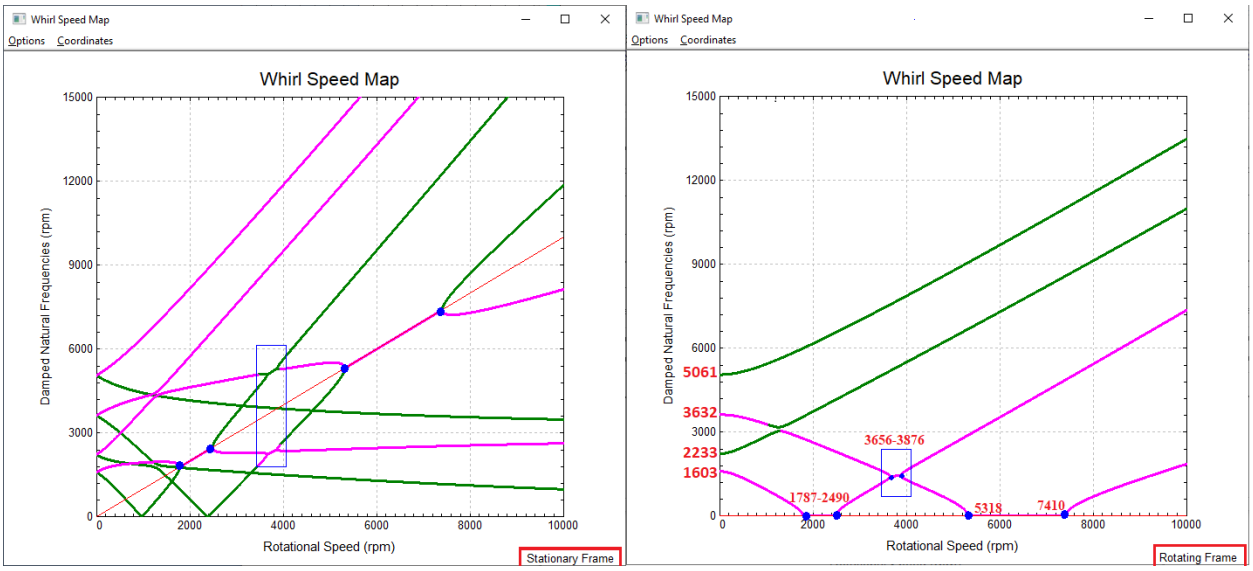

Fig. 3-10 Example 3C – Whirl Speed Map

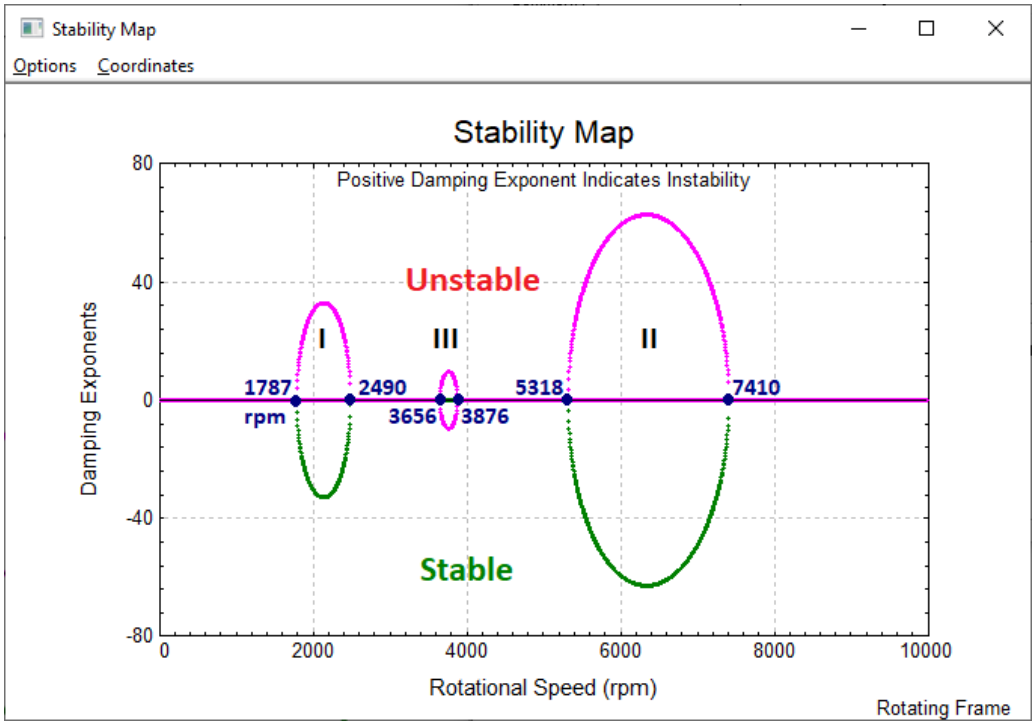

Fig. 3-11 Example 3C – Stability Map

Time transient responses at three speeds in the unstable regions are shown below. It shows that the whirl frequency in the unstable regions (I & II) between two anisotropic critical speeds is a single frequency same as the rotor speed. However, the whirl frequencies in the region III are not a single frequency.

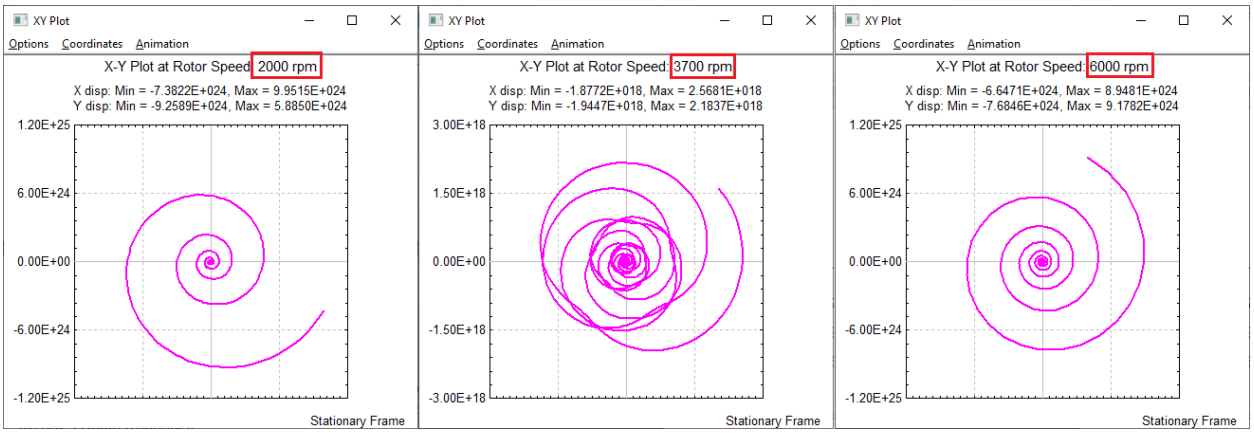

Fig. 3-12 Example 3C – Time Transient Responses at 2000, 3700, and 6000 rpm

The steady state response due to unbalance is shown in Fig. 3-13. It shows there are four peaks at 1787, 2490, 5318, and 7410 rpm in both X and Y directions in the stationary frame. In the rotating frame, the peaks at 1787 and 5318 rpm are shown in the y direction only and the peaks at 2490 and 7410 rpm are shown in the x direction only. Note that the unbalance response analysis is a linear analysis. In the unstable regions as described before, the linear theory is not applicable.

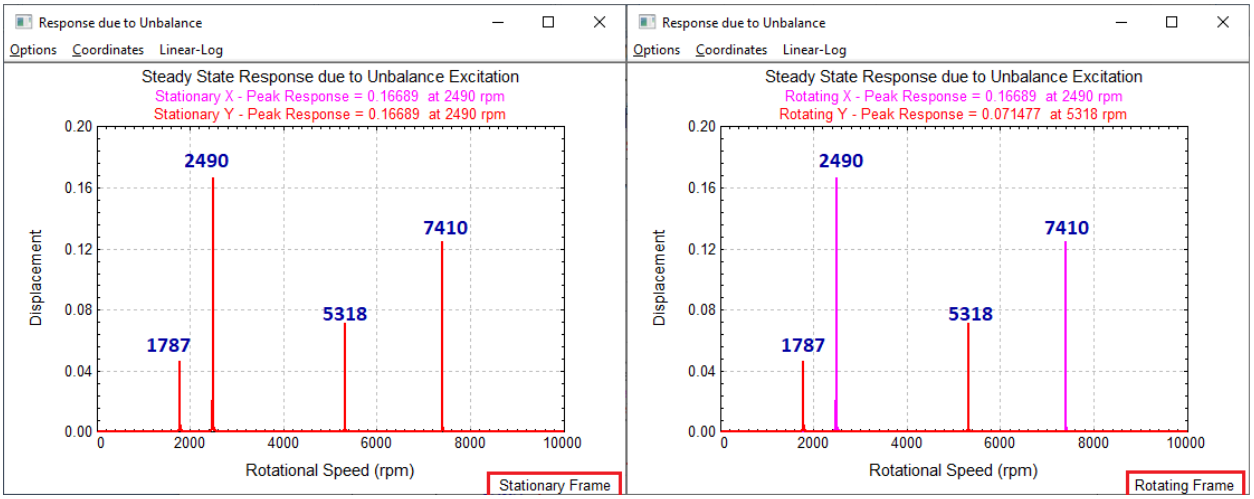

Fig. 3-13 Example 3C – Steady State Response due to Unbalance

The steady state response due to the gravity excitation is shown in Fig. 3-14. It shows that there are two peaks at 973 and 2381 rpm. The motion at the first peak of 973 rpm is predominately by the translation mode and has much higher translational displacement. The second peak at 2381 rpm is predominately by the rotational motion and has much lower response. Again, this gravity response analysis is also a linear analysis. Linear theory is not applicable in the unstable regions. Fig. 3-15 shows the gravity response orbit at 973 rpm.

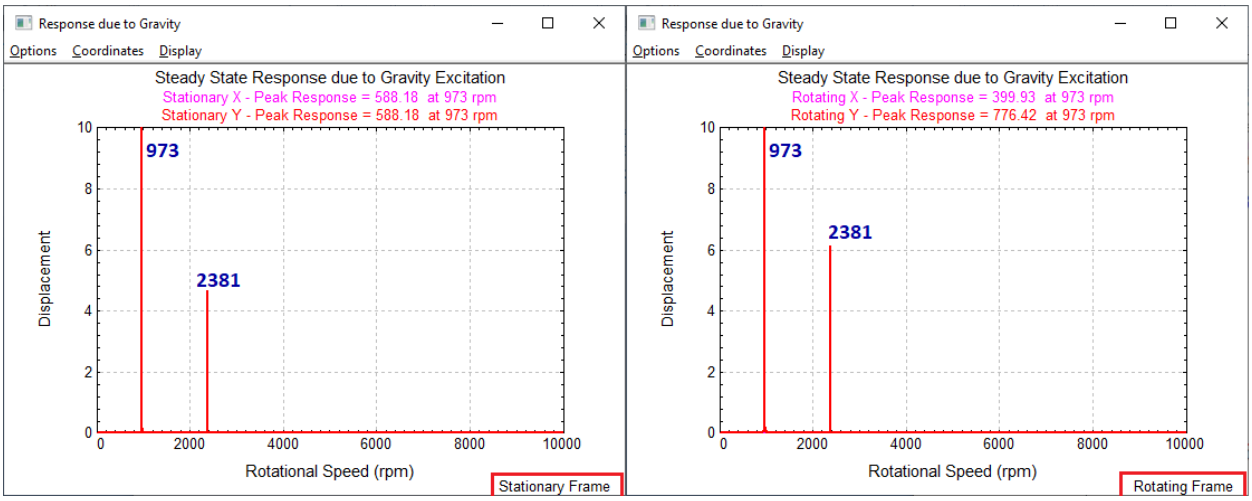

Fig. 3-14 Example 3C – Steady State Response due to Gravity

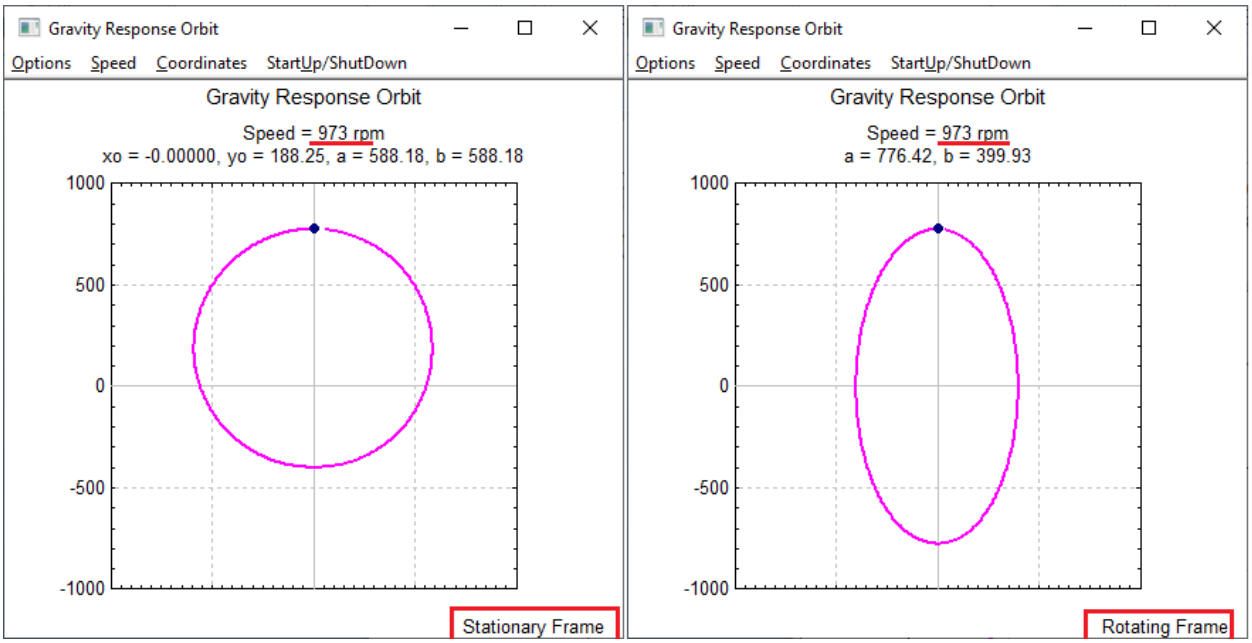

Fig. 3-15 Example 3C – Steady State Response at 973 rpm due to Gravity

4. Example 4 – A single overhung Rotor

A single overhung rotor, a disk mounted outside the bearing span on a flexible and massless shaft, is used in this example. The asymmetry occurs in the disk inertia.

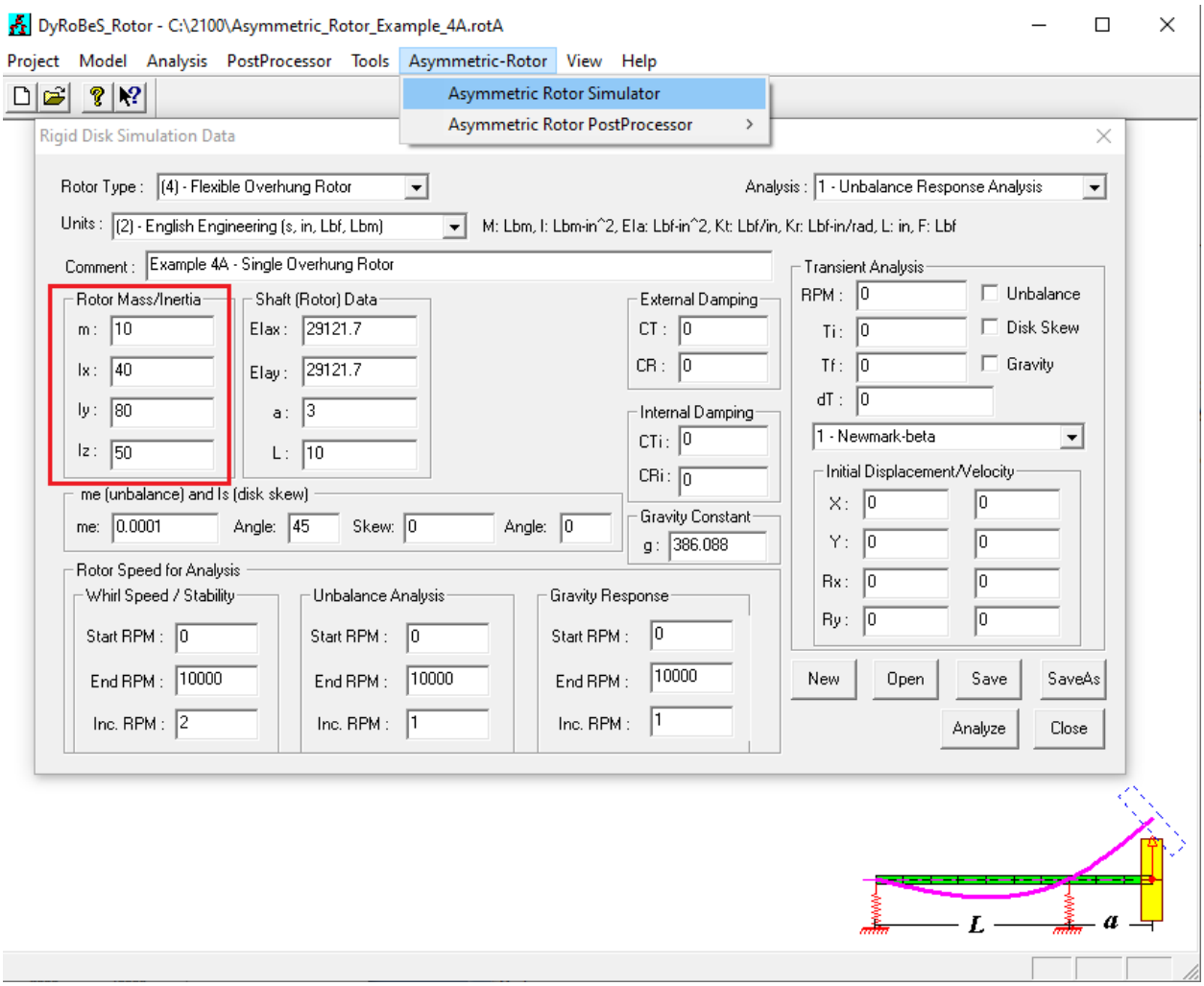

Fig. 4-1 Example 4A

A) I_x=40, I_y =80, and I_z = 50

The inertias were chosen, I_x=40, I_y =80, and I_z = 50 (polar inertia), such that $I_x < I_z$ and $I_y > I_z$. The critical speeds for the isotropic rotor with diametral moment of inertia of 40 and 80 can be calculated and listed below for reference. The first mode is mainly translational mode and the second mode is predominated by the rotational motion. When the diametral moment of inertia is less than the polar moment of inertia, the forward synchronous critical speed for the rotational motion cannot be found (or approach to infinity). The mode shapes for these isotropic rotors are shown in Fig. 4-1 and Fig. 4-2.

Critical Speed (rpm)	$I_x = I_y = 80$	$I_x = I_y = 40$
1st Critical Speed	1353	1743
2nd Critical Speed	7219	Infinity

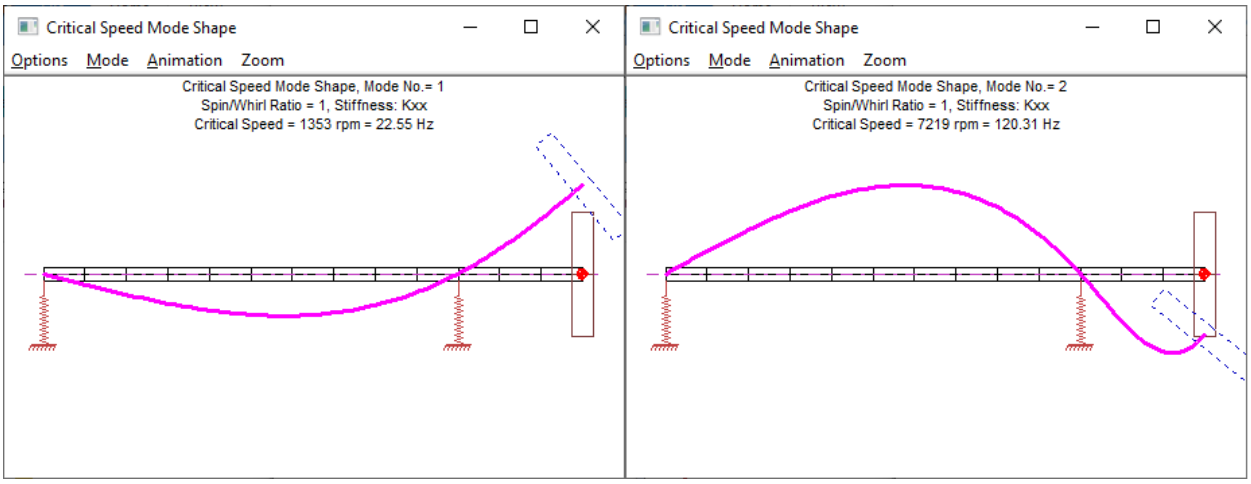

Fig. 4-2 Critical Speeds with $I_x = I_y = 80$ and $I_z = 50$

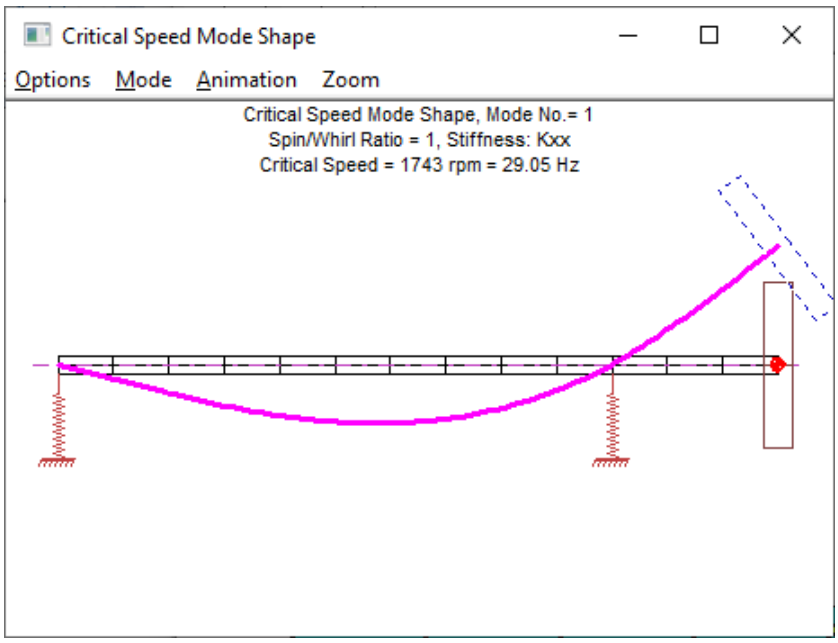

Fig. 4-3 Critical Speed with $I_x = I_y = 40$ and $I_z = 50$

The whirl speed map and stability map for the anisotropic rotor are shown in Fig. 4-4 and Fig. 4-5. The translational and rotational motions are coupled in this example. There are three unstable regions. The regions I and II are between critical speeds (1353-1743, and 7219-infinity), and region III (4263-5758 rpm) falls between two unstable regions. Since the second

critical speed does not exist for the I_x = I_y= 40, once the speed exceeds 7219 rpm, the system becomes unstable.

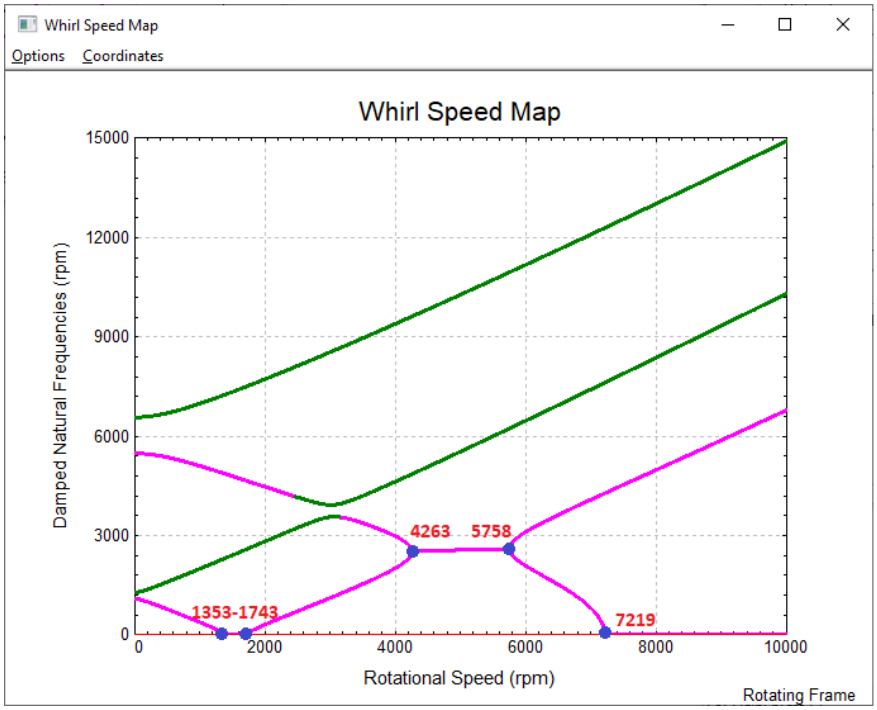

Fig. 4-4 Example 4A – Whirl Speed Map

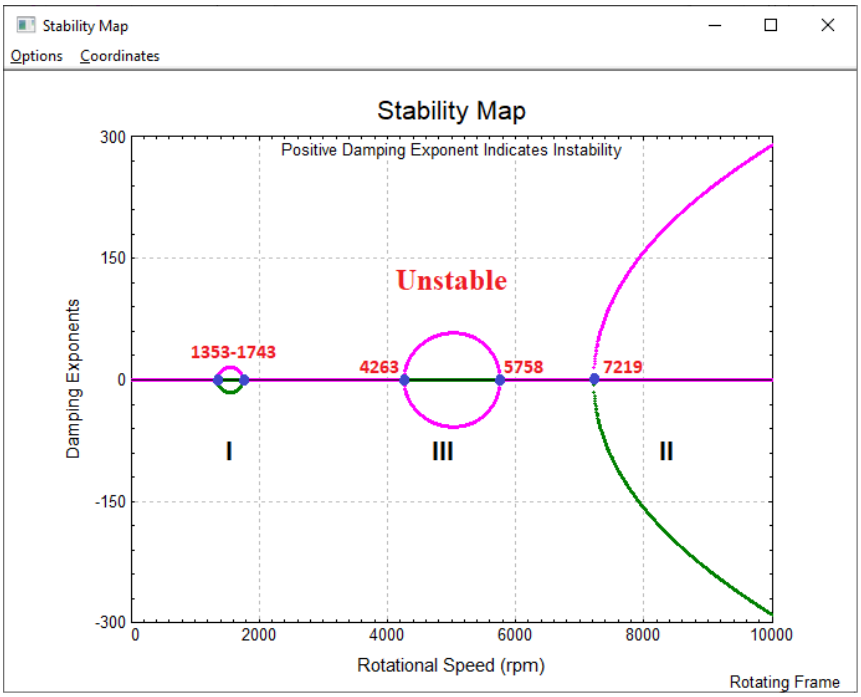

Fig. 4-5 Example 4A – Stability Map

Fig. 4-6 shows the steady state unbalance responses in both stationary and rotating frames. There are three apparent peaks at three critical speeds which are in agreement with the results from the whirl speed map. Also, the peaks at 1353 and 7219 rpm occur in the y axis and the peak at 1743 rpm occurs in the x axis in the rotating frame.

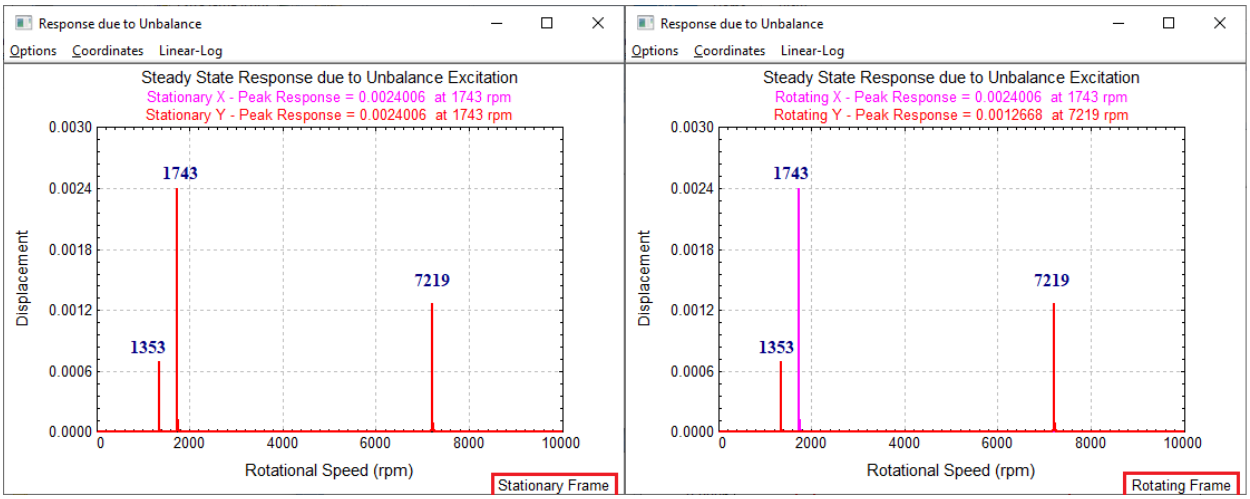

Fig. 4-6 Example 4A – Steady State Unbalance Response

Fig. 4-7 shows the steady state harmonic responses due to gravity in both stationary and rotating frame. Although there is a peak in the stationary frame at about half of the first critical speed, the amplitude is essentially zero. The harmonic response amplitude in the rotating frame is a constant. Fig. 4-8 shows the static eccentricity position (x_o, y_o) due to gravity. It shows the static equilibrium position does not change with the rotor speed and stays at the same position. As shown, the gravity excitation is present only when the asymmetry occurs in the stiffness, not in the inertia.

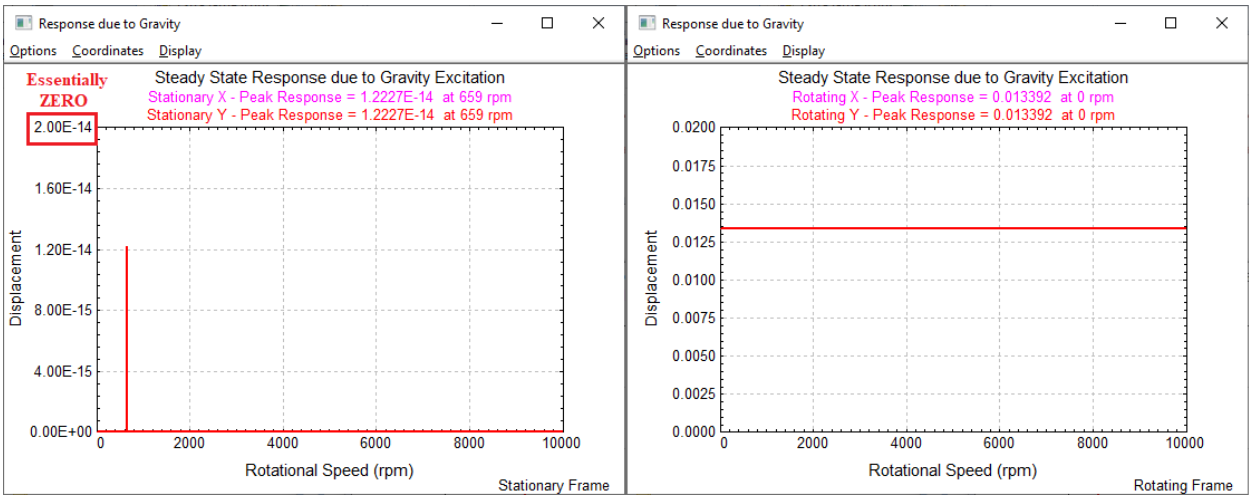

Fig. 4-7 Example 4A – Steady State Response due to Gravity

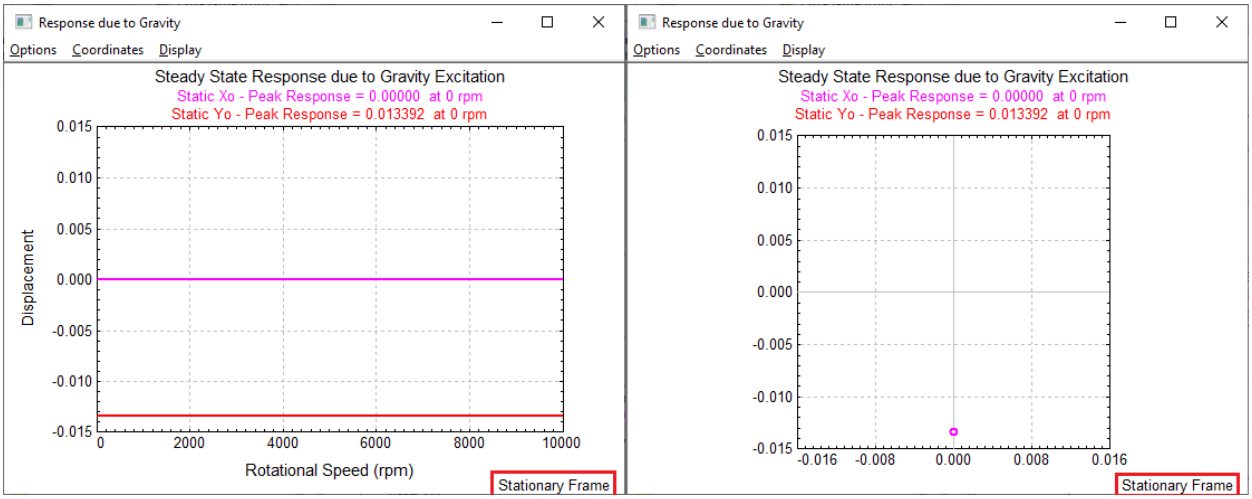

Fig. 4-8 Example 4A – Steady State Response (x_o,y_o) due to Gravity

The static eccentricity, y_o, can be verified using the following static deflection equation for an overhung load on a simply supported beam:

$$y_o = -\frac{Fa^2}{3EI}(L+a))$$

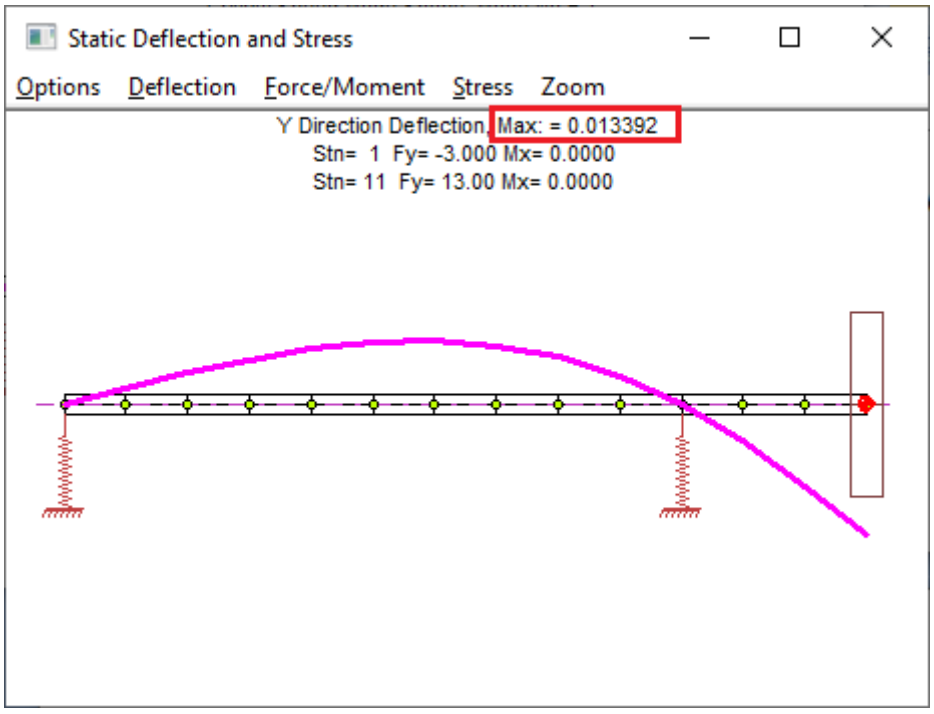

Fig. 4-9 Example 4A – Static Deflection due to Gravity

B) I_x=40, I_y =80, and I_z = 100

Next, let us increase the polar moment of inertia from 50 to 100, such that $I_z > I_y > I_x$. The rotational synchronous forward critical speed does not exist when the polar moment inertia is greater than the diametral moment of inertia. Therefore, there will be only one synchronous forward critical speed (translational motion) for each isotropic rotor as listed below:

Critical Speed (rpm)	$I_x = I_y = 80$, $I_z = 100$	$I_x = I_y = 40$, $I_z = 100$
1st Critical Speed	1884	2584
2nd Critical Speed	Infinity	Infinity

The whirl speed map and stability for this anisotropic rotor are shown in Fig. 4-10 and Fig. 4-11. In this case, there is only one unstable region. Again, it is between two synchronous forward critical speeds. Unstable regions II and III do not exist. Fig. 4-12 shows the steady state unbalance response, two peaks are at the critical speeds. The peak at 1884 rpm occurs in the y axis and the peak at 2584 rpm occurs in the x axis in the rotating frame, respectively.

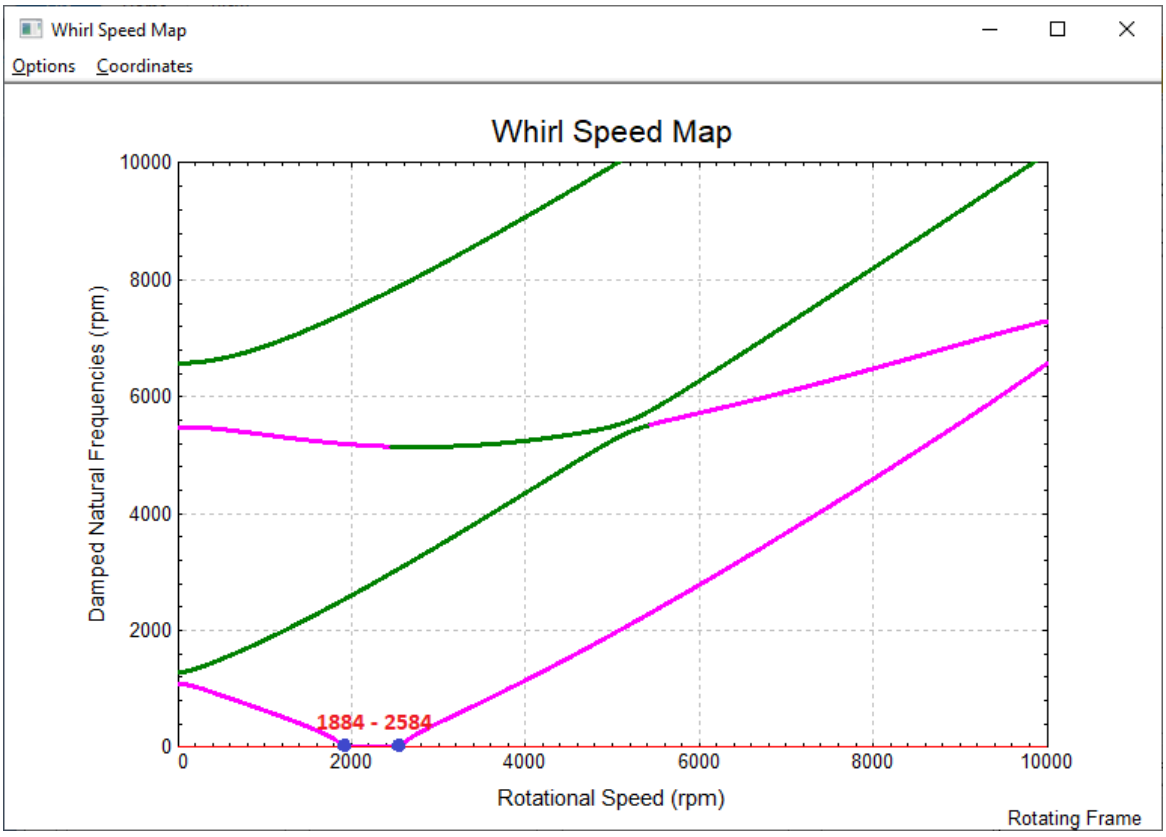

Fig. 4-10 Example 4B – Whirl Speed Map

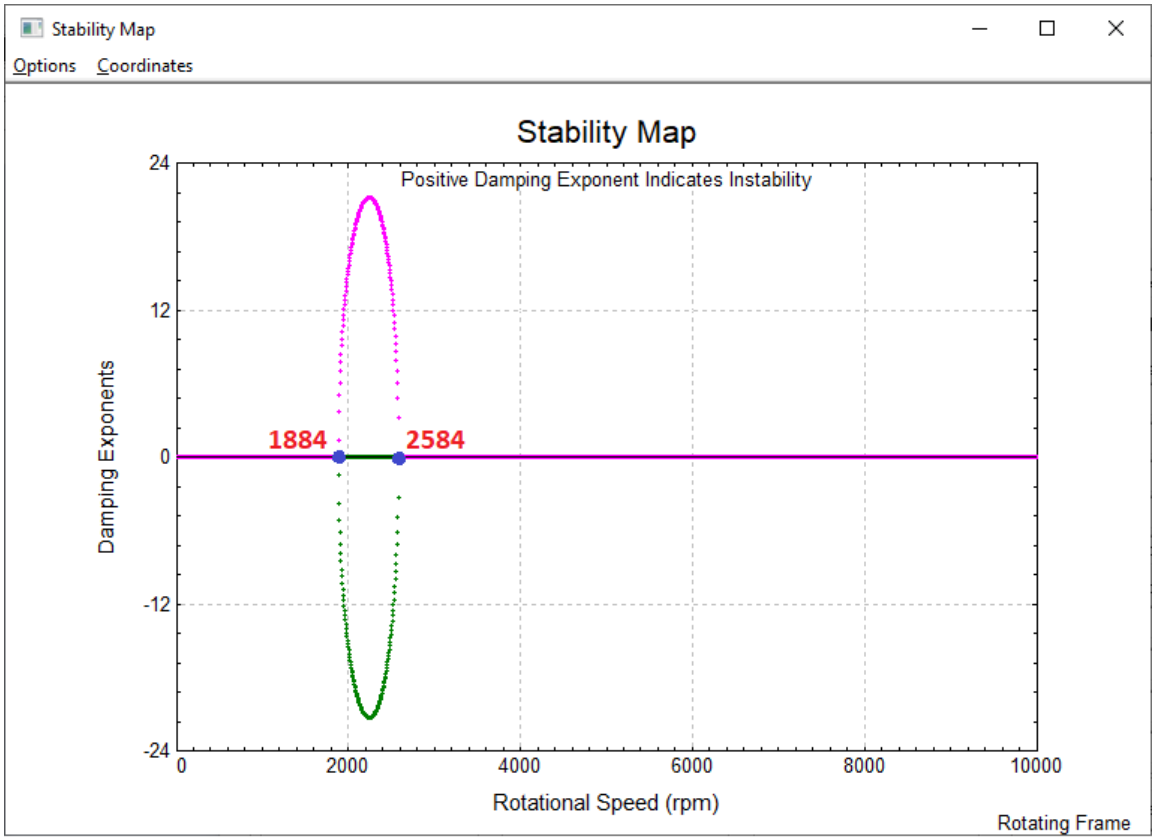

Fig. 4-11 Example 4B – Stability Map

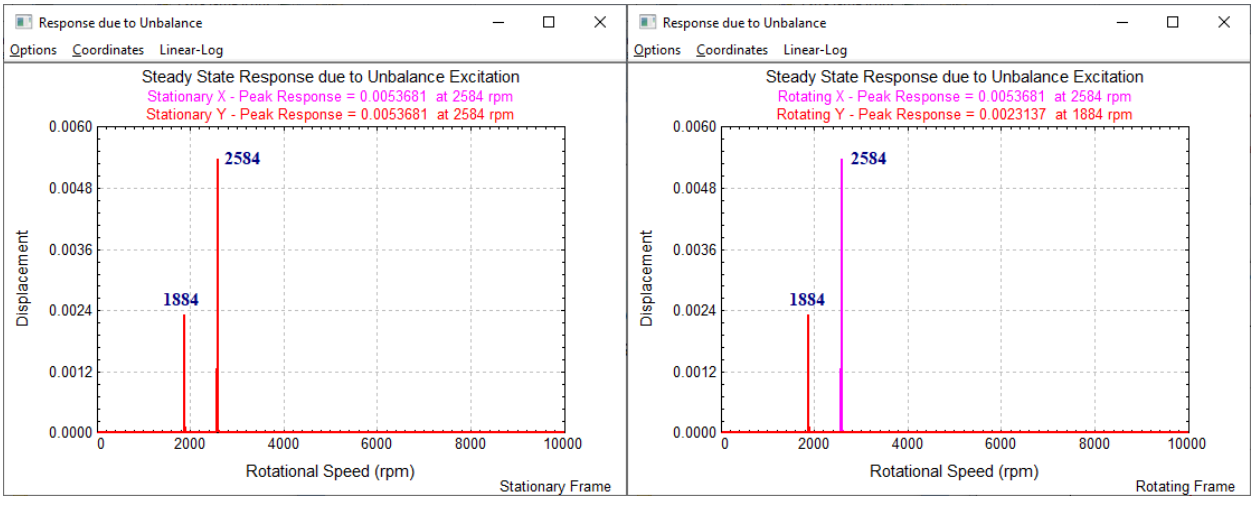

Fig. 4-12 Example 4B – Steady State Unbalance Response

C) I_x=40, I_y =80, I_z = 50 and EI_x=15000, EI_y=29121.7

Let us consider another case with shaft bending stiffness asymmetry, I_x=40, I_y =80, I_z = 50 and EI_x=15000, EI_y=29121.7. The whirl speed map is shown in Fig. 4-13. It shows that there are three synchronous forward critical speeds at 971, 1743, and 5181 rpm. And there is a range between 3639 and 4299 rpm where the two frequencies merge into one. As shown in the previous examples, this range also shows the instability. Fig. 4-14 shows the stability map. Again, there are three unstable regions as expected. The critical speeds due to gravity excitation are at 544 and 2827 rpm that are 1X in the rotating frame or 2X in the stationary frame.

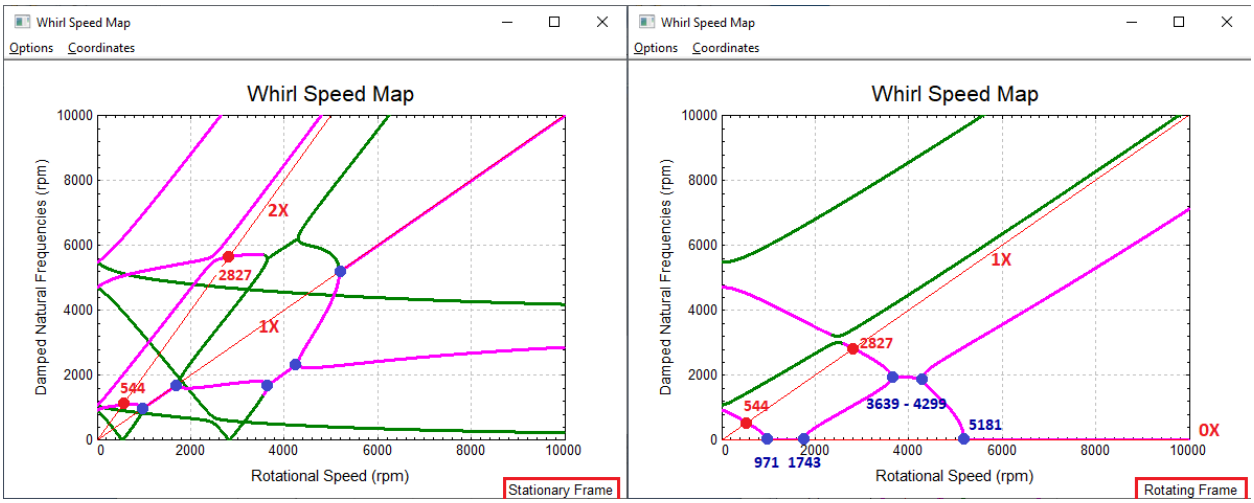

Fig. 4-13 Example 4C – Whirl Speed Map

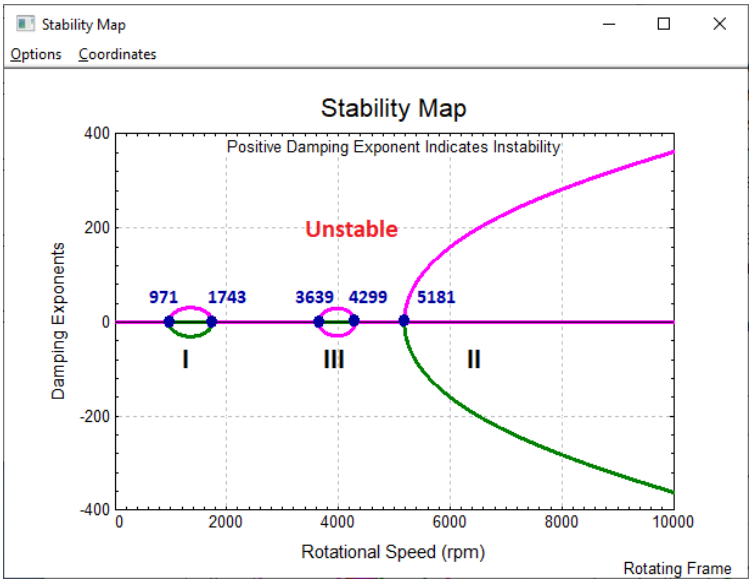

Fig. 4-14 Example 4C – Stability Map

Fig. 4-15 shows the steady state unbalance response. There are three peaks occurring at the critical speeds (971, 1743, and 5181 rpm). Since the steady state unbalance response is harmonic and the displacement orbits are circular in the stationary frame, three critical speeds are observed in both X and Y directions. The response is constant in the rotating frame, critical speeds 971 and 5181 rpm are observed in the y axis and 1743 rpm occurs at the x axis.

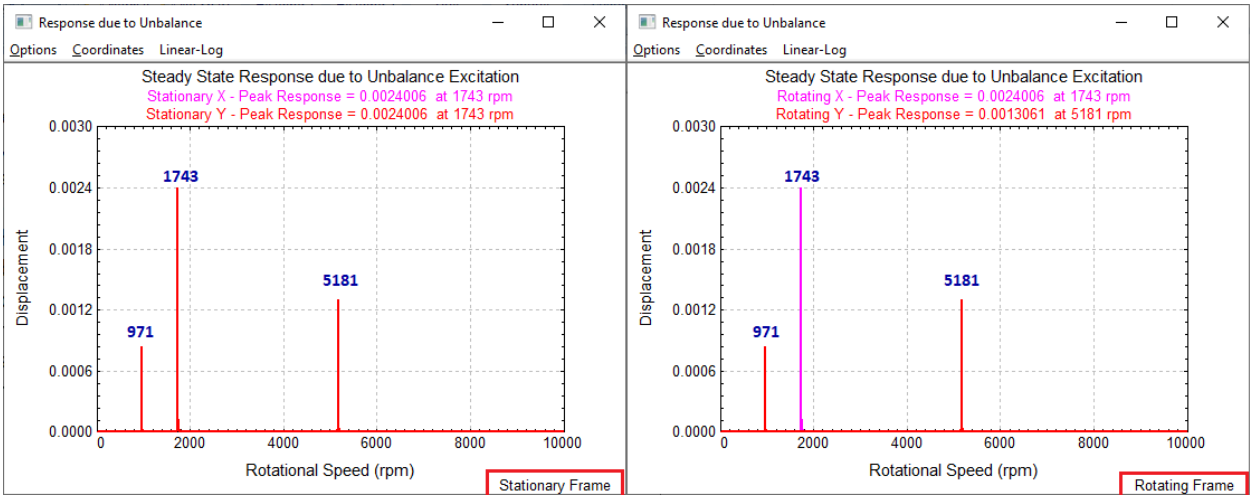

Fig. 4-15 Example 4C – Steady State Unbalance Response

Since asymmetry is present in the shaft stiffness, the harmonic response due to gravity is shown in Fig. 4-16. Interestingly, there are only two peaks at 544 and 2827 rpm. The first peak at 544 rpm is 56% of the first unbalance critical speed (971 rpm) which is the intersection between the first forward natural frequency and the gravity excitation line. The second peak at 2827 rpm is 55% of the third unbalance critical speed (5181 rpm) which is the intersection between the second forward natural frequency and the gravity excitation line.

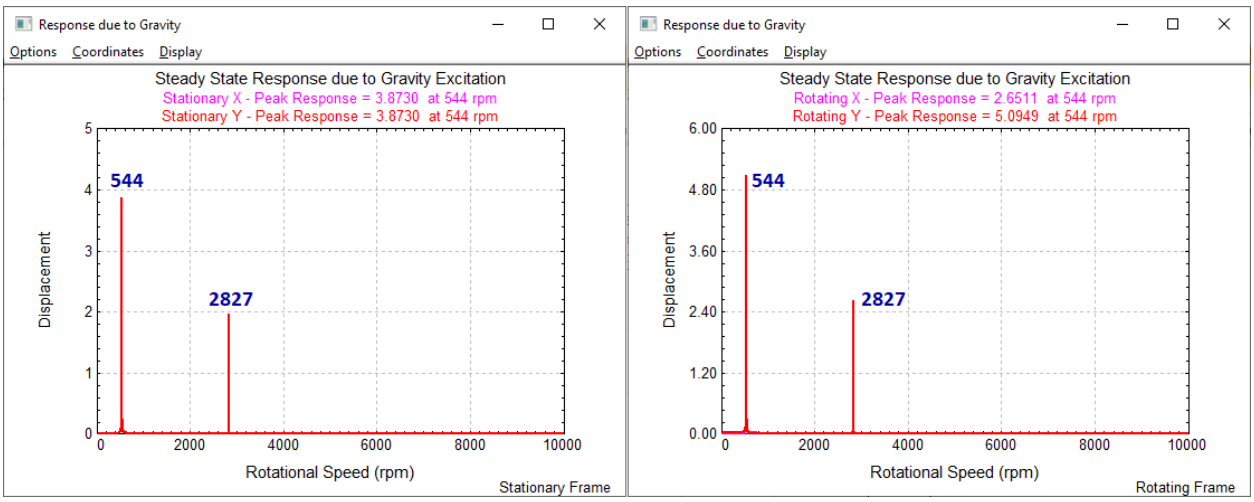

Fig. 4-16 Example 4C – Steady State Response due to Gravity

Fig. 4-17 shows the static eccentricity (equilibrium position) in the stationary frame. Note that the y_o moves along the vertical line (gravity) and the x_o is always zero for an undamped system. y_o starts from a very small negative value in the gravity direction, then moves vertically down even further until right before the gravity critical speed. The y_o changes sign when going through the gravity critical speeds. Figure 4-18 shows the responses due to gravity before and after gravity critical speeds at 543, 544, 2827, and 2828 rpm.

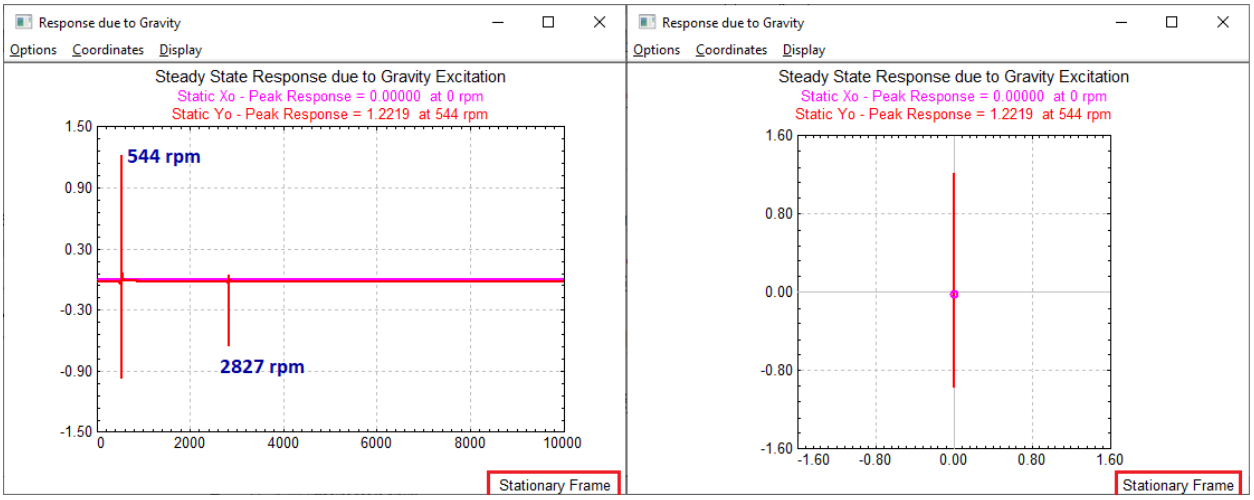

Fig. 4-17 – Static Eccentricity due to Gravity Excitation

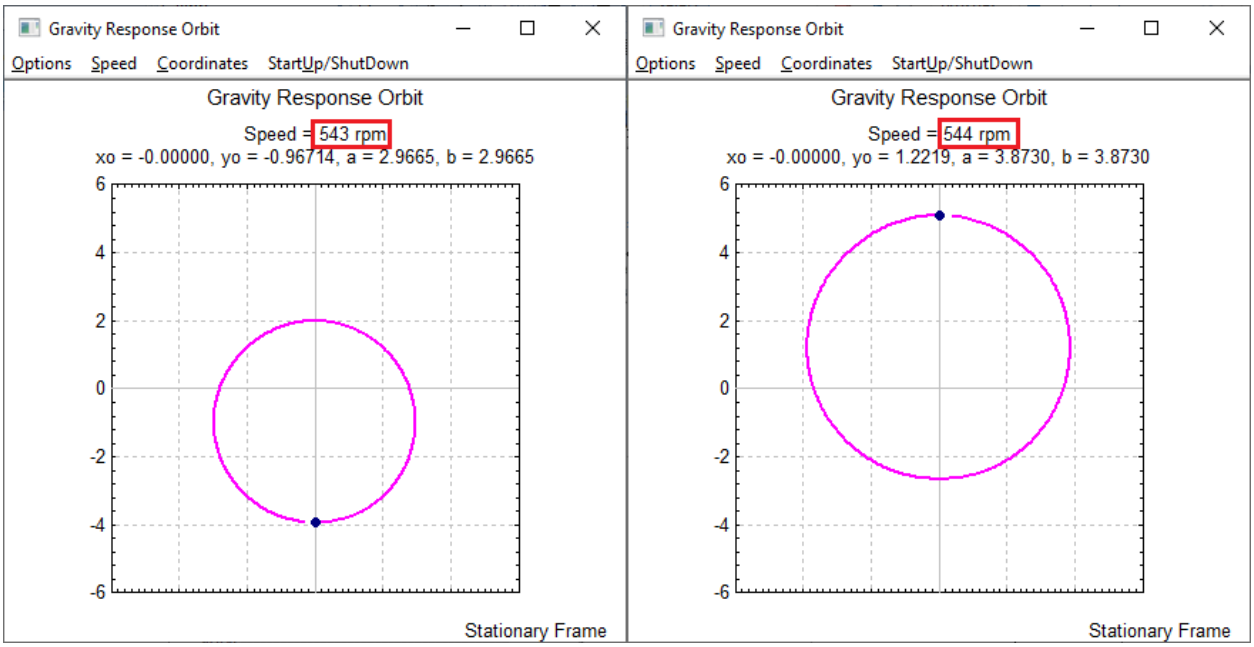

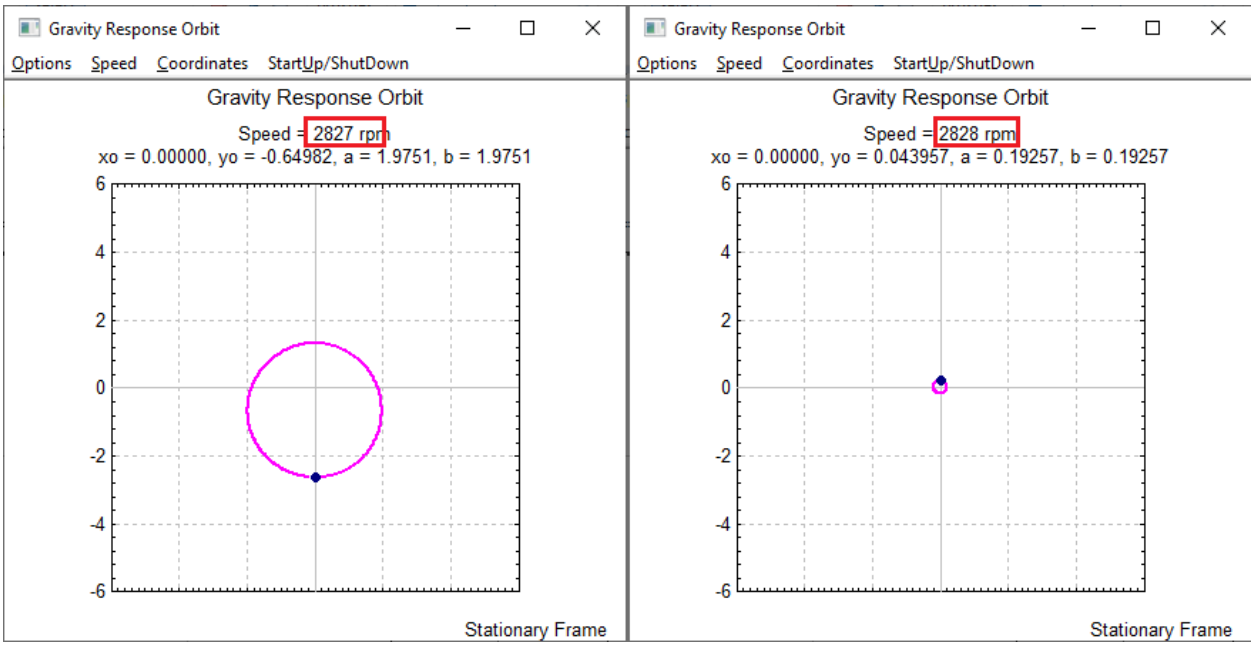

Fig. 4-18 – Responses due to Gravity Excitation before and after gravity critical speeds

5. Example 5 – An anisotropic rigid rotor mounted on two isotropic bearings

This example is a rigid rotor mounted on two isotropic bearings. The center of mass is within the bearing span. The isotropic rotor has been analyzed in details in book "Introduction to the Dynamics of Rotor-Bearing Systems", page 125-131, and not repeated here. The inertia I_x has been changed from 1.23702 (477.6 Lbm-in^2) to 2 (772.176 Lbm-in^2) for the anisotropic rotor study here.

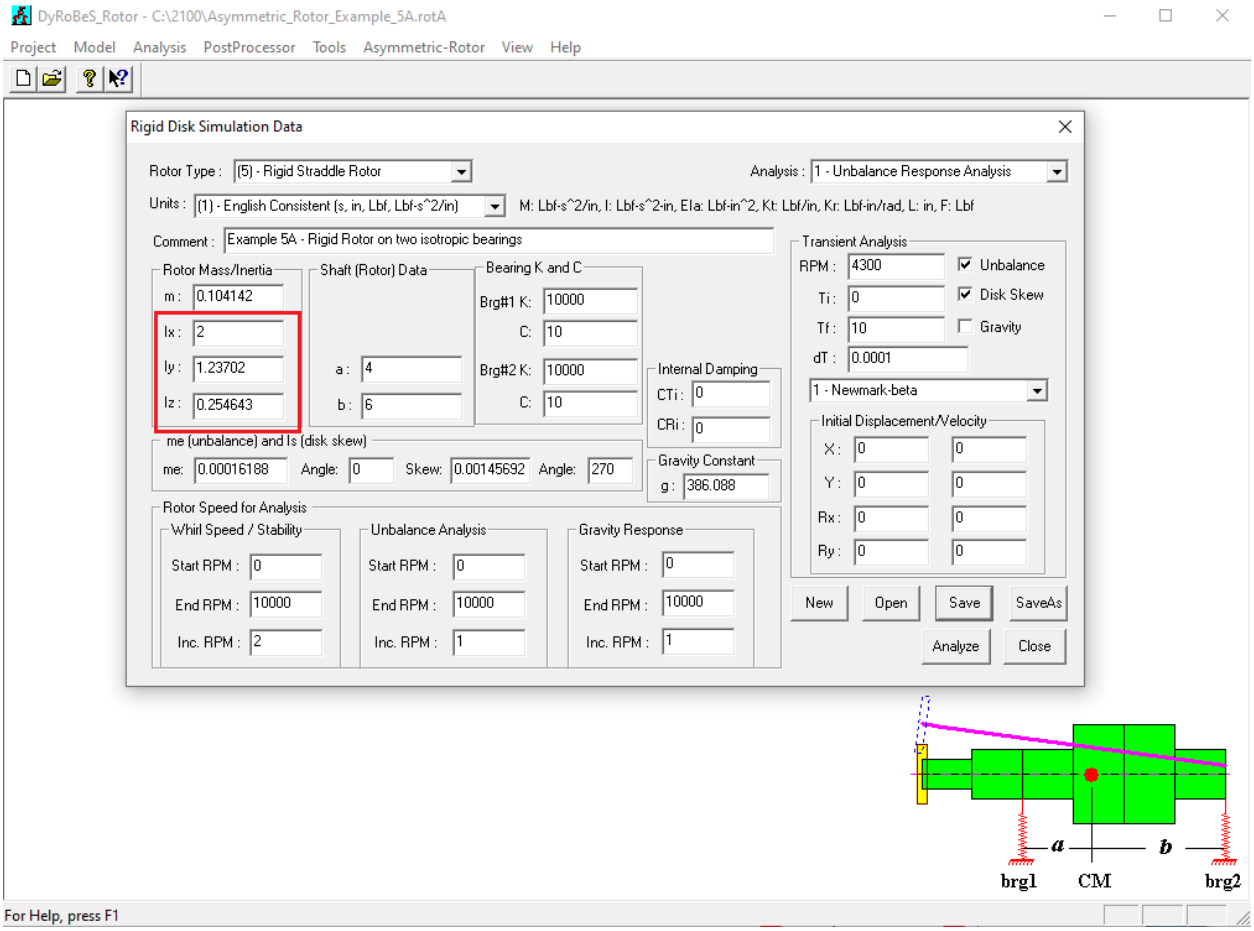

Fig. 5-1 Example 5

The whirl speed maps are shown in Fig. 5-2. It shows that there are four damped synchronous forward critical speeds at 3896, 3972, 5072, 6804 rpm where the damped natural frequencies are zero and the first two forward natural frequencies intersect at one point. However, due to high damping present in the bearings, the rotor is stable and no unstable regions between critical speeds in this example, as shown in Fig. 5-3. Fig. 5-4 shows the unbalance response at CM, Bearing 1, and Bearing 2 locations.

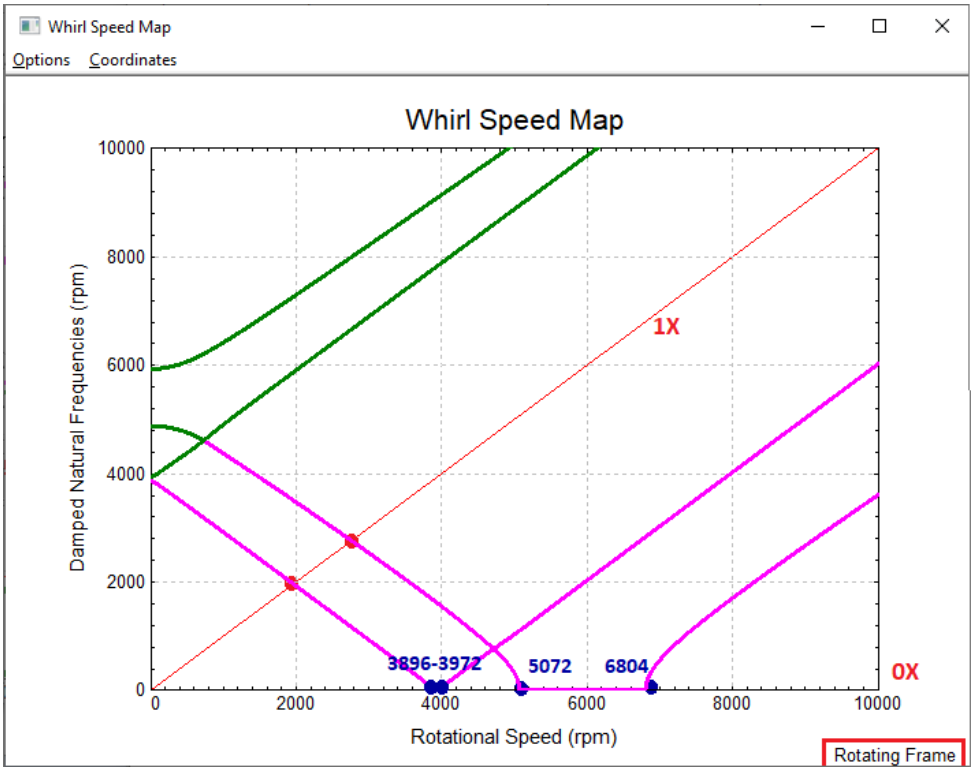

Fig. 5-2 Example 5A – Whirl Speed Map

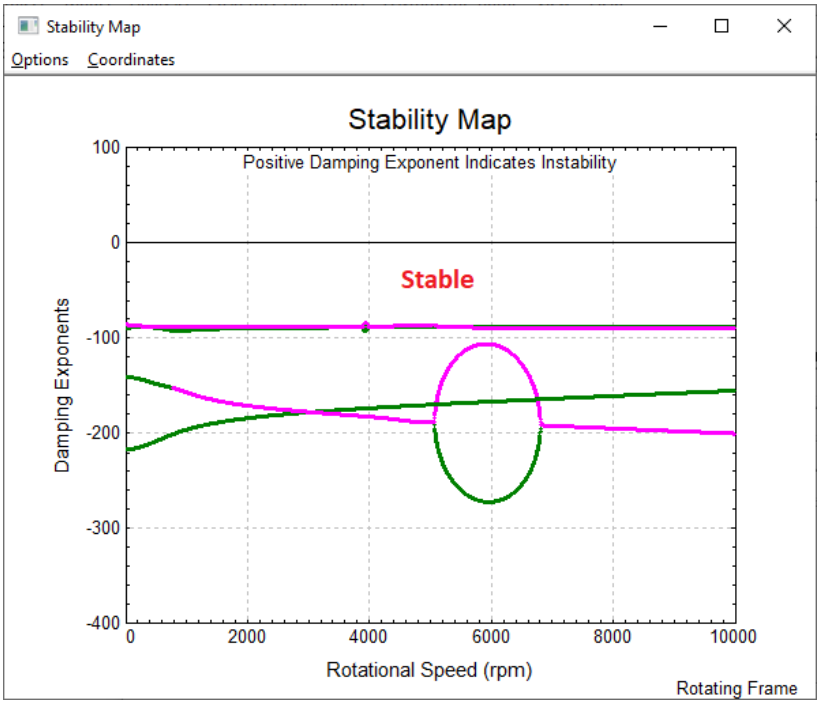

Fig. 5-3 Example 5A – Stability Map

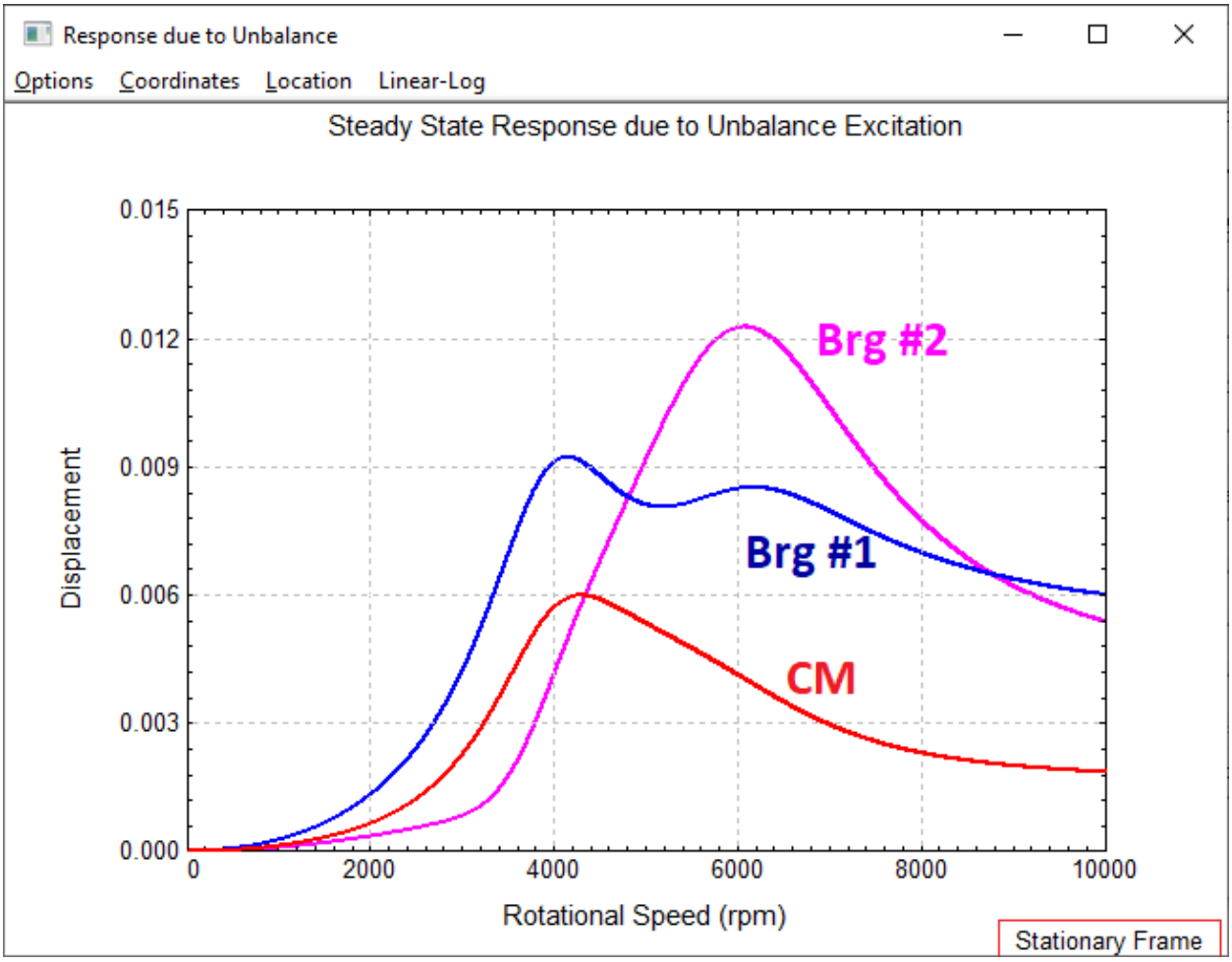

Fig. 5-4 Example 5A – Unbalance Responses at CM, Bearing 1, and Bearing 2

The response due to gravity for this anisotropic rotor with isotropic bearings contains the static equilibrium only, no harmonic response. Fig. 5-5 shows the static equilibrium position due to gravity. Fig. 5-6 shows the gravity response at 2000 rpm. It is a constant in the stationary frame, but a circular orbit in the rotating frame. Also, the orbit in the rotating frame is a backward precession since the rotating frame rotates with rotor speed. This result is verified by using the transient analysis as shown in Figure 5-7.

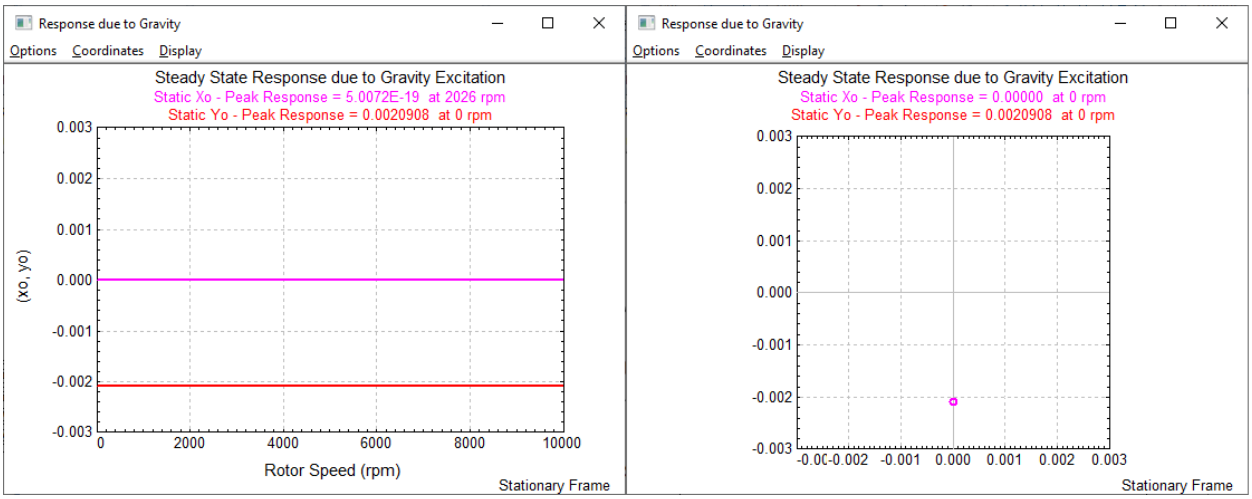

Fig. 5-5 Example 5A – Responses due to gravity

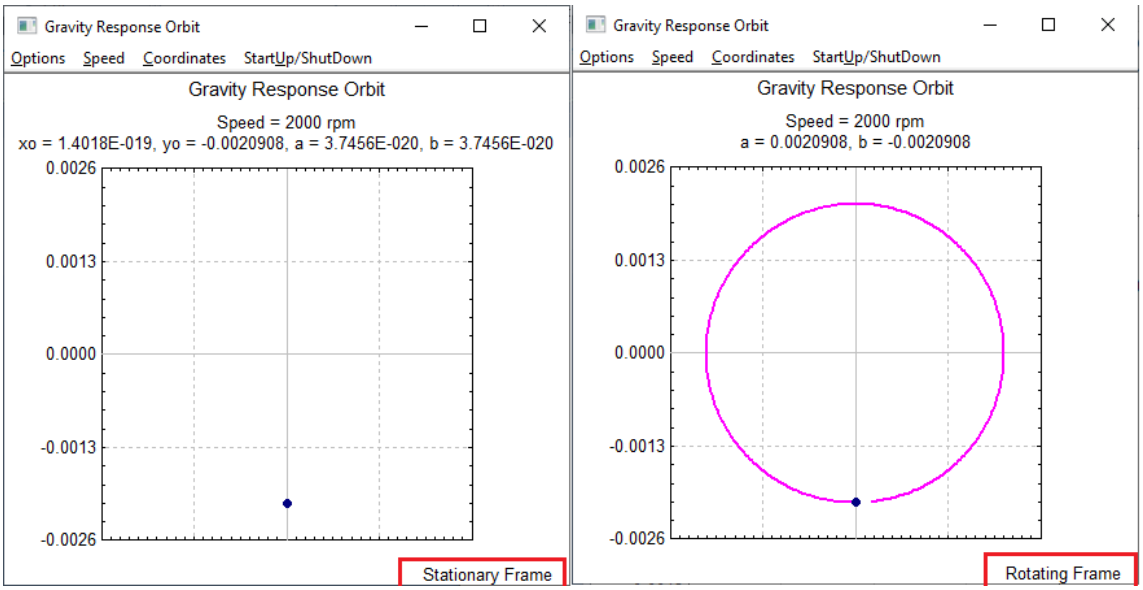

Fig. 5-6 Example 5A – Steady State Gravity Responses at 2000 rpm

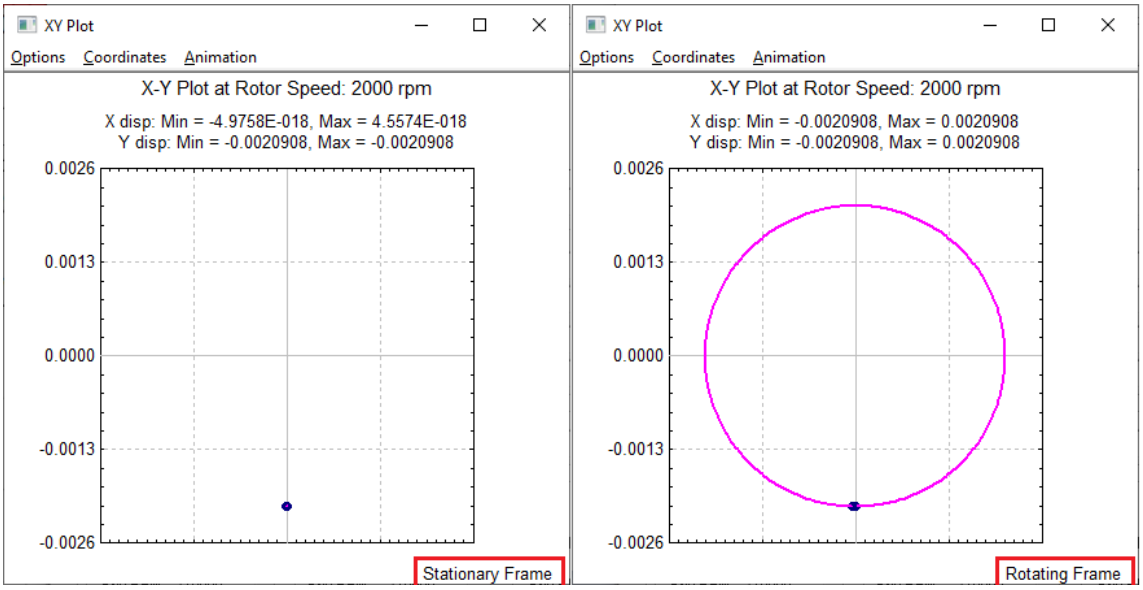

Fig. 5-7 Example 5A – Transient Responses due to gravity at 2000 rpm

Since the system stability is the major concern for the anisotropic rotor. Fig. 5-8 shows the whirl speed and stability maps for C=0 Lbf-s/in. As expected, with C=0, there are three unstable regions, two are between critical speeds and one falls between two unstable regions. Fig. 5-9 shows the whirl speed and stability maps for C=0 Lbf-s/in. It shows that as damping increases, the system stability improves. When the damping is greater than 4, the system becomes stable.

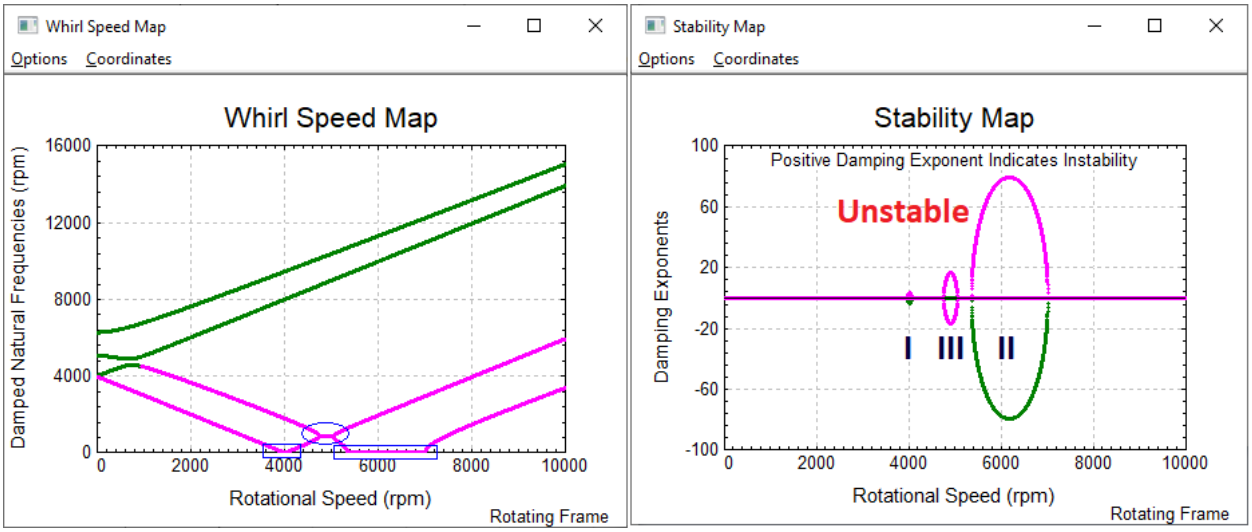

Fig. 5-8 Example 5B – Whirl Speed Map and Stability Map for C=0

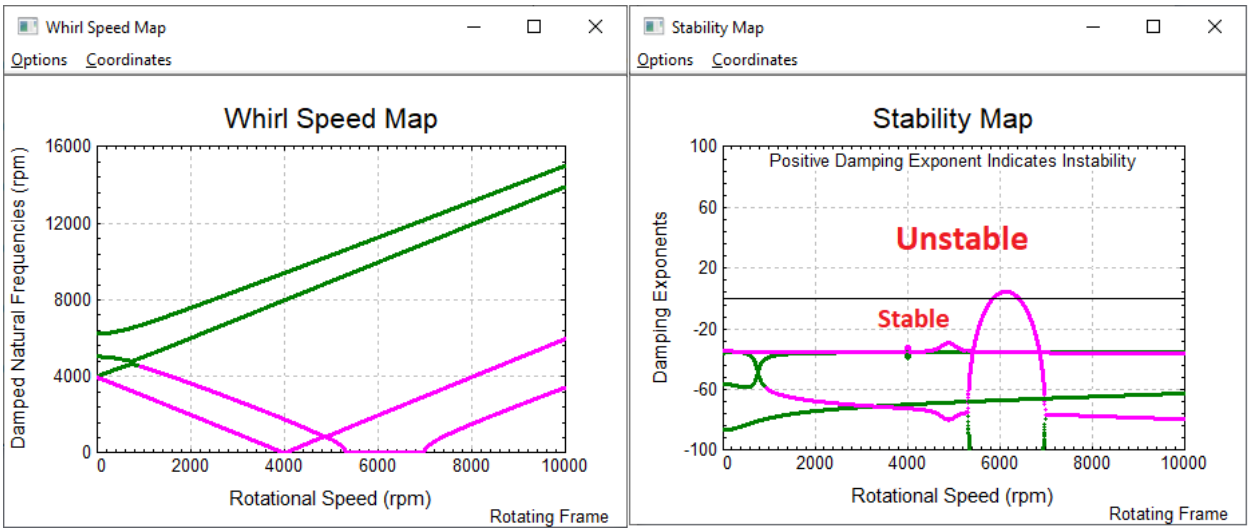

Fig. 5-9 Example 5C – Whirl Speed Map and Stability Map for C=4